Cyclically Optimized Electrochemical Processes

by

Robert Louis Ruedisueli

A dissertation submitted in partial fulfillment
of the requirements for the degree of

Doctor of Philosophy

University of Washington

1997

Approved by 
Chairperson of Supervisory Committee

Program Authorized
to Offer Degree Materials Science and Engineering

Date January 14, 1997

UMI
300 North Zeeb Road
Ann Arbor, MI 48103

In presenting this dissertation in partial fulfillment of the requirements for the Doctoral degree at the University of Washington, I agree that the Library shall make its copies freely available for inspection. I further agree that extensive copying of this dissertation is allowable only for scholarly purposes, consistent with "fair use" as prescribed in the U.S. Copyright Law. Requests for copying or reproduction of this dissertation may be referred to University Microfilms, 1490 Eisenhower Place, P.O. Box 975, Ann Arbor, MI 48106, to whom the author has granted "the right to reproduce and sell (a) copies of the manuscript in microfilm and/or (b) printed copies of the manuscript made from microfilm."

Signature 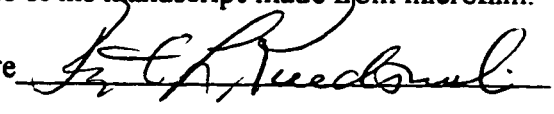

Date January 15, 1997

University of Washington

Abstract

Cyclically Optimized Electrochemical Processes

by Robert Louis Ruedisueli

Chairperson of the Supervisory Committee:
Professor Thomas F. Archbold
Department of Materials Science and Engineering

It has been frequently observed in experiment and industry practice that electrochemical processes (deposition, dissolution, fuel cells) operated in an intermittent or cyclic (AC) mode show improvements in efficiency and/or quality and yield over their steady (DC) mode of operation. Whether rationally invoked by design or empirically *tuned-in*, the optimal operating frequency and duty cycle is dependent upon the dominant *relaxation time constant* for the process in question.

The electrochemical relaxation time constant is a function of: double-layer and reaction intermediary pseudo-capacitances, ion (charge) transport via electrical migration (mobility), and diffusion across a concentration gradient to electrode surface reaction sites where charge transfer and species incorporation or elimination occurs. The rate determining step dominates the time constant for the reaction or process.

Electrochemical impedance spectroscopy (EIS) and piezoelectric crystal electrode (PCE) response analysis have proven to be useful tools in the study and identification of reaction mechanisms. This work explains and demonstrates with the electro- deposition of copper the application of EIS and PCE measurement and analysis to the selection of an optimum cyclic operating schedule, an optimum driving frequency for efficient, sustained cyclic (pulsed) operation.

TABLE OF CONTENTS

LIST OF FIGURES

Number *Page*

LIST OF TABLES

ACKNOWLEDGMENTS

I would like to thank the many individuals who have inspired and helped me along the way on this project and who ultimately made its completion possible: Professor Thomas Archbold and the Materials Science Department and all my committee members for academic support and guidance, Dr. Harold Hager for his electrochemical knowledge and advice on piezoelectric crystals, Dr. Digby MacDonald and Dr. Sam Hettiarachi for their assistance and loan of laboratory space and electrochemical impedance spectroscopy instrumentation at SRI, Dr. Claude Gabrielli for making it possible for me to participate in the EIS international symposium he organized in France in May of 1989, and with very special regard for Professor Colin Sandwith whose passion for engineering science in general and corrosion in particular inspired me into this work in the first place and who has given me encouragement and meaningful and related work at the Applied Physics Laboratory, UW, throughout the long term of this research endeavor; many thanks to my fellow employees here at APL, professors and fellow graduate students, family and friends who have shared in and helped me along over the years of this project. Finally, a very special note of thanks and appreciation for my wife, Diana, for her understanding and patience over these many years and for her assistance in preparing this final document.

DEDICATION

This work is dedicated to the author's parents, Robert W. and Elizabeth M. Ruedisueli on the occasion of their 50th Wedding Anniversary. Their loving encouragement and support has made this work possible.

CHAPTER 1

Background and Introduction

Early in the evolution of electrical power systems, **ac** (alternating current) (**av**, alternating voltage) won the dominant role, while **dc** (direct current) devices and applications became the choice where portability and compactness are the primary criteria. From the time of its invention in the late 18th century by the Italian physicist Count Alessandro Volta to the present day dry cells, lead-acid batteries, and button-sized alkali batteries, the voltaic cell remains the most convenient and readily available source of **dc** power. It is also the simplest and most common example of a device based on electrochemical principals.

Electrochemical processes constitute a special family of heterogeneous chemical reactions: an electrochemical process is a set of complimentary, bipolar reactions occurring at oxidation and reduction surface reaction sites remote from each other, but sharing a common ionic medium of reacting species and connected by an electronically conducting path external to the reaction medium.

The natural and modern industrial worlds are full of electrochemistry from the tiny mitochondria which produce energy in plant and animal cells, to fuel cells in space craft, batteries in flashlights, automobiles, and submarines, while metals are electrochemically deposited in plating process and etched away in specialized metals finishing processes. Corrosion is an electrochemical process which yields no useful energy and costs the U.S. alone tens of billions of dollars a year in lost or degraded metal implements and structures. Apart from this last example, however, electrochemical processes while in seemingly subsidiary roles alongside the internal combustion engines, the coal (oil or gas) fired

thermo-electric, hydro-electric, and nuclear power plants of the present day, play, nevertheless, key roles in our survival and present many challenging opportunities for our advancement.

While most electrochemical reactions are, to some extent, reversible, the devices applying them are (like the dry cell) conventionally irreversible. They can be, and generally are, thought of as being strictly ***dc***. The flashlight battery is used until it is drained below some acceptable voltage level and then it is discarded. One notes along the way how batteries exhibit some rejuvenation between periods of usage. The flashlight having previously grown dim appears bright again after a few hours *rest*.

There are some notable exceptions, however, to the electrochemical **dc** mode of operation. ***dc*** is taken generally to mean *steady* (or constant) current (or voltage) with no variation in polarity. Any departure from this regime pulsing (on, off) or periodic reversing (direction of) current (PRC) or (polarity of) voltage, as well as a sinusoidal (square or saw-tooth) variation at any **dc** bias (whether polarity is reversed during any portion of the cycle or not) is taken generically as ***ac***.

This researcher first became interested in **ac** electrochemical processes through a study of the effects of **ac** on the passivation of stainless steel [4]. There are many examples of processes and products that have been enhanced by the use of **ac**. For example, **ac** has been preferred for decades for etching lithographic plates and the surfaces of capacitor foils because the resulting etch is more uniform than with **dc**. Electro-deposition (plating) processes, too, have been improved by using **ac** as pulsed or periodically reversed current (PRC). The resulting plate is typically finer grained, more uniform, and exhibits better mechanical and electrical properties. Electrowinning efficiency of some metals, such as zinc, can be improved [10]. When the process is conducted in an

ac (typically PRC) mode, there is more usable plated metal product per watt of power used. In the area of energy production, a solid state switching device developed for the purpose of getting **ac** from space craft fuel cells resulted unexpectedly in higher output from the fuel cells. In corrosion, high frequency pulsed rectifiers are finding favor in cathodic protection of well casings [8,9].

Another common device taking advantage of electrochemical reversibly, but with very long cycles, is the lead-acid storage battery. Here the battery takes its place in a very highly, cyclically optimized device as it starts the engine, then recharges as the internal combustion engine runs. The timing cycle of the gasoline or diesel engine is a very evolved system for energy conversion.

The internal combustion engine and its essential auxiliaries, as in an automobile or diesel electric submarine power plant exemplify a *cyclically* optimized system or device. Hydrocarbon fuel is optimally mixed with air (oxygen) to burn, to produce hot gas expanding against a cylinder head resulting in mechanical work and motion as the desired effect, some of which is stored in the inertial mass of a flywheel, to continue the cycle; it is still evolving although limited by its Carnot cycle efficiency, as electronic devices permit finer, more sophisticated system control.

Apart from electrochemical applications of PRC schedules, chemical process engineers have been fascinated with the possibility that running at least some reactions in a cyclic or oscillatory mode may be advantageous. Douglas and Gaitonde [12] summarize their work on the subject of cyclic operation as follows: "The time-average conversion obtained from an oscillating reactor is sometimes superior to the steady-state output. This result implies that under certain circumstances, an oscillator will have a performance better than that expected from the optimum steady-state design."

Certain chemical and electrochemical reactions that have traditionally been run in a batch fashion have an inherently cyclical nature to them. Even when these processes have constant inputs, they produce periodic outputs. As early as 1824 Fechner [1] noted that under certain conditions, current oscillations occurred during the electrodeposition of silver on iron from acidified silver nitrate. This is an early example of many inherently oscillatory-like systems being reported and studied to this day. Another example is the corrosion of iron, under certain conditions, in chloride solutions [3]. The mechanisms responsible for such behavior are worthy of study in themselves. As a class, these systems raise some very pragmatic questions which are properly addressed in engineering work:

1) Are there some general criteria for which electrochemical systems can be expected to oscillate in a predictable manner?

2) Are there systems which while *critically damped* (will not oscillate) can be run in a superposed (forced) oscillatory mode, or under a pulsed or periodically reversed regime, cyclical mode of operation?

3) If we assume the answer to (1) and (2) is yes, certainly *some* at least, then how can such systems be identified and by what means can it be determined if there is an advantage to the non-steady or cyclical mode of operation?

4) Finally, how can the *right* or *optimal* cyclical mode of operation be determined?

Given the idea that cyclical operation could be advantageous, a trial and error method of finding an ac, PC, or PRC schedule that yields satisfactory results could be applied to any system under consideration. It is likely that such an empirical method was utilized to arrive at many, proprietary, industrial applications of cyclic processes currently

in use. Examples include the ac etching of capacitor foil surfaces and some electroplating processes.

The answers to question (1) and (2) may be taken as "probably yes" and the answer to (3) must, in any case, ultimately be found by an actual full scale test. The answer to (4) requires the development of a rational approach or strategy which is the object of this work: *to propose a strategy to determine an optimal cyclic mode of operation.*

Fundamental to this procedure is a perspective, the idea of examining the system not only from the conventional standpoint of its thermodynamic equilibrium states and kinetics of reaction rates and pseudo-steady states; but to consider, as well, the *dynamics* of the system: *the manner and rate at which the system responds when perturbed from equilibrium states.* Does the system drift back asymptotically to some steady state, does it tend to oscillate some before settling back into equilibrium, or does it become unstable with oscillations growing in amplitude?

An approach to designing the *cyclic optimization strategy* is described over the next several chapters. First of all, there needs to be some fundamental description of electrochemical systems in general: what common properties do they have with other physical systems in which cyclic behavior can be observed; mechanical, electrical; and what properties are peculiar to electrochemical systems? All physical systems must deal with mass and energy, changes in state with time, and shifts between potential and kinetic energy. Mechanical and electrical systems exhibit some elasticity as they oscillate between kinetic and potential energy states; they have inertia. One question asked here is: is there an analogous quality in chemical and electrochemical systems?

At some point, early on, we must introduce and define *optimal* as it pertains to physical system cycles in general and electrochemical processes in particular. Optimal is a nebulous term and depends mostly upon the desires, economic objectives, and expectations of the end users. It is easier to say what it is *not:* optimal is *not* necessarily maximum or minimum, or even necessarily required to be the most *efficient*; some criteria must be chosen.

A review of mathematically defined criteria for stability and oscillations for physical systems and the application of such criteria to electrochemical systems may be helpful in laying a basis for the selection of an operating *duty cycle*.

We will consider the options available for systems that do not oscillate naturally; those which consist of a set of competing reactions which together run asymptotically to a critically damped pseudo-steady state. Through measurement of the time constants for the competing reactions and judicious apportionment of cycle time between the competitors, an *optimal* cycle design is sought. The cycle timing device or schedule here acts like a traffic light apportioning the flow of traffic through an intersection.

Broad attention is given to describing the state-of-the-art electronics that make modern electrochemical techniques and experiments possible. The backbone of most electrochemistry experimental work is the modern, PC-supported, potentiostat-galvanostat, which can measure the performance of a fuel cell, or the corrosion rate of a metal sample in a given electrolyte in terms of conventional cell current vs. voltage plots. Modern, solid-state, operational amplifier electronics, with very short pulse rise times, fast response, and high stability make accurate control of electrochemical cells and response measurement possible over a wide range of frequencies.

Particular attention is given to the application of the frequency response analyzer (FRA) with the potentiostat to perform electrochemical impedance spectroscopy (EIS). EIS is used to measure the reaction system response to a small amplitude (voltage or current) perturbation from a given electrochemical cell equilibrium point, across a wide range of frequencies. The resulting spectrum of ohmic (real), reactive (imaginary) and phase angle responses can reveal the time constants for one or more of the reactions taking part in the system. The time constants are of fundamental importance in designing the optimal cycle.

A description is given of the relatively new and rapidly developing technique of piezoelectric crystal electrodes (PCE's) applied to electrochemistry as an in situ quartz micro-balance (QCM). This technique measures the real time mass flux to or from an electrode surface as well as the conventional cell voltage and current. With this technique the gain or loss of fractions of a monolayer from surface can be measured in real time and correlated with the cell current/voltage condition producing the mass change. The effect of current/voltage cycle tuning, therefore, can be readily observed. Additional means must be employed, however, to confirm the quality and nature of the mass change. It is also possible to monitor the energy to maintain the crystal's amplitude of oscillation as the fundamental frequency drifts in proportion to its surface loading.

Finally we will see how, with some fundamental knowledge of the system of interest and the aid of the tools and techniques described in the following chapters, a stable, useful, optimal electrochemical process mode of operation can be *designed*. With this strategy, the amplitude and frequency of the optimal *duty cycle* can be chosen by rational design rather than by trial and error.

Ultimately, the factor that determines the choice of industries in terms of which technologies to develop and what aspects of a particular technology or process favor it over another is *economics*. More specifically, the basis for decision making in industry is: *return on investment*,

$$\text{ROI} = (\text{annual profit}) / (\text{investment}) .$$

Whether the subject is the improvement of older, established processes such as the reduction of aluminum ore or chlor-alkali production or the introduction of new processes for the electrochemical production of organic molecules such as hydroquinone or benzaldedhyde, ROI will be the ultimate criterion.

Electrochemists have been very productive in developing the inventory of electrochemical reactions and the basic mechanistic knowledge about these reactions. There is, however, as indicated by Beck [6] and Spotnitz, et. al. [7], a considerable lag in the design of reactors which apply and make the electrochemical reaction technologies industrially viable. Varjian [11] describes the array of products of electrolytic processes from adipronitrile to zinc (of greatest importance, by quantity produced, are: chlorine, caustic soda, aluminum, copper, magnesium, and zinc). To make the most of the investment already in the fundamental work of electrochemical researchers, there is a need for R&D strategies which will bring additional work to bear on reactor design details which are most likely to lead to maximum ROI.

Beck and Spotnitz both illustrate the complexity of the task of developing electrochemical processes at an industrial level; it is a very long road from the laboratory flask cell to a full scale electrochemical process plant. The ROI is a function of total plant, personnel, and material and energy costs and quantity and price of material sold. Beck

demonstrates optimization analysis functions for some of the electrochemical process cell variables such as optimum cell current density, electrode spacing, or adjustment time period in order to maximize ROI.

Spotnitz develops a complete and general ROI model for electrochemical processes which includes both electrochemical and associated non-electrochemical support equipment (i.e.. mixing and separating distinct from electrochemical vat equipment) to analyze the impact of various parameters in terms of a dimensionless optimum current density and maximum ROI. Certain assumptions, e.g., that parameter effects are generally linear, may be over-simplifying the real case. However, the model clearly shows what changes in parameters realize positive effects on ROI and gives examples of which processes are most likely to become commercially viable (based on present energy and material costs and known technologies). For example, the model predicts that hydrogen should be electrochemically consumed as in a fuel cell, but not electrolytically produced; the production of adiponitrile would be viable, but not the production of hydroquinone.

Cell parameters which are expected to improve the ROI are: increased optimum cell current density, current efficiency, and reaction product selectivity. Decreased cell resistivity, and zero-current (reversible) cell voltage would also improve ROI. Thus, in designing reactors for processes which are already commercially viable (or those which are nearly so) the above are the parameters to improve; they all must be addressed on the scale of the electrochemical interface.

In general, the strategy for a step-wise, key parameter analysis-based (i.e. *rational*) optimization strategy for *cyclical or periodically controlled electrochemical processes* entails the following:

1) Obtain a general knowledge of the electrochemical reaction kinetics and the mechanisms for the processes which fit an economic criterion (ROI) for optimization.

2) Identify key parameters and "optimum" criteria necessary to arrive at periodic control duty cycles (fraction of time on/off).

3) Determine the level of accuracy and precision of measurement of parameters necessary to arrive at duty cycles.

4) Identify the instrumentation and methods necessary to make measurements.

5) Make measurements on selected process; interpret and apply data to arrive at an actual periodic control schedule

6) Test the "schedule" by running and comparing with criteria and results of tests run "off-schedule".

CHAPTER 2

Electrochemical Fundamentals: Systems in Equilibrium

Electrochemical reactions are a special branch of heterogeneous chemical reactions; the reactions occur not by species interactions within a volume but as a result of reaction species moving to or from a surface. However complex the reaction interface surface might be it is, topologically, two dimensional. Reaction rates therefore are not only controlled by the activation energies for specific reactions or reaction steps, but by the availability of reaction sites on the reaction surface and transport rates (by convection or diffusion or electrically influenced migration) of reaction species to and from the reaction surface.

What distinguishes *electrochemical* reactions form other herterogeneous reactions is that electrochemical reactions occur as bipolar cells at complimentary pairs of oxidation-reduction *half-cell* reactions proceeding at two separate but electrically connected interfaces in a conducting medium (an electrolyte). Four elements or components common to all electrochemical reactions are:

1) an anode or *oxidation* site (or electrode) where, $M \rightarrow M^{n+} + ne^-$

2) a cathode or *reduction* site (or electrode) where, $A^{n+} + ne^- \rightarrow A$

3) an ionic conducting medium, an electrolyte (typically an aqueous salt solution) and

4) an electronic conduction path between the anode and the cathode, an external circuit.

The oxidation and reduction processes are stated in (1) and (2) as half-cell reactions. Typically the electrodes of the electrochemical cell (see Figure 2.1), where these reactions occur, are metals, but they could also be semi-conductors. If these are semi-conductors, such materials act as either the ionic (electrolyte) or the electronic (external circuit) conducting medium. The sum of the two half-cell reactions gives the full, electrochemical cell reaction, expressed as:

$$M + A^{n+} = M^{n+} + A$$

Unlike other chemical reaction systems, the electrochemical cell, due to its distinct bipolar character allows for a simple, direct electrical measure of its thermodynamic potential. When a standard, high resistance voltmeter is connected in the external circuit between the two electrodes (see Figure 2.2) or between one of the electrodes and a standard reference electrode (see Figure 2.3), the measured voltage and its polarity are used to determine the magnitude and sign of the *Gibbs free energy* as:

$$\Delta G = - nFE$$

In this equation E is the measured voltage (in volts), F is the Faraday constant (96500 coulombs) and n the number of electrons exchanged in the reaction. While this equation gives the magnitude of the free energy, the driving force for the reaction, it is the sign of the free energy which is the more crucial information: it determines the spontaneous direction of reaction of the cell.

For reactions not in the standard state, where the activity of either product or reactant is not unity, the correct half-cell potential is given by the Nernst equation:

$$E = E^{o} + 2.3\ (RT/nF) \log\ (a_{oxid} / a_{red})$$

where a_i is the activity of the reacting species, oxidation and reduction, respectively.

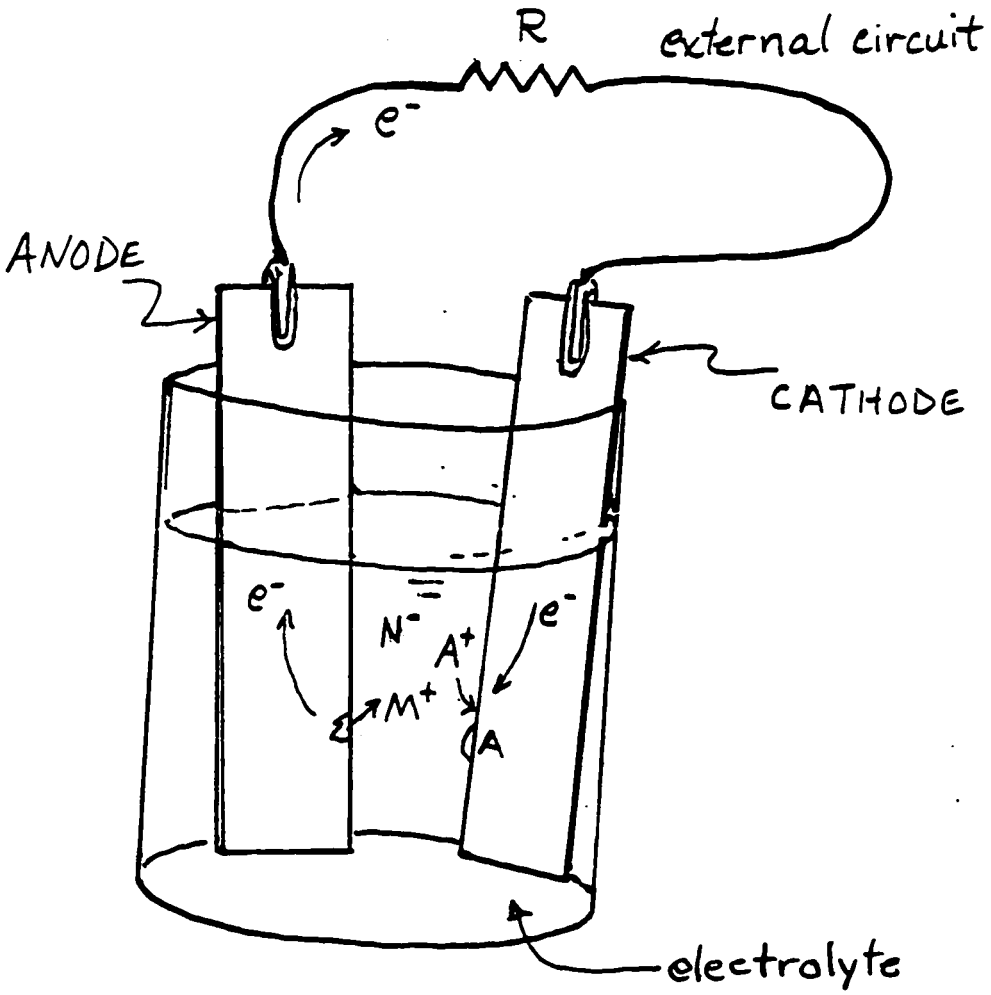

Figure 2.1. THE ELECTROCHEMICAL CELL consists of two sets of complimentary, heterogeneous reactions occurring at sites which are remote from each other:

1) ANODIC (oxidation) reaction $M \rightarrow M^{n+} ne^-$

2) CATHODIC (reduction) reaction $A^+ + e^- \rightarrow A$

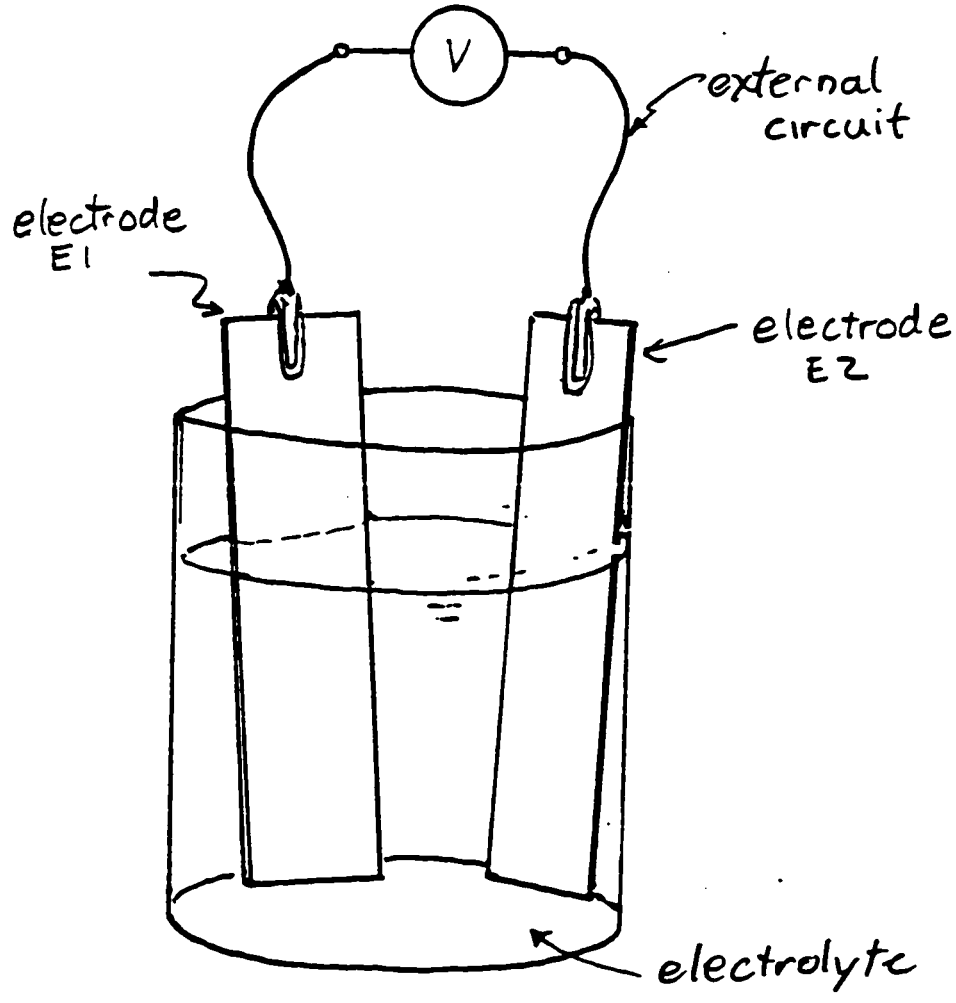

Figure 2.2. THE CELL ELECTRICAL POTENTIAL can be measured with a voltmeter in the external circuit. The process (anodic or cathodic?) at a given electrode (E1 or E2) is not known unless the voltmeter (v) has been calibrated to a known cell.

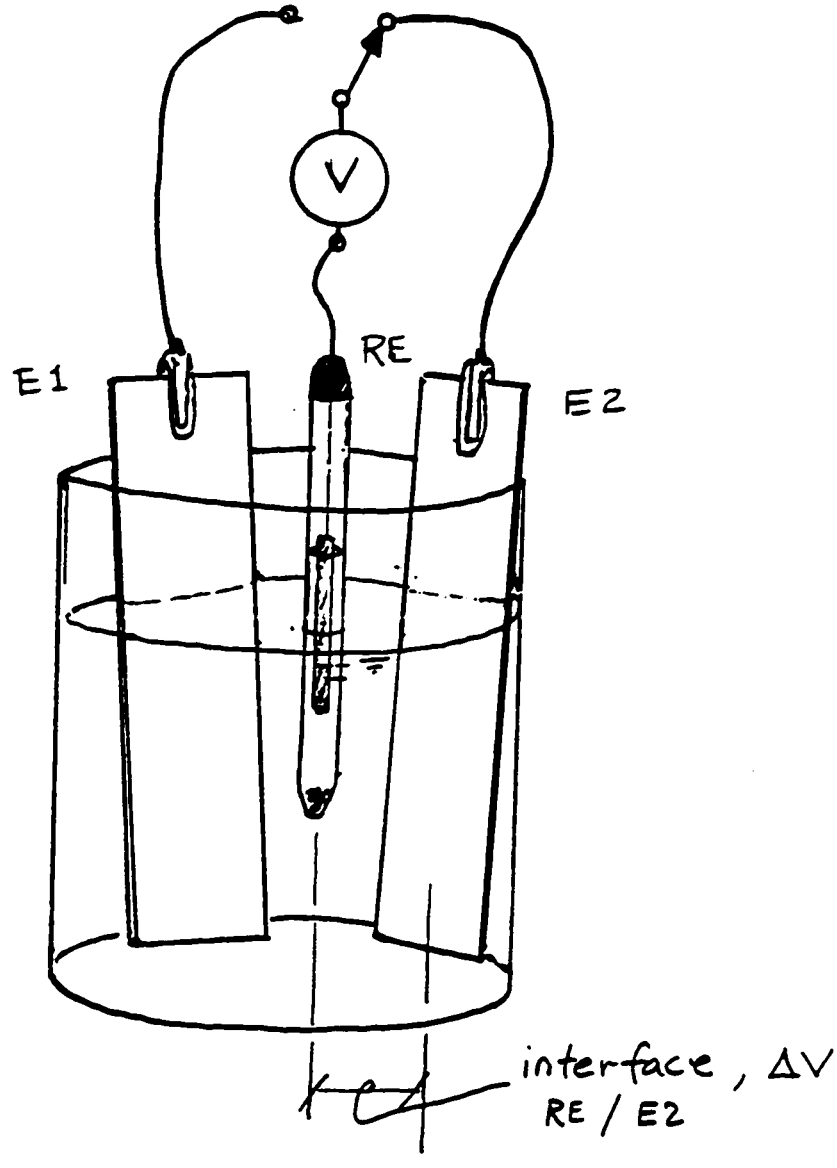

Figure 2.3. THE MEASURED POTENTIAL, ΔV, between any two electrodes is proportional to the Gibbs free energy of reaction occurring between them. While potential can only be measured between two electrodes, one of the two electrodes can be a standard reference electrode, RE, such as silver-silver chloride or mercury-mercurous chloride (calomel).

It is important to emphasize that this is the equilibrium condition. The measured potential gives thermodynamic information only: the magnitude and direction of the driving force. This information suggests only what *can* happen, not what *will* happen or how fast. It does tell what *cannot* happen. This is, however, a useful starting place in analyzing an electrochemical system. Marcel Pourbaix assembled an atlas of equilibrium diagrams or maps for metals in aqueous solutions [2, 3]. The possible equilibrium species (metal, metal oxide, metal hydroxides, etc.) for many metal/water systems are described in terms of the phases within the boundaries of the potential versus pH *Pourbaix* diagrams. Figure 2.4a and 2.4b show the Pourbaix diagrams for nickel and copper, respectively.

For the electrochemical cell in equilibrium, there is no net reaction at either electrode, and no net current through the external circuit. This is not, however, a static situation. On the reversible hydrogen electrode (consisting of platinum in 1 N hydrochloric acid solution), for example, both the reduction and oxidation reactions are proceeding simultaneously at different points on the platinum surface, but at the same reaction rate which is proportional to the *exchange current density*.

$$r_{red} = r_{oxid} = i_o / nF \qquad (\text{moles/cm}^2\text{-sec})$$

The reversible electrode reaction can be plotted as a point corresponding to its equilibrium potential, 0.0 volts, and its exchange current density on a log current vs. potential plot. The exchange current density for hydrogen on different metals varies by many orders of magnitude. For mercury, it is 10^{-12} amp/cm^2, while for bright platinum it is 10^{-3} amp/cm^2 and ten times still greater for platinized platinum [1].

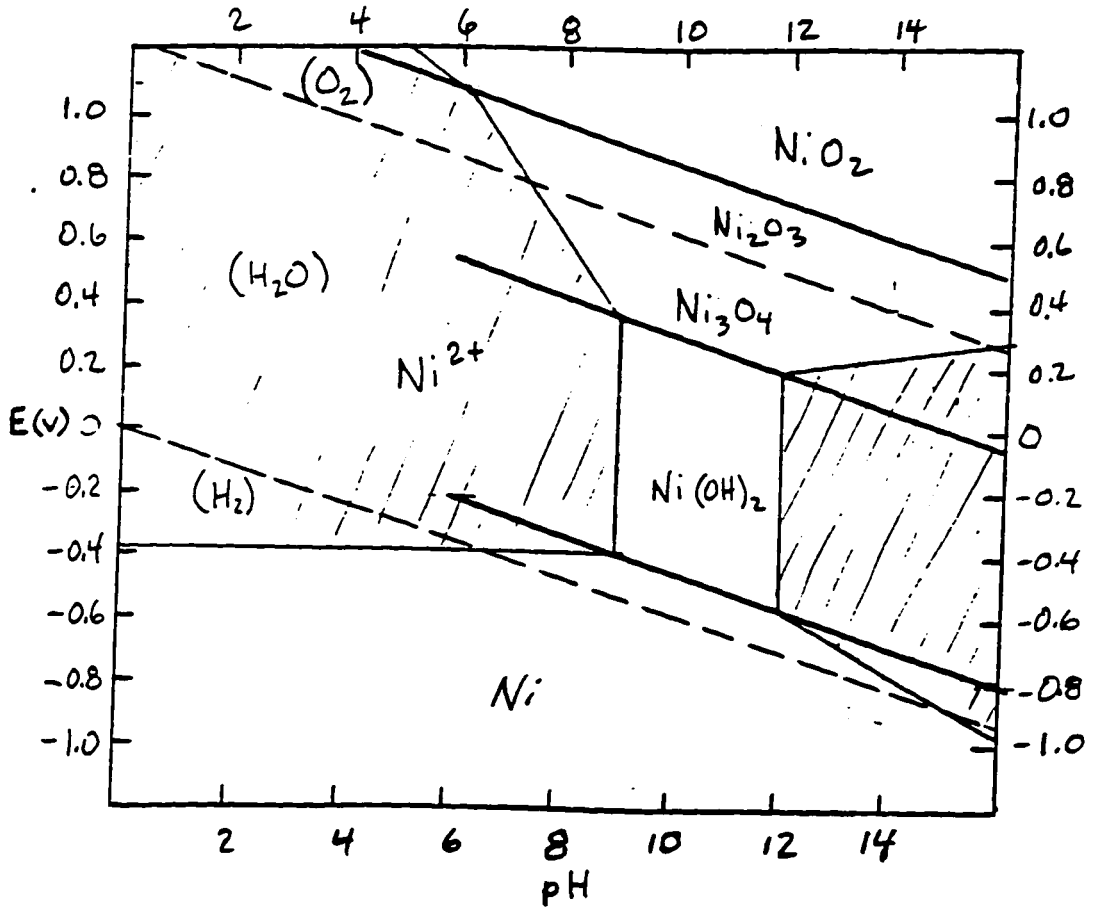

Figure 2.4a. POURBAIX DIAGRAMS are thermodynamic equilibrium plots showing the species of a metal that will predominate in the aqueous electrochemical system over a range of pH and E(v) electrode potential values. Boundary lines are derived from the Nernst equation. Above example is for nickel. (Jones, [1], p. 61)

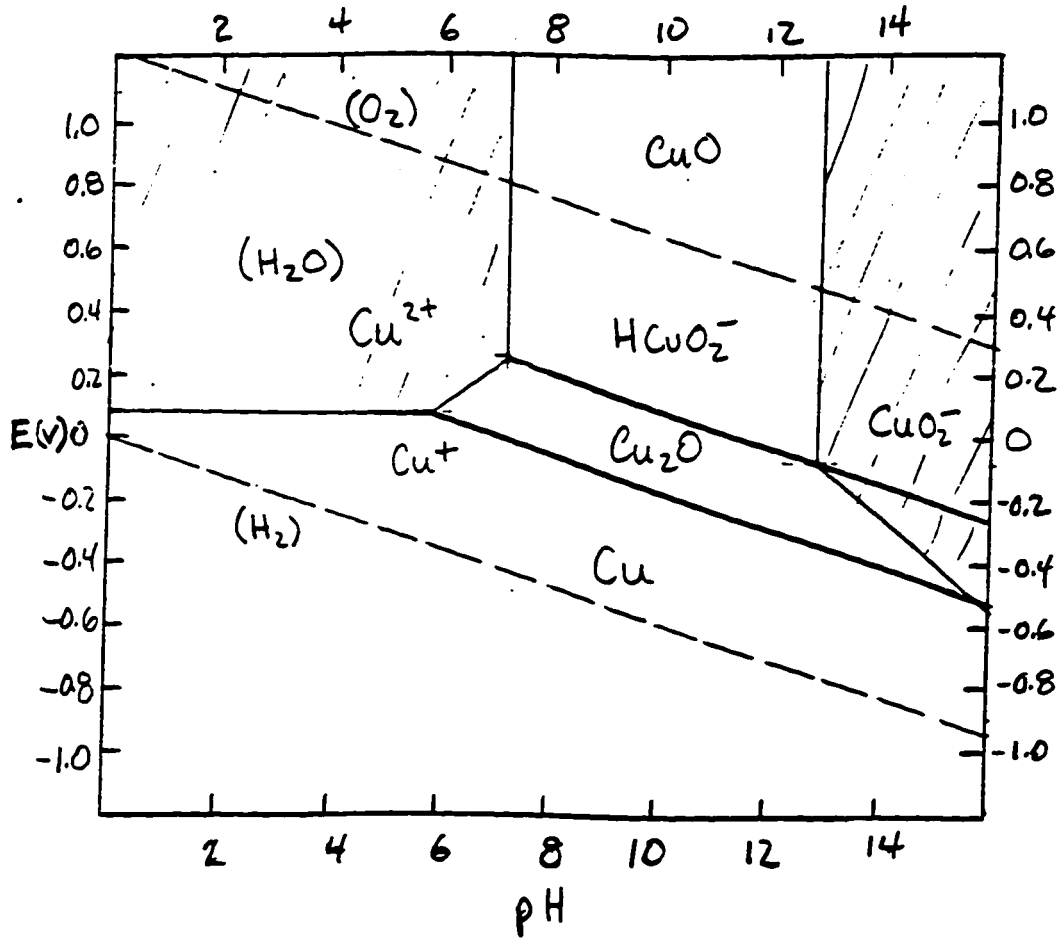

Figure 2.4b POURBAIX DIAGRAM FOR COPPER, like preceding diagram for nickel, shows regions where the metal is stable, actively corrodes, or forms oxides. The diagrams show what can happen not what will happen or how fast; kinetics are not known. (Jones, [1], p. 61)

If the high resistance voltmeter between the electrodes of the cell in the measurement set-up is replaced by a low resistance copper wire, current flows freely through the external circuit and the cell is no longer in equilibrium as reactions proceed in their respective spontaneous directions at both electrodes. In a cell consisting of electrodes of zinc and platinum, the zinc is oxidized. The zinc ions go into solution, providing electrons through the external circuit for the reduction of hydrogen ions and the formation of hydrogen gas on the platinum electrode surface. As the electrochemical system proceeds to a new equilibrium, the electrodes are said to *polarize* towards each other: the anode (zinc) becoming more noble (more positive) and the cathode (H/platinum) less noble (more negative). The rate, the *kinetics*, of this process are dominated by two kinds of polarization: *activation* polarization and *concentration* polarization.

Activation polarization is due to the energy required to initiate the *rate determining step* (rds) in the reaction: the combination of two hydrogen atoms to form a molecule or the gathering of some critical number of molecules to form a hydrogen gas bubble on the platinum surface. The potential shift from equilibrium required to overcome the activation energy barrier is referred to as the *overpotential*, n_{red} (for reduction) and n_{ox} (for oxidation):

$$n_{red} = b_{red} \log i_{red} / i_o \quad \text{and, similarly,} \quad n_{ox} = b_{ox} \log i_{ox} / i_o$$

The slope, b, in these expressions relating the reaction rate to the overpotential is the Tafel constant. These constants are particularly important in this work: they are a measure of a reactions sensitivity to potential control. The value of b typically ranges between 0.05 and 0.15 volts and is typically about 0.10 volts.

In the absence of a slow rds, the reaction rate will generally be limited by the concentration polarization which is defined by the rate at which reactants (hydrogen ions, for example) can reach the electrode surface by diffusion from the bulk electrolyte solution across the diffusion layer. The reaction rate limit then is the *limiting current density*, i_L :

$$i_L = DnFC_B / x$$

where C_B is the concentration of reacting species in the bulk solution and x is the diffusion layer thickness. If the reaction is controlled by concentration polarization, the overpotential is:

$$n_{con} = 2.3 (RT / nF) \log (1 - i / i_L)$$

The reduction reaction is more likely to be controlled by concentration polarization. In general, the reaction rate at an electrode is controlled by both activation and concentration polarization. The resulting total overpotential then is:

$$n_T = n_{red} + n_{con} \text{ or } n_{ox} + n_{con}$$

$$\text{i.e.: } n_{red} = b_{red} \log (i / i_o) + 2.3 (RT / nF) \log (1 - i / i_L)$$

is explained by the *mixed potential theory* of Wagner and Traud [9] and Stern and Geary [10]. An electrode surface may be involved in several reactions simultaneously and the resulting equilibrium potential measured at an electrode, according to mixed potential theory, is derived from two hypotheses:

1) Any electrochemical reaction can be divided into two (or more) partial oxidation and reduction reactions.

2) There can be no net accumulation of electric charge during an electrochemical reaction.

Therefore, the total of all the oxidation reactions must equal the total of all the reduction reactions at any electrode reaction site. This is true whether the electrode reaction sites are distributed over a single metal in an electrolyte or on two (or more) separate reaction surfaces which are electrically connected and immersed in separate but ionically connected electrolytes. A separate reference half-cell connected through a voltmeter (as in Figure 2.3) to any part of the electrode (or electrically shorted electrode system) will read the same equilibrium potential, E_{corr}. Knowing the reversible half-cell potential and exchange current density for the participating reactions and the electrode metal involved, along with the respective Tafel constants, an Evans plot can be constructed as shown here in Figure 2.5. The open circuit, equilibrium potential, *Ecorr*, is at the intercept of summed reduction and oxidation reactions.

The measured Ecorr is the sum of the desired interface potential and a standard reference half-cell electrode. A good standard reference electrode consists of a highly reversible, non-polarizable half-cell reaction which leaks current readily and therefore has a relatively high current density (10^{-3} to 10^{-2} amp/cm^2.) but when used with a high impedance electrometer draws no current. The standard hydrogen electrode is not a convenient reference electrode to use. Examples of other good reference electrodes are: saturated calomel, silver-silver chloride, and copper-copper sulfate.

Accurate, reproducible Ecorr measurements are essential (1) to make maximum use of available information about a given system, (2) to aid in gauging the degree of stability of a system and, (3) as a reference point for dynamic studies of systems undergoing perturbation in some prescribed manner in order to meaningfully observe its dynamic response.

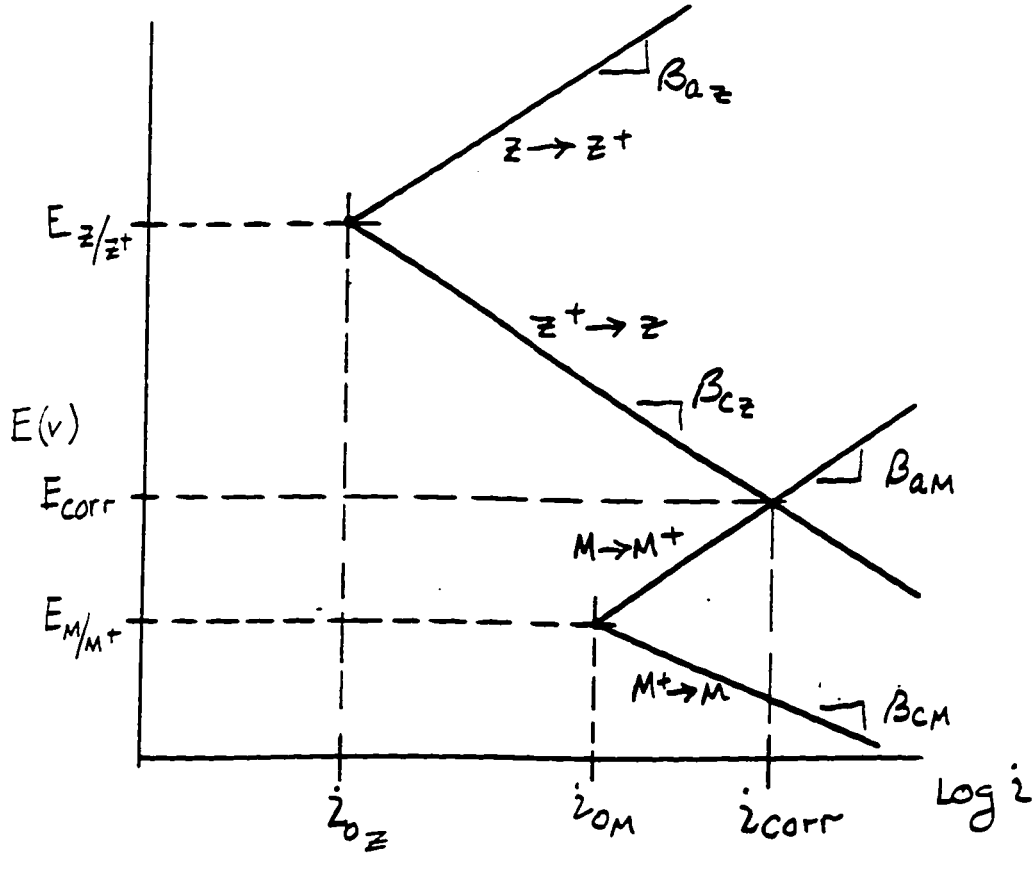

Figure 2.5. EVANS DIAGRAM used by Stern-Geary mixed potential theory to describe how the oxidation/reduction reactions at a single electrode are resolved to an open circuit equilibrium (corrosion) potential, E_{corr}, and corrosion current, i_{corr}. $E_{Z/Z+}$ and $E_{M/M+}$ are the reversible oxidation/reduction potentials for the reactive electrolyte species, Z, and electrode metal, M, respectively; i_{OZ} and i_{OM} are exchange currents for these reactions; and β_{aZ} , β_{cZ} and β_{aM}, β_{cM} are anodic and cathodic Tafel constants.

Reproducible Ecorr measurements require strict controls on the electrolyte/electrode interface composition and conditions. The concentrations of electrolyte solution species, dissolved gasses, pH, temperature, conductivity, and degree of convection all must be maintained within strict limits along with electrode surface oxidation condition.

Some time is required for an interface to establish a stable Ecorr. Even if all electrolyte conditions are maintained, a stable Ecorr reading will not necessarily appear immediately when the potentiometer is switched across the reference electrode and the interface of interest. Ecorr can be quite stable over long periods of time (days, weeks); immediately after the measurement is first made, however, Ecorr may appear to drift one way or the other, a few millivolts at a time. The stable Ecorr is approached gradually over minutes to hours and will change gradually as the cell electrolyte conditions and or composition change. A cell open to the atmosphere will adsorb carbon dioxide from the air. Dissolved carbon dioxide will depress the pH which in turn has an effect on the Ecorr.

Acquiring a stable Ecorr is the starting point for conducting further electrochemical studies. The study and characterization of an electrochemical system is accomplished by constructing the system in the form of a three-electrode cell (similar to that shown in Figure 2.3) which includes one acting as an anode, one a cathode, and the third a reference electrode. Typically, the interface at only one electrode is the object of study. This electrode is the working electrode (WE); the second is the counter electrode (CE). The external circuit to this experimental cell, shown in Figure 2.6, includes instrumentation which not only measures but accurately controls the voltage between the working and reference electrodes, and the current across the cell, between the working

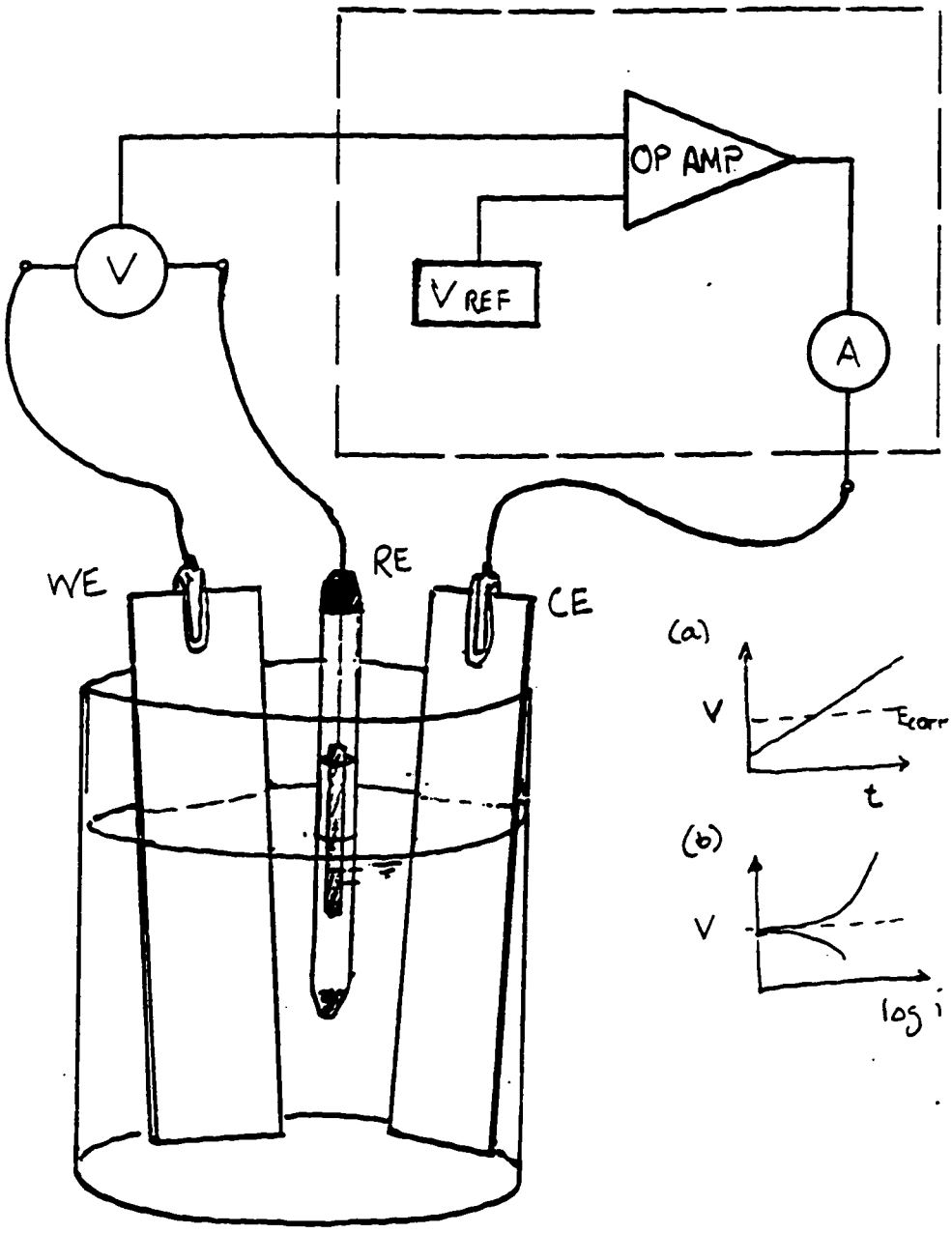

Figure 2.6. THE THREE ELECTRODE CELL permits not only the measurement but the control of the potential of one electrode, the working electrode, (WE) whose voltage/current response is to be studied. The control circuit (more symbolic here than functional) in the external circuit applies and measures the current required to ramp the WE-RE potential over a predetermined range and at a specified rate.

and the counter electrode. Ecorr is the initial set or reference point for experiments such as, anodic polarization plots (AP-scans) or polarization resistance measurements.

The electrochemical cell is studied by measuring and recording the current which must be applied to the cell by a potentiostat in order to attain some overpotential with respect to Ecorr either by stepping the voltage or ramping it at a specified sweep rate (mV/sec). The current density across the electrochemical interface as it is polarized away from equilibrium (Ecorr) and results in a log-current versus potential plot shown in Figure 2.7 and 2.8, is described by the Butler-Volmer equation:

$$i = i_0 [\exp ((b_{ox} F / RT)(E - Ecorr)) - \exp ((b_{red} F / RT)(E - Ecorr))$$

This current which can be measured as it flows through the external circuit is equivalent to the ionic flux across the electrode/electrolyte interface which is the sum of electric migration, diffusion, and convective terms, respectively:

$$N_j = -z_j u_j F c_j - D \nabla c_j + c_j V_f$$

The cell must, in any case, obey Ohm's law:

$$E = i A R = IR$$

The mass of the species oxidized or reduced at the electrode interface is proportional, according to Faraday's Lay, to the charge passed during period, t, of current flow, thus:

$$\Delta W = k \int_0^t i(t) A dt$$

$$\text{where, } k = M / nF$$

Finally, the efficiency, n, of the reaction process is defined as the ratio of the theoretical (Gibbs free energy) to actual (enthalpy change) charge passed:

$$n = \Delta G / \Delta H$$

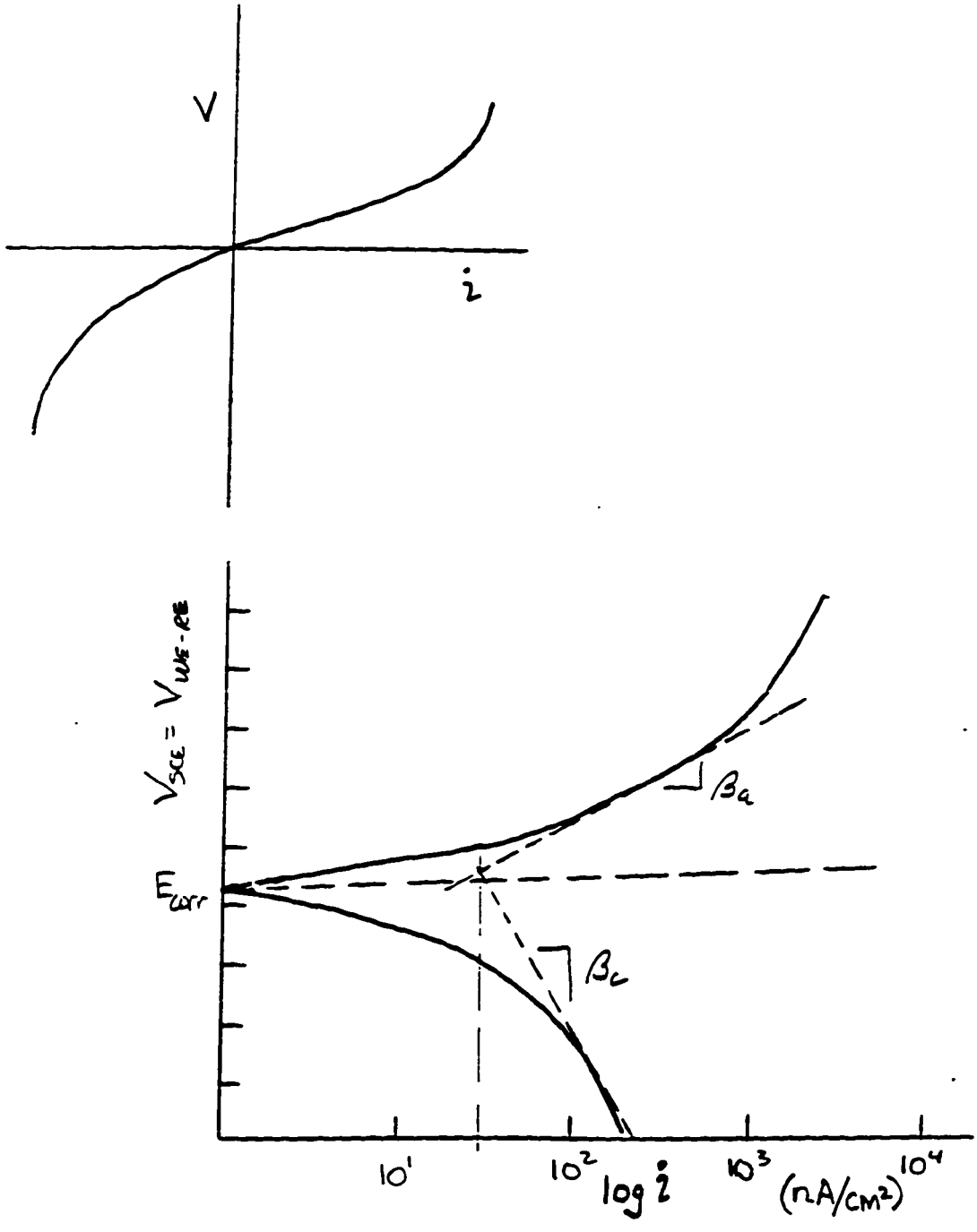

Figure 2.7. THE BUTLER-VOLMER equation describes the V-log i curve generated in the operation pictured in the previous figure

$$i = i_o [\exp(-\beta_a \Phi) - \exp(-\beta_c \Phi)]$$

where, i_o is the exchange current density, and the reaction driving force $\Phi = V_{SCE} - E_{corr}$; β_a and β_c anodic and cathodic Tafel constants, respectively.

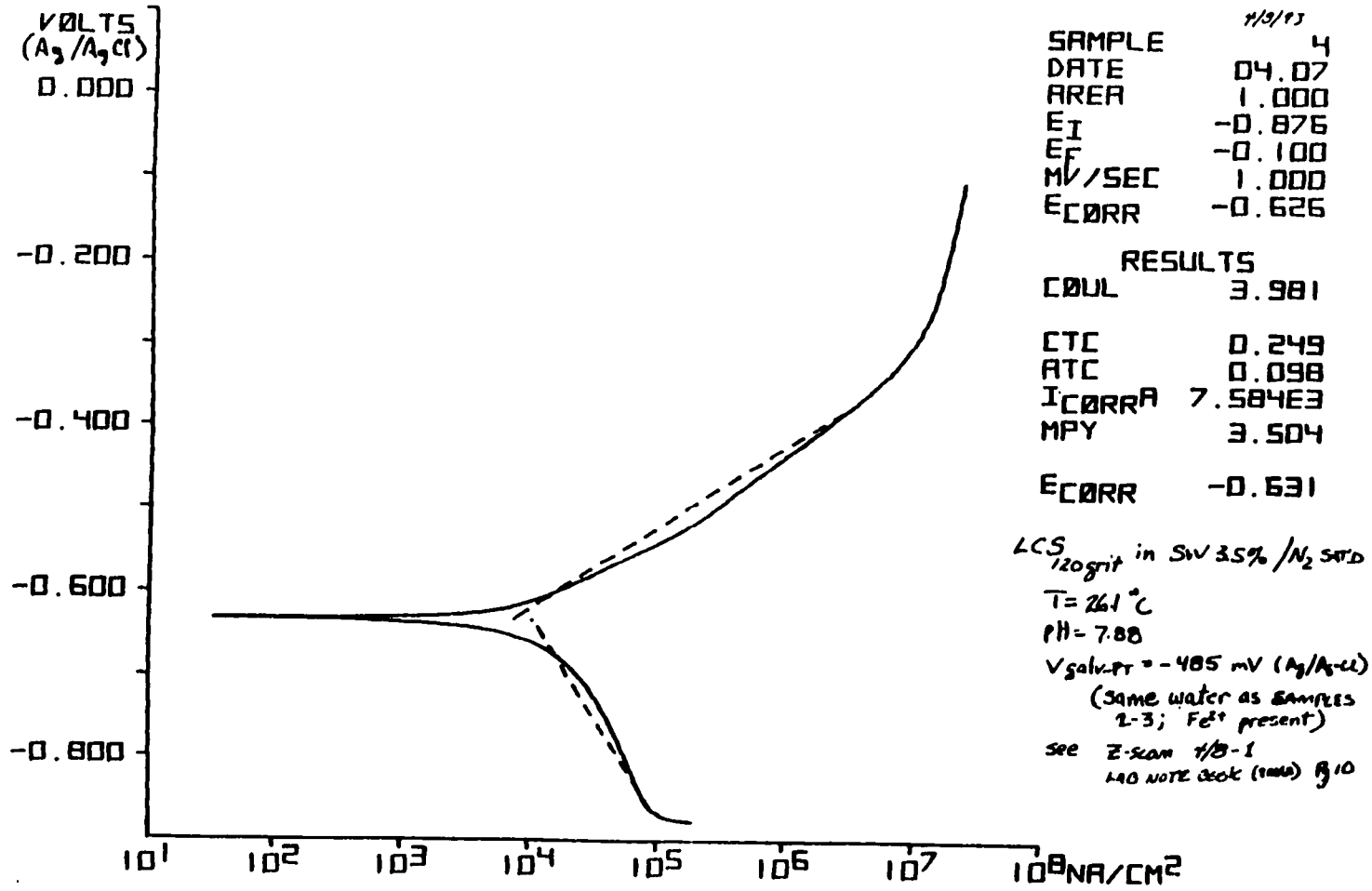

Figure 2.8. CORROSION RATE MEASUREMENT by the anodic polarization (AP)-Tafel intercept method, exemplified here by low carbon steel in seawater, using a silver-silver chloride reference electrode.

The equations noted here all describe the electrochemical interface in a state of equilibrium or near equilibrium as the system is gradually moved away from its initial equilibrium Ecorr, its measured response is largely independent of time. Perturbation study methods, to be discussed in Chapter 3, also start from the time-independent state [5]. The *dynamics* of the interface are not observed on the time scale of electrochemical equilibrium measurements. In measuring the polarization resistance, however, the slope, $\Delta E / \Delta i$, is noted to be a function of the rate at which ΔE ramp is performed. For more detailed discussions of electrochemical equilibrium, see references [1, 4-8]. Also, see Appendix G for details on voltmeter calibration and the interpretation of the sign of the measured potential. At this point, the dynamics of the interface and basis for the third interface measurement mentioned above, the electrochemical impedance, must be addressed.

CHAPTER 3

Perturbation Response and Relaxation in Electrochemical Systems

The strategy for electrochemical process optimization is based on the assumption that electrochemical systems have natural frequencies for cyclic operation which correspond to their controlling step or process relaxation time constants. The natural frequency of a physical system (and chemical systems can be described as statistical aggregates of micro-physical systems) is the preferred frequency of oscillation for that system following a perturbation about some equilibrium (or pseudo-steady-state operating) point. To sustain the oscillation, the perturbing force must be of sufficient amplitude and persistent at the right frequency to overcome the internal restoring and damping forces of the system.

The period corresponding to the natural frequency is the *relaxation time constant* of the system. The relaxation time or period is observable when the system is perturbed sufficiently to engage all of its internal restoring and dissipative forces but not to the point of becoming non-linear: any system hysteresis as a result of the perturbation should be negligible on the scale of the system. The initial state should be discernible even after indefinite repetitions of the perturbation. In this condition the system could be described as linear and dimensionally stable. The relaxation time is that period required by some rate determining characteristic or step such as a rate-determining reaction step. Relaxation time is the time required for initial conditions or dimensions or new steady-state conditions to attain following the system perturbation.

The characteristics of an electrochemical system which determine its response to a perturbation of the equilibrium of the electrode surface/electrolyte interface by an externally imposed electric field include:

(1) The electrode surface geometry (atomically smooth, electronically-conductive plain to rough, tortuous, insulative, diffusion barrier) and distribution of charge transfer sites; the heterogeneity of the surface (i.e. single crystal; few, fine grain boundaries; large grain boundaries; multi-phased).

(2) The nature, size, magnitude of charge, concentration, distribution, and mobilities of ionic and dipole species (and mean free path of motion) in the interface. Also, the number and extent of the reactions these species engage in both the interface and on the electrode surface.

(3) The state of thermal equilibrium at the interface: degree of convection due to thermal and/or density gradients at or in the vicinity of the interface.

(4) The degree of convection at the interface by electrode rotation or stirring.

The details of the foregoing will determine how the system will respond to and propagate a perturbation in the electric field across the interface. The interface response, shown in Figure 3.1a and b, is measurable in terms of:

(1) A voltage/current lag or phase angle (between the perturbing signal and the response).

(2) Applied voltage to measured change in potential and/or IR drop across the interface.

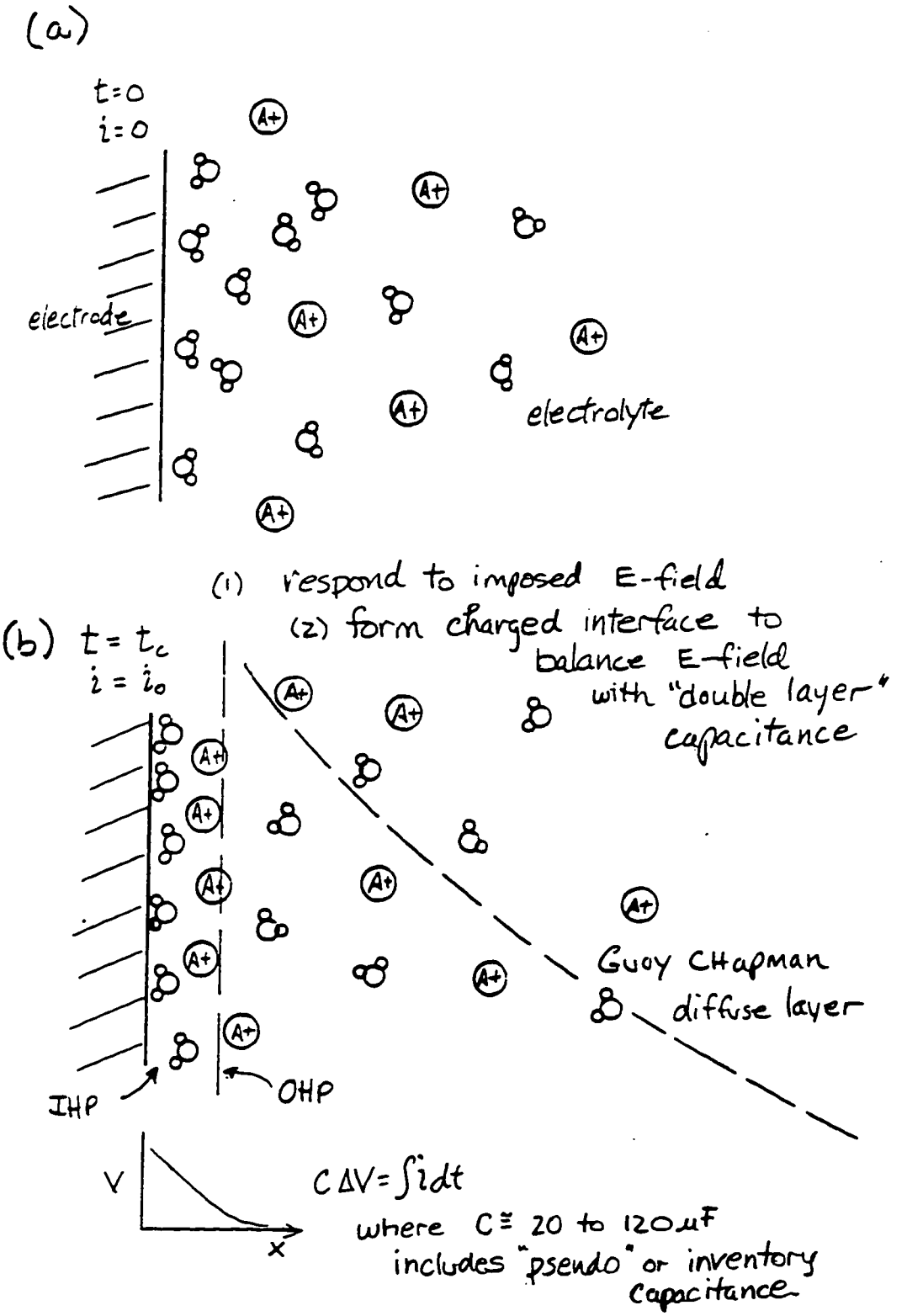

Figure 3.1. DYNAMIC BEHAVIOR OF THE INTERFACE: ion mobility and polar molecule orientation result in the electrolyte/electrode interface picture (a) before and (b) after the imposition of an electric field.

(3) A charging of the double layer as ionic electrolyte bordering electronic metal (or semi-conductor) lattice become opposing faces of a capacitor.

(4) Establishment of a diffusion layer thickness and concentration gradient of active charge transport species.

(5) Evolution of reaction products at a rate proportional to charge transfer across the interface (expressed as exchange current density).

(6) A characteristic deBye-Huckle length [5] for the diffuse charge density of the system of interest.

(7) Accumulation of reaction intermediaries and products and occupation of active electrode surface sites constituting a *pseudo-capacitance*, which may contribute significantly in combination with the double layer capacitance (3) in producing the total capacitive reactance of the interface.

The end point of the (interface) electric field perturbation is a fully charged, polarized interface with an increasing tendency to *leak charge*, i.e. pass net current (via the external circuit) by means of actual charge transfer (of electrons) across the electronic/ionic boundary. The charge transfer mechanism is a quantum mechanic event, the tunneling of an electron from an ion at (or very near, within angstroms of) an active metal (or semi-conductor) surface site into the electronic conduction band of the solid phase lattice, (or vice verse, from metal to electrolyte species).

The positioning of the ion, which was most likely fully hydrated (wrapped in an envelope of water or other solvent molecules), may have been the slowest in a series of

transport and intermediary reaction steps, but this last step, actual electron transfer, is surely very fast.

The charge transfer step, while not controlling in the timing sense, is the crux of an electrochemical process: it permits the equilibration of external EMF's and internal Gibbs free energies across the interface. It brings into play the bipolar nature of the process. It is not a single isolated heterogeneous reaction surface, but two sets of complimentary (oxidation-reduction) reactions at two interfaces connected by an external, electronically conducting circuit. The electrical circuit laws of Ohm, Faraday, and Kirchoff must all be satisfied:

(1) Ohm: $E = IR$

(2) Faraday: $G_j = n F E_j$

The Gibb's free energy (thermodynamic statement of Faraday's Law) for a given reaction at the interface is equivalent to the magnitude of the charge transferred and the emf (over-potential) at the interface of exchange.

(3) Kirchoff, First Law: $(\text{sum}) E_j = 0$

The sum of all the EMF's must be zero around any complete (closed) circuit.

A fourth law is invoked by the response of the two (electronically connected) interfaces to a perturbation in the electric field,

(4) Le Chatlier's principle:

The system will react in such a way as to oppose any change exerted upon it by external forces, in order to restore itself to its initial condition.

A primary restoring force in the electrochemical system is the establishment of concentration gradients of the active species in the interfacial region of the electrolyte. This is concentration polarization.

Other factors which must be overcome and balanced with the propagation of the perturbing electric field include:

1) dipole moment reorientation,

2) ionic charge distribution in the electrolyte (coulombic forces) which constitute attractive and repulsive forces, and

3) existing convection due to balancing of gravitational and thermal effects constitute inertial forces in the initial state of the system,

all react to oppose and balance the perturbation to the system.

In the balancing process, the foregoing laws are satisfied. The sign of the sum of the free energies, G_j's at the two interfaces will indicate whether and in which direction there is a spontaneous (if the sum is negative) net reaction upon the establishment of an external circuit between the two interfaces with a resulting electric field, or, that a reaction proceeds only if the external circuit includes an externally imposed EMF (battery, generator, etc.). (The external circuit being an electronically conductive path between two active, complimentary, reaction sites on a single electrode surface, or, an actual external path, wire, between to separate electrodes.)

In any case, the sum of the external EMF's, interfacial "over-potentials",

$$\sum E_j = \sum G_j/nF ,$$

the external circuit IR (current x resistance) (voltage) drops, and electrolyte (ionic flux x electrolyte resistance) drops is zero, $\sum E(i) = 0$, satisfying Kirchoff's law, an electrical equivalent of the equilibrium state in a balanced, Newtonian mechanical system, where:

$$\sum F_j = 0$$

While the zero-sum of forces always exists, the attainment of the final values in the equation is not instantaneous. The perturbation is initiated, grows, to some maximum value, propagates; all the while, the opposing, balancing forces grow in the complex system dimensions described above, establish, and, when the external circuit is opened (perturbing force ceases), relax. Figure 3.2 shows the progress in time at the interface as the *leaking charge* and charge transfer results in a changing concentration gradient in electroactive species acting in accordance with Fick's law of diffusion. The interface response occurs, however, slowly or rapidly, in finite time.

The time required to impose a perturbation, and relax, is the system *relaxation time*, or *time constant*. The system modulus (ratio of forcing to response function) is dependent on the rate of perturbation. In a mechanical system, the measured response to a perturbation is a function of stiffness, which depends on material modulus and section geometry. The relaxation time will depend on shape (or wave form), amplitude and frequency of the perturbation function. Figure 3.3 illustrates an effect due to the amplitude of the perturbation in relation to the asymmetry of the system about its equilibrium point. Faradaic rectification as illustrated here, would not be frequency dependent.

A metallurgical wire *torsional pendulum* specimen provides, by way of analogy, a good example of the relationship between a material (or interface) modulus and the

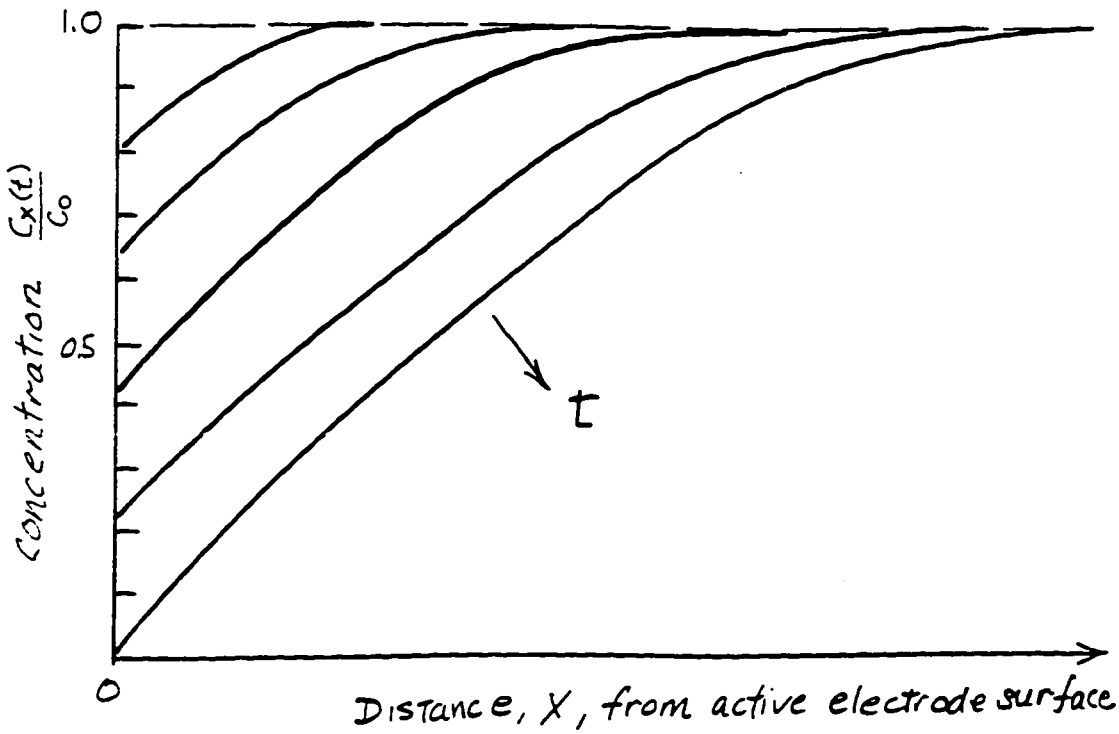

Figure 3.2. FICK'S SECOND LAW is a basis for time-dependent behavior of the electrochemical interface:

$$C_A: \quad A + e^- \rightarrow R$$

C_o = bulk concentration of electroactive species

$C_x(t)$ = concentration of electroactive species at a distance x from electrode surface

$$\frac{\partial C(x)}{\partial t} = D\nabla^2 C(x)$$

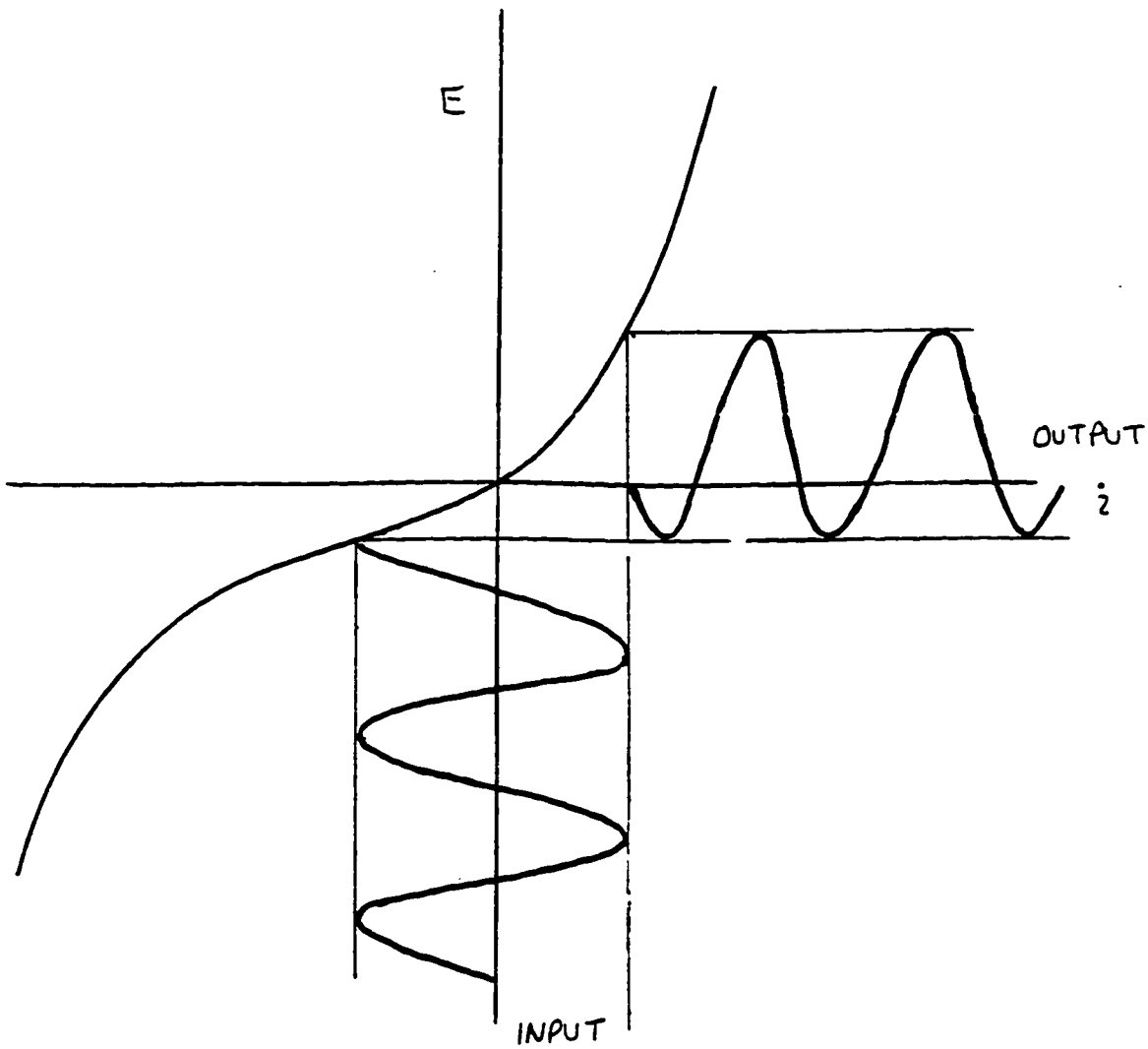

Figure 3.3. FARADAIC RECTIFICATION, asymmetric output from symmetric input, results from nonlinearity of the i vs V polarization curve. Note that the effect would not vary with frequency.

relaxation time for a rate controlling internal material process. The wire torsional pendulum is used to determine the diffusion constant of interstitial atoms moving through the metal lattice. In this system the primary dimension of perturbation is the lattice parameter which is worked (expanded, contracted) in a periodic fashion as the wire twists and untwists with a perturbing torque acting against the restoring force proportional to the torsional modulus of elasticity of the wire. The preferred period of oscillation corresponds to the time required for mobile interstitials to make the move from one interstitial lattice site to the next, in a succession of jumps. This interstitial movement time, or jump frequency, is a measure of the diffusion constant.

The period of oscillation at the natural, or minimum stiffness, of the wire is a measure of the controlling step, the movement of the interstitials. The natural frequency for the pendulum occurs midway between low frequencies dominated by the fully relaxed modulus, (time for anelastic processes to take place) and high frequencies dominated by the unrelaxed modulus (no time for anelastic processes) [7]. This is the frequency for which the energy lost to total energy ratio is a maximum.

In an electrical system the modulus is the complex impedance function $Z=V(t)/i(t)$ which consists of real (ohmic resistance) and imaginary (capacitive or inductive reactance) components. Figure 3.4 (a, b, c) illustrates the time dependent nature of the interface modulus and work. Electrochemical Impedance Spectroscopy (EIS) measures the complex impedance (resistance, reactance) response spectrum of an electrochemical interface to a specified range in frequency and amplitude of voltage (or current) perturbations, about a specified equilibrium potential of the interface. The response spectrum is characteristic of the set of reactions occurring across the interface at the specified potential, [3, 4].

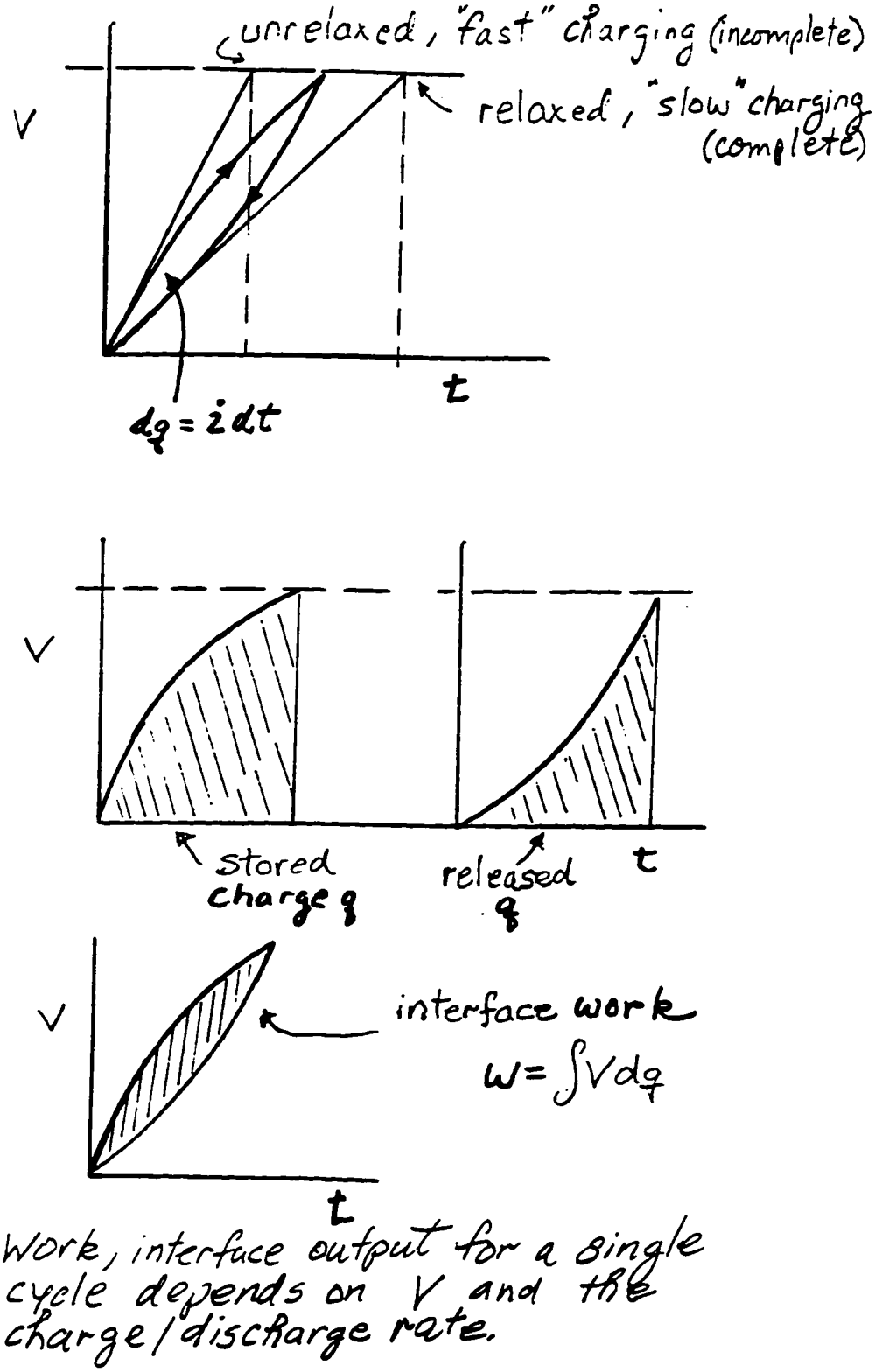

Figure 3.4a. THE INTERFACE TIME-DEPENDENT BEHAVIOUR capacitive (charge-discharge), is analogous to material anelastic processes.

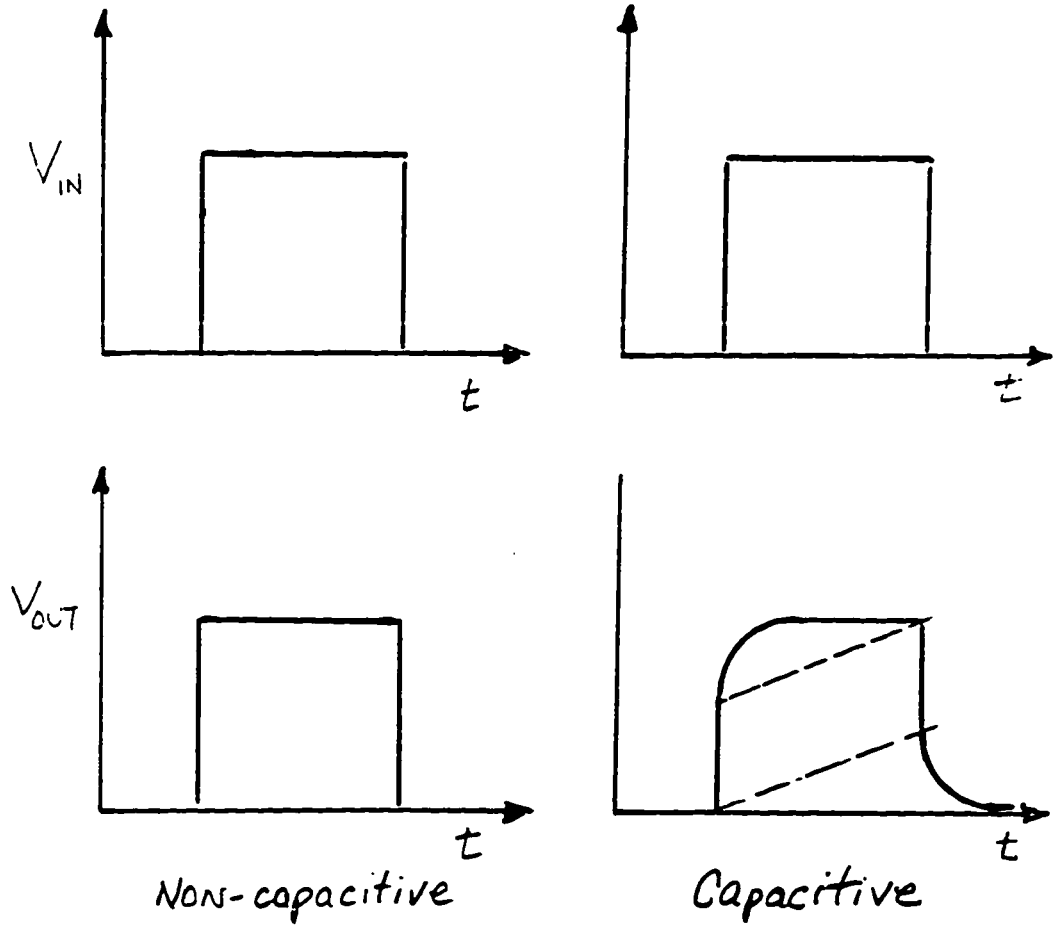

Figure 3.4b. TIME DEPENDENT VOLTAGE RESPONSE across a non-capacitive (elastic) interface compared to capacitive (anelastic, energy-storing) interface. (Charge is stored in double layer and chemical inventory.)

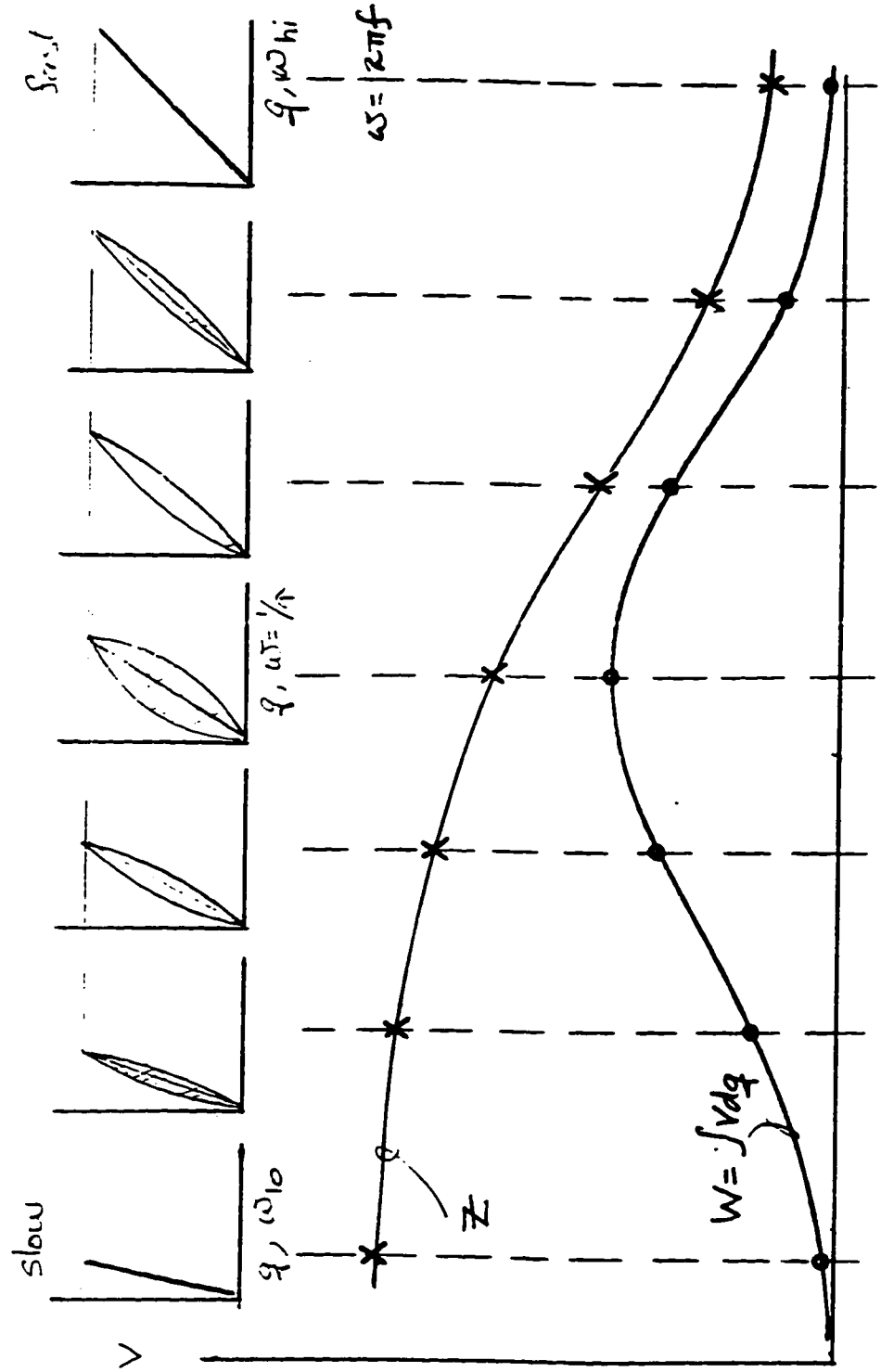

Figure 3.4c. IMPEDANCE OF THE INTERFACE MODULUS, Z = V/I.
The maximum interface work occurs where $f = 1/t_r$

The interfacial reactions and all the processes discussed above are reflected in the impedance spectrum in the magnitude (of real, ohmic, or *imaginary*, reactive impedance) and in the phase angle (between the perturbing signal and the interface response voltage/current).

In particular, the resistance to the charge transfer step across the over-potential of the interface, referred to as the *polarization resistance*, R_p, can be determined. For a given electrode equilibrium potential, the charge transfer reactions between the interfacial species and the electrode surface proceed at a rate proportional to the exchange current density. In accordance with Ohm's law, the current is inversely related to the resistance across the interface, such that

$$I_0 = B / R_p$$

The Faradaic current density measure of reaction rate is the object of many conventional electrochemical experimental methods:

(1) The anodic (or cathodic) polarization/Tafel intercept method, based on the mixed potential theory derived by Stern and Geary (wherein a projection is made on a log i vs. E plot from a near-linear portion of the high field region of the exponential polarization curve to the current at the intercept with the equilibrium potential).

(2) The exchange current is computed from a measurement of R_p which is the slope of the dE/dI curve very close to the equilibrium potential, E_{corr}.

Both (1) and (2) are essentially dc methods. A third method utilizes small amplitude ac perturbation, ac impedance or EIS scans of the frequency range from near dc (10 mHz or less) into mid audio frequencies (10 kHz or higher). It is found that

$$R_p = |Z|_{\omega=0} - |Z|_{\omega=\infty}$$

Experiments run with a Princeton Applied Research (PAR) 350 corrosion measurement instrument utilizing the AP/Tafel intercept method compare quite well with results obtained from ac impedance scans run on a Schlumberger 1260, frequency response analyzer (FRA).

As a measuring technique, the ac impedance spectroscopy has several advantages over the dc methods:

1) Minimal perturbation of the system from equilibrium ensures the condition of linearity.

2) The electrolyte resistance is readily distinguishable from the polarization resistance.

3) The capacitive properties of the interface are measurable.

4) Electrode surface film and diffusion barrier effects can be measured.

ac measurements reveal the intrinsic time-dependent nature of the system. Analogous to the torsional measurement on metallurgical specimens pendulum discussed earlier, ac instrumentation can measure the anelasticity of the electrochemical system; the interfacial properties, which are time-dependent and have relaxation time constants, are quantifiable.

In impedance spectrum measurements, the low frequency impedance value, $|Z|_{\omega=0}$, corresponds to the fully *relaxed* modulus, M_r, of the mechanical system; while the high frequency value, $|Z|_{\omega=\infty}$, is the *unrelaxed* modulus, M_u.

The simplest description of the time dependent mechanism behind the behavior of the electrochemical impedance scan is the Randles equivalent, R-C, circuit model [10]. In this simplest case, the R_S, series resistor corresponds to the solution (electrolyte) resistance; while the parallel resistor, R_p, is the polarization resistance and the parallel

capacitor element, C, corresponds to the interfacial "double layer" capacitance (typically 15 to 40 μf). Many systems actually conform quite nicely to this simple model.

Other more complicated systems involving multiple reactions and time constants and/or diffusion barrier porous film electrodes call for the addition of more R-C parallel elements and/or Warburg (diffusion) impedance elements [11]. Still more complex circuits are derived from network element transmission line models. It is possible to design equivalent circuits for the fractal response of a rough-surface electrode which exhibit a characteristic 1/f noise response to perturbation.

Equivalent circuit models, however, do not uniquely identify a particular system. Not all researchers find them the best way to model the time dependent characteristics of a system. (Some prefer more direct identification of electrochemical mechanisms and associated rate constants [3].)

Taking the modeling a step further draws on the analogy between a mechanical lumped mass (restoring, viscous damping, and inertial terms included) and the electrical R-L-C circuit where the L is an inductor (an electrical "inertial" element). These elements in both systems may be in parallel or series, depending on whether "through" or "across" variables are "driving force" or "displacement". This approach can be extended to the electrochemical interface, given that the flux, J, is a "displacement" (rate of charge displacement) variable analogous to x (length) in the mechanical and i, current, in the electrical system. It would appear that, J' (the temporal derivative of the flux) corresponds to an inertial type term, possibly related to the rate of change of $\Delta C(x)$, the interfacial concentration gradient...(or ion convection current/electrical field interaction). In any case, the 'L' term introduces a special property into the system of interest: the possibility of resonance.

All the foregoing models are readily subject to some form of frequency response analysis, EIS; electrical, and electrochemical response, directly measured as a function of

frequency. The results are plotted in Nyquist, complex phase diagram, (real vs. imaginary impedance components) or Bode (frequency vs. impedance magnitude and phase angle) format. Information revealed in these plots includes:

1) the moduli (Z_{lo}, and Z_{hi}) at the extremes of the frequency spectrum, which give the polarization resistance value, R_p ,

2) the maximum phase shift angle, θ , a measure of lag between the perturbing force and responding displacement, and

3) the corresponding maximum quality factor, Q.

The last two quantities, (2) and (3), occur at the frequency of the maximum fractional energy lost. This is analogous to the logarithmic decrement damping of the wire pendulum. The reciprocal of this frequency is the relaxation time constant t_r for the process. The relaxation time constant corresponds to the frequency at which the anelastic properties are *fully engaged.*

EIS Bode plot data identifies frequencies at which impedance decreases most dramatically, rolls off; the Nyquist plot data shows at what frequencies the impedance is purely ohmic and what frequencies the impedance is reactive (capacitive or inductive). A process operating at a frequency dominated by ohmic impedance would be nearly charge transfer or activation controlled as opposed to a capacitance dominated frequency which would indicate diffusion or double layer charging control. The initial expectation is that the impedance roll-off (in the Bode plot of an impedance plot) occurs at the frequency most nearly synchronized with the natural relaxation time of the dominant reaction or step of the process. This is the frequency that is most likely a natural balance point for competing reactions involved in the overall process as well. There may be a problem in operating the process at this frequency in that the voltage (or current) perturbation used in the test scans is very small and what actually occurs at a practical operating level of voltage is considerably different.

CHAPTER 4

PCE Measurement of Electrochemical Cell Mass-Flux Response

Certain crystalline materials, barium titanate and quartz among them, are excellent electro-mechanical transducers. Due to an asymmetric charge distribution, the dipole moments and resulting electrical fields of these materials are altered in proportion to the mechanical stresses on the unit cells and, visa versa, the mechanical stresses are in proportion to the surrounding electrical field strength. Crystals with this *piezoelectric* property readily convert mechanical to electrical and electrical to mechanical energy; acoustic waves to electrical and visa versa [1]. They have found wide application in acoustics as sonar transducers. Piezoelectric materials illustrate the case where the balancing of perturbing and restoring forces result in sustained oscillations.

Piezoelectric crystals have also found use as nano-balances because their fundamental frequency of oscillation is very sensitive to changes in the mass on the surface of the crystal. They have been used in vapor deposition for some time as indicators of the amount of material condensing on surfaces in a target area.

More recently piezoelectric crystal sensitivity to surface mass loading has been applied to the liquid phase as well. Metallic tabs or flags plated on either side of a quartz crystal wafer support an alternating electric field across the thickness of the crystal. A specially designed oscillator circuit with an automatic gain controls the electric field and excites the crystal in such a way as to allow it to oscillate at its own natural frequency but at a constant amplitude. If one face of the crystal is sealed into an electrochemical cell, its

flag exposed to the cell electrolyte and connected in the cell external circuit, it becomes an electrode in the cell, a *piezoelectric crystal electrode* or PCE.

Typically quartz crystals used as PCE's are AT cut wafers approximately one half inch in diameter and about 10 mils thick. The fundamental frequency of oscillation for these crystals is typically one, two, five, ten, or twenty megahertz. As long as the surface mass change does not produce a shift in the fundamental frequency more than one to two percent of the initial value, the PCE response to an increase or decrease in surface mass loading is a linear change in the crystal's fundamental frequency of oscillation which, as shown in Figure 4.1, can be very accurately monitored (to 0.1 hertz in 1Mhz). A sensitivity factor can be determined experimentally to calibrate the PCE accurately. The surface mass (areal density) change is expressed as the Sauerbrey equation:

$$\Delta m = -S\,\Delta f_0,$$

where S is the sensitivity factor for the monitored crystal, and Δm is the areal density (g/cm^2).

Hence, the negative temporal derivative of the fundamental frequency, df_0/dt, is directly proportional to the mass flux response of the PCE to the electrochemical cell. The PCE adds mass flux to the conventionally monitored electrochemical cell current and working electrode potential. Figures 4.2 and 4.3 show the relation between df_0/dt and the copper electrodeposit and iron dissolution current, respectively. Not all charge transfer reactions result in surface mass changes. For dissolution or deposition reactions, the current is directly proportional to the mass flux. This is simply the temporal derivative of Faraday's Law,

$$dm/dt = Ki_m = -S\,df_0/dt$$

where, K=M/nF is the electrochemical equivalent constant for the reaction in question and i_m is the corresponding electrode reaction current density.

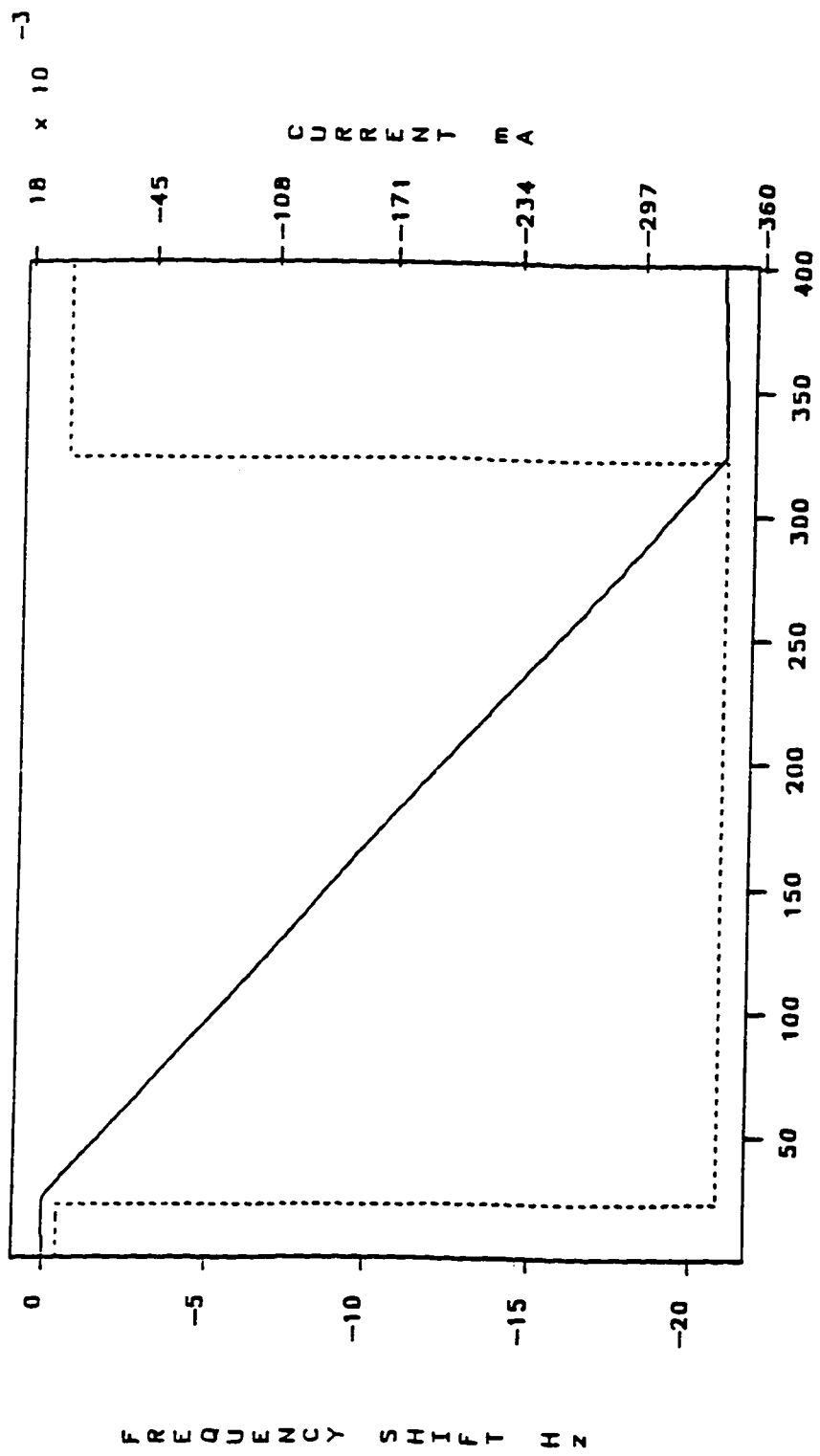

Figure 4.1. THE PCE FREQUENCY SHIFT AND CATHODIC CURRENT as a function of time for a 250 mil electrode during dc Plating in 0.1 N $CuSO_4$/ 0.01 N H_2SO_4/ 0.21 N Na_2SO_4, [2].

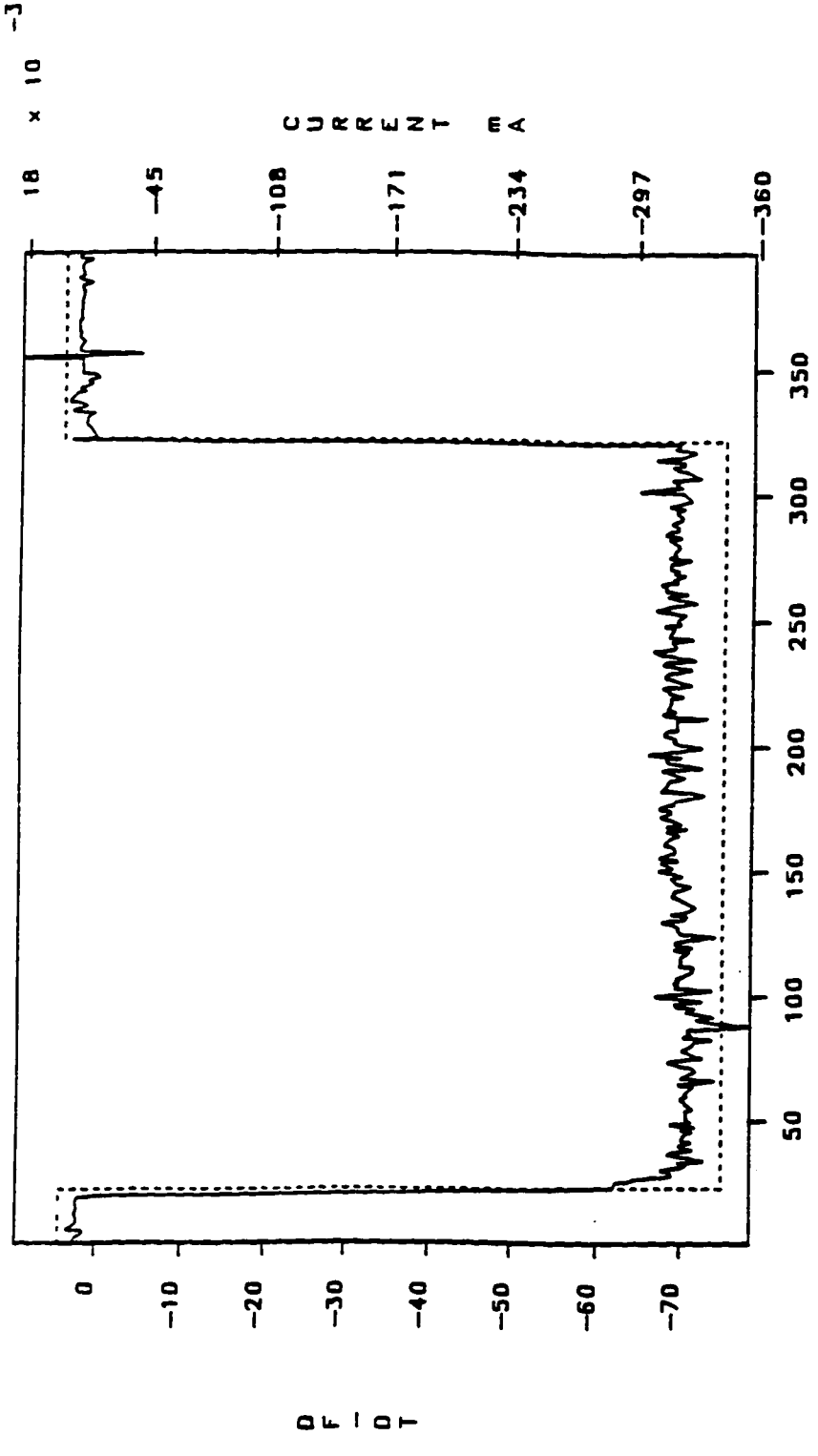

Figure 4.2 THE PCE TEMPORAL DERIVATIVE AND CATHODIC CURRENT VERSUS TIME for dc copper plating on a 250 mil electrode in 0.1 N $CuSO_4$/ 0.01 N H_2SO_4/ 0.21 N Na_2SO_4, [2].

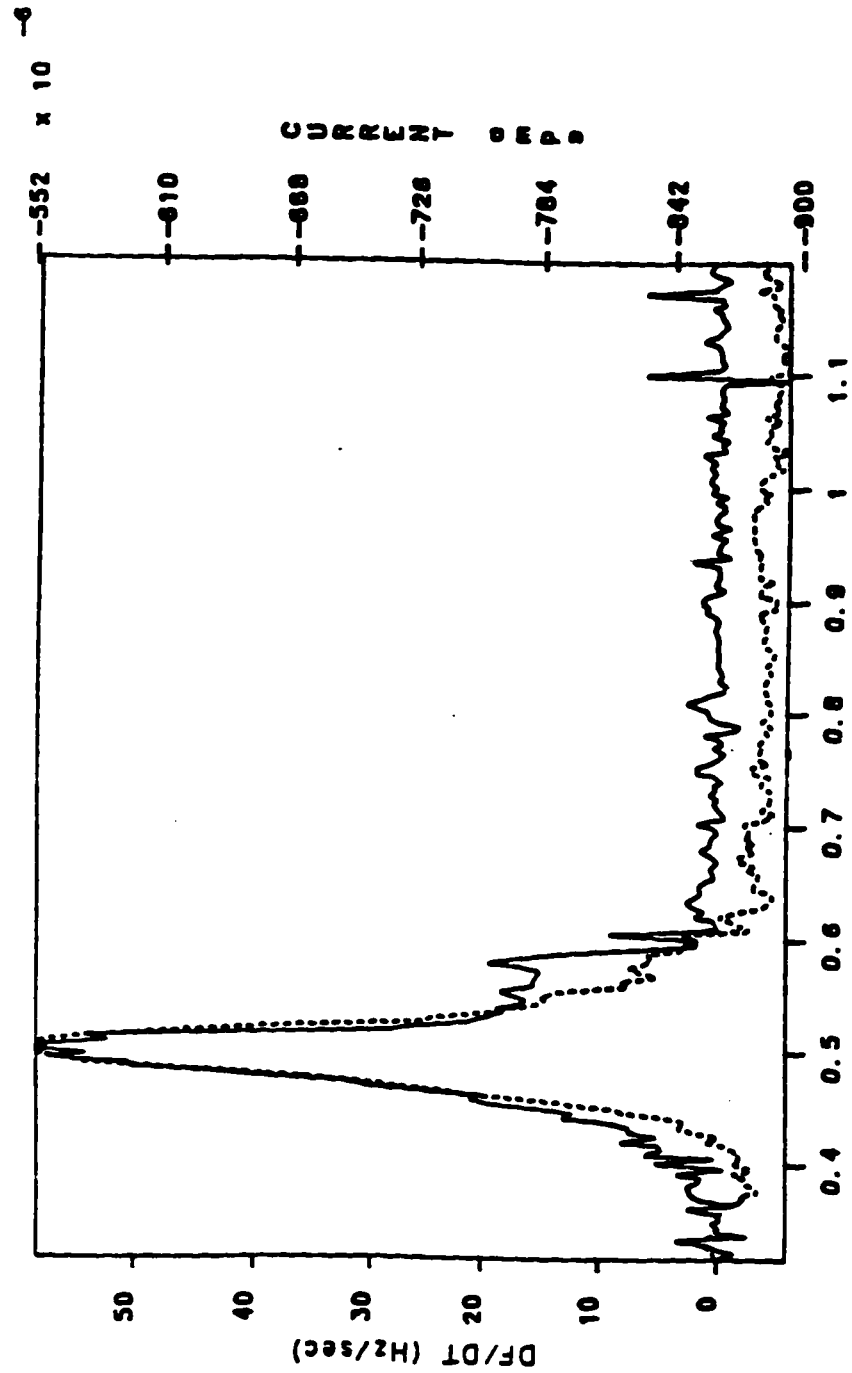

Figure 4.3. THE PCE TEMPORAL FREQUENCY DERIVATIVE (solid line) AND CELL CURRENT (dashed line) VS. POTENTIAL during the linear potentiodynamic sweep for ron plated at 400 mA/cm^2 on a 5 Mhz PC: the dissolution range, [4].

The monitored cell current meanwhile is the sum of all the cell reaction current densities multiplied by their respective active reaction surface areas,

$$I_{cell} = \Sigma_{k=1.n}[i_k A_k]$$

Direct mass flux measurement permits the resolution of cell current due to two or more reactions at the working electrode (PCE). In metal deposition processes, which may also be accompanied by hydrogen reduction, the amount of current contributing to the metal deposition will be measured as mass flux, that portion going to hydrogen reduction will be the difference,

$$I_H = I_{cell} - I_m$$

Ideally, in metal electrodeposition, the hydrogen current is eliminated or kept to a bare minimum, by whatever means practical.

Work by numerous researchers over the past decade verifies the effectiveness of the PCE as an analytical method in electrochemistry, [6, 7]. Typically a surface mass loss or gain of fractions of a monolayer is detectable. Hager [4] analyzed the dissolution and passivation of iron during anodic polarization in sodium sulfate solutions, clearly demonstrating the correlation between the time derivative of the PCE fundamental frequency change and cell current. Buehler [2] demonstrated the application of a fast data acquisition PCE system to the study of the pulse plating of copper. The real time mass flux for a single pulse was successfully recorded along with the applied pulse potential and cell current on a time scale of microseconds.

There were several significant results of Buehler's work. Mass-flux data make possible the computation of mass-to-charge ratios for corresponding electrochemical reactions. Resolving these data for a single pulse (5 to 20 msec duration, galvanically controlled) made it possible to measure the efficiency of the pulse for comparison with

pulses of different duration and current density. This charge to mass ratio efficiency may be a very useful *figure of merit* in designing an optimal pulsed schedule.

Equally interesting in the resolved pulse data was the *current off* period during which the mass flux decayed in an exponential manner. Reaction parameters used to fit the decay curve supported a two-step reaction mechanism and gave strong indication as to which was the rate controlling step. This information is of further use in arriving at the duty cycle and pulse spacing for an optimal cycle.

The curve fit appears to be satisfactory, but does it account for all the processes that are represented in the resolved pulse data? The model assumes the response of the PCE to be due entirely to reaction kinetics at the interface during the decay curve immediately following the actual current pulse. In fact the initial response of the PCE at the very beginning of the pulse appears to be fluid dynamic rather than kinetic. There is an initial *increase* in crystal frequency which would be due to either mass loss (rather than the expected mass accretion) or a decrease in the fluid viscosity at the interface.

The processes in the interface immediately before, during, and after the current pulse are not only kinetic but electrosterric, diffusional, hydrodynamic, and convective as well. The charging of the double layer is rapid but not instantaneous and depends on the electrical field strength and the nature of the species at the interface. The reaction is dependent on (although not necessarily controlled by) the diffusion of reactive species to and from the reaction interface. Time is required to establish a concentration gradient in the species reacting at the interface and there is a characteristic relaxation time associated with the decay of the gradient immediately after the current pulse even if the reaction itself ceased immediately. No current, no excess of electrons at the interface, no charge transfer, no more reaction; but, the excess (or inventory) of participating species in the

concentration gradient would persist, however briefly, into the post-pulse, current-off period. The frequency of the PCE is dependent upon the density-viscosity product of the fluid in the interface which, in turn, is determined by the concentrations of the species in the interface. Thus the establishment of a concentration gradient has a hydrodynamic effect. Furthermore, the PCE's own oscillatory motions might have a convective effect on the species moving to and from the interface.

Recent work by Ivanov and Yelon [12] shows that the accuracy of the Sauerbrey model for calculating changes in deposited crystal film mass (areal density) breaks down for thick films. Their work with 1 micron thick films of aluminum, lithium, and nickel on 6Mhz AT-cut quartz crystals showed that, unless the film and quartz acoustic impedances are very closely matched (as is the case for Al), the *acoustic wave model* must be used to compute a composite quartz/film fundamental frequency and subsequent mass changes.

The PCE oscillates at a fundamental resonant frequency precisely because it possesses balanced capacitive and inductive properties (as seen in the Butterworth model). As discussed earlier the fundamental frequency varies linearly with the surface areal density of mass loading making it a natural micro-dynamic scale. This property is exploited by the PCE *in situ* measurements to obtain mass-to-charge ratios which, in pulsed plating experiments as conducted by Buehler (1986) [2] reveal the efficiency of individual pulses of given duration and current density. Also indicated by these experiments are rate controlling step and interface concentration gradient relaxation times.

CHAPTER 5

Electrode Surface Condition Effects on EIS and PCE Responses

A true atomically smooth plain is difficult if not impossible to achieve over any substantial surface area even on the surface of a single crystal let alone the surface of a polycrystalline material. While the thermodynamic equilibrium potential Ecorr discussed in Chapter 2 is not directly affected by the geometry of the solid/liquid interface, the kinetics of the reactions and supporting processes occurring at the interface will very likely be affected. The simplest description of the macroscopically, uniform, plain solid (electrode)/liquid (electrolyte) interface is *roughness*. Roughness is a relative measure best expressed as the final degree of mechanical finish used to prepare the surface: a course 120 grit, a finer 600 grit, on down to 0.1 micron (or finer) finish. Surface roughness can be expected to effect *all* solid/liquid interface interactions: added or trapped (fluid) mass, convection, double layer thickness and, hence, diffusion. Roughness determines the actual surface area and hence the number of reaction sites. Electrically, roughness determines the actual capacitance of the interface, the *double layer*. All of which underscores the importance of consistency in electrode surface preparation techniques in conducting electrochemical experiments. Uncontrolled surface variations can mask variations due to other parameters or produce effects which are inaccurately attributed to controlled parameters.

Surface roughness calls into question two of the important new techniques discussed. It is reasonable to expect that both EIS and PCE techniques will be sensitive to electrode surface conditions. These techniques could therefore lead to erroneous conclusions especially in electrochemical deposition or dissolution which can result in

substantial surface roughness changes over the course of an experiment. It then becomes increasingly difficult to decouple electrochemical reaction mechanism effects from mass transport and solid surface/liquid fluid dynamic interactions as the electrode surface is altered from its initial prepared, *known* condition. In applications using these techniques to determine reaction kinetics, mechanisms, and rate determining steps, they must be applied only briefly and to freshly prepared surfaces.

Ibl [3] suggests comparing diffusion layer thickness with surface asperity height. Thirsk [2] gives a simple relationship based on the thickness of the Nernst diffusion layer compared with the surface dimension parameter. Roughness effects become important for diffusion controlled reactions when :

$$D\,t / b^2 \ll 1 \text{ , where } b = \text{surface roughness height}$$

For example, a copper deposition / dissolution reaction on a surface with a 1 μm finish ($b=10^{-4}$ cm) and $D_{Cu} = 7.6 \times 10^{-6}$ cm^2 / sec, roughness becomes a factor if the time scale of the process is $t \ll 1.32 \times 10^{-3}$ seconds or at a frequency of 760 hz; for $b=10\mu m$, the critical frequency drops to 7.6 hz. These frequencies are within the range of frequency analyzed by the EIS technique.

To the extent that EIS and PCE techniques are surface sensitive, they might be useful in observing electrode surface changes. Work has been reported on surface sensitivities of both techniques. The constant phase element response of EIS to some electrochemical interfaces suggests that some electrode/ electrolyte interfaces are fractal. Liu [5] used a Cantor bar structure to model the interface and show that a fractal dimension could be calculated. It is important to note whether such a model would work as well for activation controlled as for diffusion controlled processes at such an interface.

Bates [6], however, argued that the fractal electrochemical interface model could not be verified experimentally.

Fractal or not the sensitivity of EIS to surface roughness variations could be experimentally verified. A standard flat, 5/8 inch diameter (PAR K47) cell specimen of low carbon steel can be easily tested sequentially at three different surface polish conditions, say: 120, 400, and 600 in the same electrolyte solution, 3% NaCl (or sea salt) at STP. The same specimen is resurfaced for each test from course (120) to fine (600). Then, as a check on reproducibility, the sample is resurfaced to the course condition and retested. The resulting EIS scans (Bode plots of 0.1 to 10kHz at 5mV) are compared for variations. If substantial variations are noted along with identical scans for the same surface condition, additional tests could be run at finer grades of polish and on different materials, stainless steel, and bronze. Some tests could be run on electrochemically etched specimens as well using AC and DC etch schedules and comparing the results. It has been known for decades that AC produces a more uniform etch than DC. Can the differences be detected by variations in EIS scans? Tests of this type should also be done on pure metals iron, copper, aluminum as well as the alloys mentioned above.

The PCE is sensitive to surface roughness because the extent of hydrodynamic coupling is dependent upon the degree of fluid trapping which occurs at the interface. The greater the roughness, the greater the trapping. Finish is usually not an important variable in PCE experiments as the surface condition is determined by the method of metal deposition: either vapor or electrochemical deposition on the PCE specimen flag substrate. The deposited test metal surface is then either accreted or dissolved depending on the experiment and the hydrodynamic coupling can be ignored so long as the surface

roughness is assumed to remain nearly constant. For experiments of short duration, this assumption of near constant roughness is reasonable.

Schumackar, et. al.[1], however, give a quantitative description of the degree of fluid trapping and use the PCE as a roughness gauge. This suggests some follow-up work to the AC/DC etch experiments suggested above. The same etch schedule variations could be used on PCE specimens and compared with the EIS results. Indeed EIS scans could be made on the PCE specimens themselves to see if surface roughness can be resolved. The PCE apparatus reported by Simpson [4] has an automatic gain control (AGC) to maintain the crystal oscillations at constant amplitude. The gain level, which is really a measure of energy required to maintain the oscillation amplitude, will be proportional to fluid trapping at the interface, roughness. The AGC can be monitored along with frequency to give an indication of roughness variability.

Critical frequency calculations, noted above, indicate that electrode surface roughness must be judiciously taken into account. Depending on the approach taken, the roughness sensitivity of EIS and PCE techniques can interfere with, or mask other parameters of interest, or add useful information to the data base. Compared to other factors in the experiments to be conducted, roughness may not play a measurable role, especially if the roughness is constant throughout the experiment.

CHAPTER 6

A Cyclic-Process Optimization Approach

In the previous chapters, the motivation for finding an optimum process cycle design, has been established. Even a small improvement in process efficiency can make it economically practical or improve its profitability. Many processes of commercial value which are presently conducted in a steady state (dc) mode [19], would very likely yield better results if they were conducted in a cyclic (ac) mode. Some of the work done (1952-1977) to apply cyclic operation to conventional chemical separation process equipment (for distillation and liquid-liquid extraction) is described in references [1-4]. The reported results were increased output, efficiency, and/or enhanced selectivity for the desired product.

More recently, considerable work has been devoted to exploring the application of cyclic operation (as av or ac, periodically controlled potential, or pulsed current, PC) to electrochemical processes. The focus of this study is on electrochemical processes and on the use of certain electrochemical techniques (EIS and PCE), the fundamentals of which have been reviewed previously, as methods of obtaining cycle optimizing information on process for the electro-deposition and -dissolution of metals in particular. References [5-8] explore the application of pulsed plating with particular interest in its applicability to the printed circuited board industry. Berube and Piron [9] investigated the advantages of pulsed reversed current (PRC) in zinc electrowinning which may have implications for the recycling of zinc galvanizing. Other applications of cyclic current control may help prevent unwanted metal dissolution due to corrosion; references [10, 11] report the application of pulsed current to cathodic protection in deep well casings. References [12-

15] describe work applying cyclic current or potential control to the modification or preparation of metal surfaces as in metal etching or passivation.

A complete description of an electrochemical process candidate for optimization would include: the cathodic and anodic reactions and reaction mechanism steps; reaction overpotentials, Tafel constants, and cell working electrode open circuit potential (Ecorr); the optimal pH (for each reaction), temperature range; reaction species concentrations and solubility products and diffusion coefficients; electrolyte solution resistivity and support requirements; the controlling or rate determining reaction and step, whether or not the key reactions are activation or diffusion limited and the limiting current density; also, what by-products are likely, such as hydrogen; and, for some systems, whether or not oscillations and perhaps resonance can occur naturally under certain conditions. In addition to this list, which would be desirable for the design of a conventional dc process cell, the key to optimization is a reasonable estimation or, preferably, a *direct measurement* of the controlling process *relaxation times* which can be used to design a cycle for current leveling and current apportionment for improved process control.

An optimization criterion must be chosen. The optimization criterion would be specific to a particular candidate process. It could be as simple as a maximum or minimum factor measurement. More likely, the criterion is a combination of factors such as: product purity and quality as well as quantity; energy efficiency; surface deposit or etch condition, grain size and uniformity, hardness; electrical or thermal conductivity; mechanical elasticity and yield strength. One relatively simple measure is the density of electrodeposited material. With the optimization criterion chosen, use the electrochemical impedance spectral (EIS) analysis and piezoelectric crystal electrode (PCE) response data

(or other means) to obtain critical relaxation times, those times which will most likely control the process.

If the chosen criteria is simply energy efficiency the answer to the pulse design problem might be given by the pulse current efficiency or mass-to-charge ratio data obtained by Buehler, for a series of tested pulses. The true picture is however a bit more complicated and a pulse schedule design would need to incorporate the relaxation time and reaction mechanism data for the principal reactions involved. Where multiple competing reactions are involved, we could envision something analogous to a Weber traffic control model [18] to determine pulse widths and duty cycle. The EIS and PCE data provide or lead to the time constants needed to determine pulse widths, cycle position, and overall duty cycle (on/off and reversed current or potential periods) and also to arrive at a pulse current density.

Once chosen, the candidate pulse schedule must be tested. The test is accomplished by varying the pulse cycle about the chosen "optimum" and the results compared (with dc results) against the selected criterion. For example, product purity is checked with EDAX or other emissions spectroscopy methods; grain size and uniformity can be appraised optically under a microscope; a method can be devised to measure deposit conductivity or resistivity; a reverse bend flexure test can quantify elasticity; and roughness can be evaluated optically.

The optimization approach can be demonstrated and evaluated by applying it to one or more electrodeposition processes. Candidate materials are copper, silver, zinc, or calcareous deposit from sea water. The dissolution of iron, copper, zinc, or aluminum also present good illustrative cases.

CHAPTER 7

Periodic Potential or Current Control Models

Over the past two decades, researchers [1-11] have used mathematical models to explore the effects of ac on electrochemical processes. The models, based on reaction and mass transport limits for particular systems, can serve as a basis for comparison with experimental measurements and later as design and operational guidelines for electrochemical processors such as electro-platers and commercial chemical producers.

The criterion for electroplating or electrowinning of metals would typically be purity, morphology, or alloy composition of the desired deposit. Similarly, the criterion for chemical substance production reactions would be selectivity and productivity for a desired product. Recent work done on certain branched electroorganic reactions, such as the reduction of nitrobenzene [1-3], shows that enhanced productivity and selectivity for key intermediaries can be realized under periodic potential or current control. The advantages of periodic- over dc- control, as pointed out in reference [1], are evident provided:

1) The sensitivity to potential change is greater for the reaction producing the desired product. Product selectivity is greater for whichever reaction has the greater sensitivity to potential.

2) The duty cycle length (fraction of total cycle length for which current or voltage is high) is sufficient to allow for double layer charging and to prevent the *average* electrode polarization potential from falling below the *dc* polarization potential necessary to promote the desired reaction.

3) The duty cycle length is such that the period of oscillation t is (preferably much) less than the characteristic (or relaxation) time t_c for the process.

4) The cell current levels can be maintained below the H_2 evolution limiting current.

5) The desired product results from a heterogeneous reaction at an electrode surface or a homogeneous reaction in the bulk solution.

6) There is a satisfactory trade-off between desired productivity and acceptable selectivity. (Typically, as productivity increases, selectivity diminishes.)

The problem is to arrive at an *optimal potential (or current) control profile* (or periodic control schedule) which defines the potential / current maximum (or minimum), duty cycle, and frequency. Figure 7.1 illustrates the product selectivity problem. The allowed reaction time determines which species dominates. Bakshi and Fedkiw [1] developed a numerical search technique to determine the optimal potential control profile for a general class of electroorganic batch reactions. In the class of reactions considered, the reactant is reduced electrochemically to an intermediate. The intermediate is then consumed by two parallel reactions: a chemical decomposition to a desired product or a further electrochemical reduction to an undesired product.

The model employed in reference [1] assumes: (1) no mass-transfer limitations (so species concentrations at the electrode surface are taken to be equal to bulk concentrations), (2) no side reactions (such as solvent electrolysis) occur. Based on these limiting assumptions, the state equations describing the reaction kinetics as a function of the control inputs (potential) are applied to gradient search techniques which were developed from optimal control theory. The theory of optimal control, as described in text

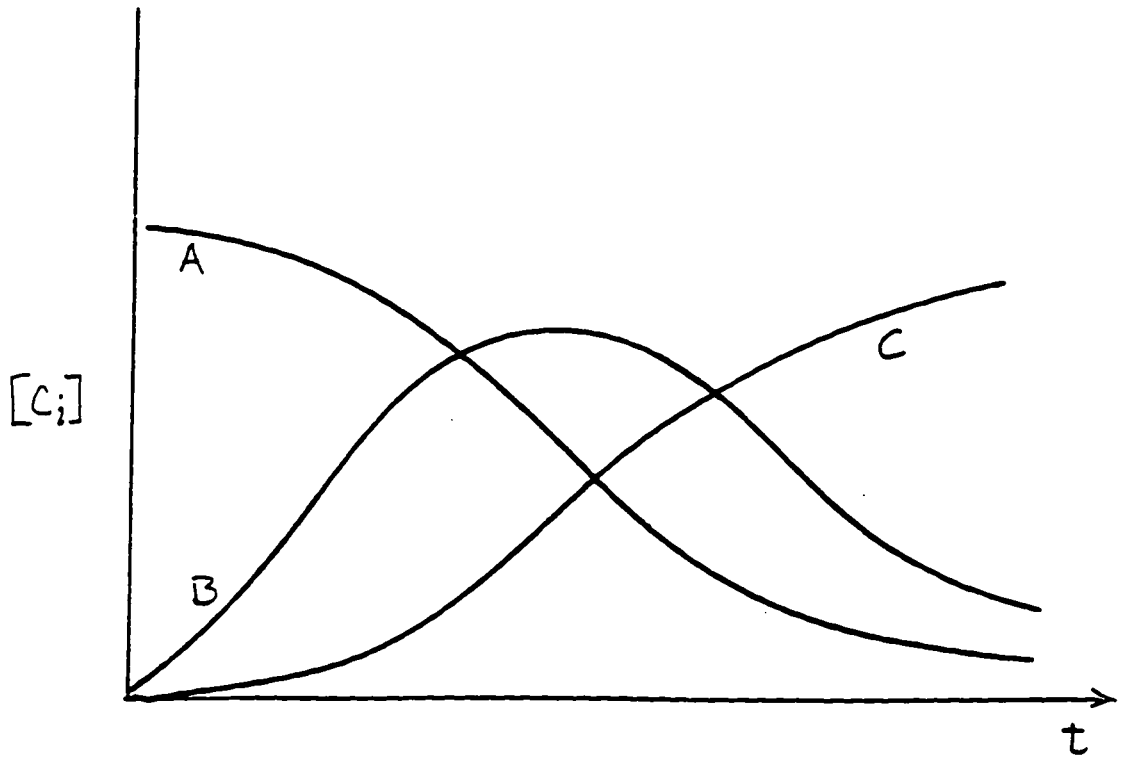

Figure 7.1. PRODUCT SELECTIVITY for species in the reaction:

$$A + e^- \rightarrow B \rightarrow C$$

varies with time as the reaction proceeds. The desired product could be B or C.

books [13-17], has been previously applied in the chemical industry to reaction temperature control. The easier, actually more promising, case of manipulating potential in electrochemical reactions, is yet to be employed in large scale production. In optimal control theory, the problem can be defined mathematically in terms of a *functional* which, in this case, is the concentration of the desired product to be maximized at the end of the batch reaction period. State equations describing the reaction kinetics in terms of reaction rate coefficients and control inputs which are related to the applied cell potential are satisfied as are restrictions on the potential. It is further assumed that reaction irreversibility is assured by proper setting of the control parameters (e.g. sufficiently high potential setting). The optimal potential control profile is then found by using a numerical search technique based on the projected gradient method.

An example of this type of branched electroorganic reaction is the reduction of nitrobenzene (NB). At the cathode of the electrochemical cell NB is reduced to phenylhydroxylamine (PHA) and subsequently to either aniline (AN) by a further electrochemical reaction or by chemical reaction in the bulk solution to p-aminophenol (PAP), the desired product.

$$NB + e^- \rightarrow PHA$$

$$PHA\ (\text{cathode interface}) + e^- \rightarrow AN \quad \text{-or-} \quad PHA\ (\text{bulk}) \rightarrow PAP$$

Except for cases in which the electrode processes are intrinsically slow or are at low overpotentials, the reaction rates will be governed by the mass transport rates to and from the electrode surface. The model prepared by the authors of [1] is instructive, but restrictive. A more general case requires the solution of Fick's second law, convective diffusion equation,

$$dC / dt = D \nabla^2 C - V \cdot \nabla C$$

Nolen and Fedkiw [3] studied the enhanced selectivity in NB reduction on a rotating disk electrode which can result under periodic current control. In this case the diffusion layer and hence the mass transport is a well defined function of the disk rotation rate. The Duhamel superposition principle is used to derive the solution for the convective diffusion equation. Mass transport and kinetic effects are coupled. Based on the fact that the sum of the individual electrochemical reaction currents equals the total electrochemical cell current, the model apportions the cell current to the different reactions involved.

The Nolen-Fedkiw model is based on an earlier work by Verbrugge and Tobias [11] developed for periodic electrodeposition of metals. Unlike the earlier work, the Nolen-Fedkiw model treats the electrochemical reactions in series rather than in parallel. Double layer capacitance charging (not included in the Verbrugge-Tobias model) and hydrogen evolution currents are taken into account. Cycle-averaged parameters are determined for the stationary-state. The results of two computational models are compared: (1) differential conversion (assuming bulk concentrations are constant); (2) integral conversion (changes in bulk concentrations are accounted for with a series of differential conversion calculations). One of the most important results of the Nolen-Fedkiw model, because it addresses double layer charging current which becomes increasingly important with frequency, is that the optimum duty cycle at constant current is shown to be greater than zero and optimum frequency less than infinity.

Smeltzer and Fedkiw [2] treat the more commercially significant case for NB reduction in a parallel plate reactor under periodic cell voltage control (periodic potential control). The transient diffusion equation is solved for stationary-state conditions (conditions prevailing after all non-periodic responses have decayed). Only mass transfer normal to the plane of the electrode surface is significant. The boundary conditions are

applied to the solution of the one-dimensional Laplace equation which relates the total current at the cathode and the anode to the solvent potential,

$$d^2 \Phi / d y^2 = 0$$

The current is controlled by the $\Phi(y)$ profile across the cell ($\Phi = \Phi_c$, at the cathode to $\Phi = \Phi_a$ at the anode). The potential profile is, in turn, governed by the concentration profile for the electro-active species.

The Smeltzer-Fedkiw model then applies an iterative solution method in which: (1) the potential in the cathodic interface is estimated as a function of time over one cycle and applied to (2) solve the linear equations for the Fourier coefficients for the NB concentration in the cathodic interface which is used to (3) solve the linear equations for the PHA concentration in the cathodic interface; then (4) the NB and PHA cathodic interface concentrations are used to solve the non-linear equations for cathodic and anodic interface potentials for a number of points in time over one cycle; (5) convergence is checked (if not achieved, the process iterates returning to step 2) and finally, (6) the cycle-average selectivity and productivity for PA is calculated. (A high interfacial PA concentration indicating that the chemical reduction to PAP is favored over electrochemical reduction to AN.)

Preceding [1-3,], MacDonald [12] derived in detail a Laplace solution to the time-dependent behavior of the most basic electrochemical case which can serve as a foundation for more complex models. A quiescent system with a well supported electrolyte results in minimal electromigration of electroactive species in a cell whose dimensions are sufficiently large to ensure that electroactive species concentrations at the cell boundaries are constant over the time frame of the experiment. These conditions rule out forced convection, rotating disk electrodes, vibrating electrodes, or thin layer systems.

The only mode of mass transport is diffusion under semi-infinite conditions. Two simplifying assumptions are made: (1) the convection term, V = 0 and (2) only diffusion through the plane of the electrode is of concern. The Laplace transform is used to convert this second order partial differential equation into a total differential equation whose solution is a function of a single independent variable. A new concentration variable representing the extent of perturbation of the system from equilibrium, $C^*(x,t) = C^b - C$, is introduced, reducing the equations for three of the common electrode geometries (planar, spherical, and expanding plane) to the same general form of the transformed equation:

$$d^2\underline{C}^*/ds^2 - (p/D)\underline{C}^* = 0$$

for which the general solution is

$$\underline{C}^* = A_s e^{-as} + B_s e^{as}$$

where $s = x, r, z$ for the planar, spherical, and expanding planar diffusion cases, respectively, and $\underline{C}^*$ is the Laplace transform of the time-dependent concentration perturbation.

(The complexity of the solution for cylindrical geometries discourages the use of microcylindrical electrodes in experimental work. When the radius is large compared to the diffusion layer thickness, as would be the case with a macrocylindrical electrode or if the experiment is limited to short times, the cylindrical diffusion may be approximated by the planar case. This approximation would apply as well to a macrospherical electrode.)

Initial and boundary conditions which express mathematically the physical restraints on the experiment are applied to refine the general solution to fit the particular case in question. These conditions define the state of the system parameters, at specified boundaries, just prior to the initiation of the experiment and after the experiment has been

running for some period of time:

$$t = 0, \quad x \geq 0 ; \quad C = C^b$$

Prior to the start of the experiment the concentration is uniform up to the electrode surface (assuming that the potential drop across the double layer has negligible effect on the distribution of electroactive species within the layer). Then, some time after the experiment has been initiated:

$$t > 0, \quad s\,(x,r,\text{or } z) \rightarrow \infty, \quad C \rightarrow C^b$$

This is the case for "semi-infinite" diffusion, the bulk concentration at some distance from the electrode surface can be taken as time independent. (Otherwise, an evaluation of the time dependency of the concentration at the wall of the vessel must be made.) For "semi-infinite" diffusion at $t > 0$, $s \rightarrow \infty$, $\underline{C}^* \rightarrow 0$, and therefore, B_S must also be zero. Meanwhile, at the other system boundary, the electrode surface, where the concentration depends on the relationship between reaction kinetics (reversible or irreversible), current, and mass fluxes; for

$t > 0$, $s = 0$, $\underline{C}^* = \underline{C}^*(s = 0)$, and therefore the coefficient, $A_S = \underline{C}^*(s = 0)$.

The general equation for the Laplace transforms of the time dependent concentration perturbations at a distance, s, from the electrode surface now reduces to:

$$\underline{C}^* = \underline{C}^*(s = 0)\, e^{-as}$$

where $a = (p / D)^{1/2}$. In terms of the Laplace transformed concentration variable this is:

$$\underline{C} = C^b / p + [\, \underline{C}(s = 0) - C^b / p \,]\, e^{-as}$$

where p is the Laplace variable (chosen sufficiently large to force convergence of the Laplace transform integral). This equation may now be inverse transformed to obtain concentrations as functions of distance and real time.

Many systems of interest involve coupled electrochemical and chemical reactions. While the foregoing may adequately describe the change in concentration of species resulting from charge transfer reactions at the electrode surface, which are controlled by pure diffusion, additional terms must be included for mass fluxes due to chemical reactions in the vicinity of the electrode. The added terms account for forward and reverse reaction rates, for example, in the simple case

$X \Leftrightarrow O$ with forward and reverse coefficients, k_1 and k_{-1}, respectively.

The product O from this reaction is electrochemically reduced in the reaction:

$O + ne^- \Leftrightarrow R$ with forward and back reaction coefficients, k_f and k_b, respectively.

The concentration changes for X, O, and R in the vicinity of the electrode surface (but not $x = 0$) can be expressed in the following equations:

$$dC_X/dt = D_X (d^2C_X/ds^2) - k_1 C_X + k_{-1} C_O$$

$$dC_O/dt = D_O (d^2C_O/ds^2) + k_1 C_X - k_{-1} C_O$$

$$dC_R/dt = D_R (d^2C_R/ds^2)$$

The reaction coefficients k_f and k_b are not considered in this set of equations because they are involved only in the charge transfer reaction which occurs only on the electrode surface and must therefore be considered in the equations for the boundary condition ($t > 0$, $x = 0$). The charge transfer reaction parameters k_f, k_b, and

$P(E) = \exp[(nF/RT)(E - E_O)]$ are all dependent on the potential at the electrode and hence on the form of the potential input signal at $t > 0$.

The coupled process equations are of the general, partial differential form

$$dC/dt = D(d^2C/ds^2) +/- kC$$

the Laplace transform for which is the total differential equation

$$d^2\underline{C}/ds^2 - [(k +/- p)/D]\underline{C} + C^b/D = 0$$

for which the general solution is

$$\underline{C} = A\exp(-bs) + B\exp(bs) + C^b/(p +/- k)$$

where $b = [(p +/- k)/D]^{1/2}$. Applying the boundary conditions as in the foregoing case for pure diffusion, the Laplace transformed solutions are of the form

$$\underline{C} = C^b/(p+/-k) + [\underline{C}(s = 0) - C^b/(p+/-k)]\exp^{-bs}.$$

MacDonald [12] gives the foregoing derivation in greater detail and tabulates reaction/diffusion rate expressions for a number of coupled charge transfer/diffusion processes. The Laplace transformed solutions can be inverse transformed (using known inverse transform functions and the convolution theorem) to reintroduce the time variable. It is further pointed out in [12] that in some cases, when the inverse transformation cannot be performed or the inverse form handled by approximation, and since the Laplace transformed current is often simpler anyway, it may be more convenient to analyze the data in Laplace space.

Another model, based on a reaction-limited case, is presented by Hager [4] considering the role of the *pseudo*-capacitance due to reaction intermediaries on thickness leveling in certain pulsed-current controlled electroplating processes. In this view, the reaction intermediary inventory, like the double-layer, constitutes a capacity for charge storage. The final step in a multi-step deposition reaction is rate determining in the process

which occurs on a poorly conducting substrate; the electrolyte solution resistance is negligible, and the reaction pseudo-capacitance, C_p, is large relative to the double-layer capacitance, C_{dl}, which is assumed to be constant over the potential and electroactive species concentration range for the system. C_p is strongly potential dependent and varies with the surface coverage fraction and is an order of magnitude greater than C_{dl} to values much smaller than C_{dl} as the surface coverage approaches unity. The disk electrode in this case is modeled as a continuum of concentric rings. The rate of reaction (or reaction *velocity*) across the rings is proportional to the availability of electroactive surface sites, expressed as a fraction of electrode surface coverage. Determining the pulse duration, and current level and subsequent current-off time, now becomes a matter of balancing the reaction rate against the reaction intermediary inventory and double-layer discharge rates. The task is complicated by the nature of the current distribution which varies across the electrode with the local impedance, a function of radial position on the electrode.

The semi-quantitative results of the Hager model show a weak dependence of deposition thickness leveling on overall electrode current within a fairly wide range of the *optimal* current level. The expression for the optimal *on-time* period while explicit in terms of system parameters is also dependent on functions of relaxation coefficients which are themselves dependent on the *on-time* period. The *off-time* period is the prime influence on thickness leveling and is selected at the expense of duty cycle, on the basis of relaxation time scales (related to C_{pmax} / C_{dl}) such that the ratio of *off-* to *on-*time is typically on the order of ten.

The importance of the Hager model, even more than consistency with experimental results, is that, based on given system parameter ranges and constraints and the selected criterion of *thickness leveling* for electroplating, the model demonstrates the development

of expressions for optimizing the operating parameters: *current-on period, level, and duty cycle*. It is an *approximation* procedure, but is *rational*.

CHAPTER 8

Natural Consequences of the Dynamic Interface: Structure, Periodicity, Fractals, and Chaos

The strategy for electrochemical process optimization will, at some point, need to address the *self-similarity* of scale and structure suggestive of *fractals* [5, 6, 24-27] and, at the same time, the *irregularity* and *randomness* described as *chaos* [4-6, 9] in the responses of many physical systems perturbed from, or moving between, states of equilibrium. Examples include the intricate structures observed by Barkey [2] in electroplated copper and zinc, oscillating chemical [1, 8] and electrochemical [10-14, 17, 23] systems. surface structure-process interactions [16, 17], ocean mixing processes [3], and bistable and noise-sensitive systems [18-22]. Such systems, Prigogine [4] would suggest, tend to be more *dissipative* and irreversible (in a general sense, compressible) than conservative and reversible (incompressible). Their time-dependent behaviors are very sensitive to initial conditions and their trajectories in phase space [7] take the form of *strange attractors* [6, 9].

The study of oscillating chemical reaction systems proves to Epstein [1] the usefulness of the *thermodynamics of irreversibility* formulated by Prigogine [4] which apply to reactions far from equilibrium either because they are in an early stage of reaction or because they are in a system which is open to the flux of energy and/or matter from outside its boundaries. Many systems of this type exhibit bistability, oscillating between two (or more) stable states. The conditions prerequisite to this kind of behavior, as summarized by Epstein are:

1) system is far from equilibrium (as in a continuous-flow stirred-tank reactor

2) feed back (auto catalysis)

3) bistability (a change in external conditions results in hysteresis).

Recognizing and following this criteria, Epstein was able to identify and *design* oscillating reactions from three different families of systems (bromates, chlorides, and iodates) with regular periodic behavior. Some of the systems, however, exhibited quite irregular oscillations which, if genuinely due to dynamics inherent in the systems themselves and not to mere experimental artifacts, serve as physical examples of what mathematicians refer to as *chaos*. While some researchers [12, 28] are skeptical, others, Hudson and Bassett [10, 11] and [13,14] maintain that the experimentally observed behavior is real and inherent in the systems.

Hudson and Bassett studied the electrodissolution of copper in acidic ($1N$ H_2SO_4) chloride (0.1, 0.3, 0.5 M) solutions. They observed current oscillations starting, regardless of fresh electrode, initial surface roughness, at potentials sufficiently high (ie., sufficiently far from equilibrium). No oscillations were seen during film building at 250 mV (SCE), but at 310 mV (SCE), after a brief induction period during which the film grew to approximately 10 μm, aperiodic oscillations in current commenced and continued until the film grew to a thickness of approximately 30-70 μm at which point the thick film surface appeared uniformly cratered. They noted that if a portion of the film was removed at any time during the process, the oscillations would cease (if in progress at the time) and the initial film building process recommence, followed by oscillations and the final thick film formation. Using a standard time series displacement method, a three dimensional phase portrait is plotted for each set of oscillations. The resulting plots appear to be

strange attractors, trajectories recorded in phase space which are aperiodic and very dependent on initial conditions.

Hudson and Bassett, while making careful observations with regard to current oscillations, take the constant potential as a given, without regard for the mechanism by which a particular potentiostat (in this case a PAR 173) maintains that potential. Herein lies the problem in identifying or separating real system behavior from experimentally induced artifacts. The entire phenomenon of oscillations is treated as if the working electrode interface were isolated from the external world when, in fact, an external black box senses the electrode potential with a half-cell reference electrode and maintains the ordered potential with an electronic feedback circuit.

Some researchers suggest, as does MacDonald [28], that the oscillations occur because of the negative load line of the typical potentiostat circuit (the system voltage/current source). Electronics texts [29, 30] point out that the operating (or quiescent) point for the coupled electronic component (or electrochemical cell) and its power source will be bi-stable in cases where the characteristic (E vs. i) curve of the component (such as a tunneling diode) has regions of negative resistance, particularly if the power source (potentiostat) load line is flatter (less negative) than the component negative resistance region.

As an example of an experimentally induced oscillation, consider the following. In an electrochemical system that passivates (requires less current at some point along its characteristic E vs. i curve) as a result of surface film formation, oscillations may occur because, as the cell current begins to drop but the potential across the film increases, partly because the film is more resistive, but also because the potentiostat applies a higher potential at the lower current demand. The increase in potential breaks the film and the

electrochemical reaction resumes at a higher current level, until the film rebuilds and the process repeats.

Cattarin and Tributsch [12] noted that the oscillatory behavior of the H_2O_2 reduction system depended on having a suitable resistor in the external circuit in series with the cell working electrode. The frequency and amplitude of the observed oscillations was influenced by the value of the external resistor as well as by the mass transport processes internal to the cell. The three conditions they cited (after Degn [31]) for current oscillations were:

1) A range of negative slope in the real current-voltage curve connecting "active" to "passive" branch of the cell characteristic curve.

2) A large enough external resistance to cause distortion in the characteristic curve to the point where multiple states are generated under potentiostatic control. This requires the total series resistance, $R_t > R^* = -(di/dV)^{-1}$, (negative reciprocal of the slope of the characteristic in a region of negative values).

3) A time-dependent feed-back due to concentration polarization which shifts the instantaneous characteristic curve back and forth, causing the system to cycle around a loop.

In the H_2O_2 reduction study, the feed-back is due to the relative interfacial reactivities for the two electrode states: activation, fast; passivation, slow.

Hudson and Bassett, in a later study [11], suggest that it would take a minimum of four ordinary differential equations to construct a model which reproduces all the dynamics observed in their copper dissolution in acidic chloride experiments.

Hibbert and Murphy [13] take exception to the rule that oscillations occur only because of (1) a negative resistance (either in or in series with the characteristic cell) and/or (2) coupling between mass transport and chemical reaction processes. They show that while a system of three equations for a two-surface oxide system taking into account OH^- diffusion, leads to a current which is three-valued as voltage becomes more positive (an indication of bistability); the upper corrosion branch and the lower passivation branch are stable unless perturbed by some external means. They go on to demonstrate, following the work of Epelboin [32], a system of only *two* equations, one of which is exponentially dependent on potential, for an oxide $\Leftrightarrow$ salt film system, where in "the energy of dissolution of the surface oxide increases with increasing surface coverage and gives a collapse in the current-voltage curve at passivation and predicts limit cycle behavior in the current with time". A seemingly simple set of equations replicates the conditions for an oscillating system observed experimentally.

Li, et. al. [14] studied the electrodissolution kinetics of iron in chloride solutions. They observed current/potential oscillations recorded as time series which were later characterized by power spectral densities, phase portraits, and correlation dimensions of chaotic attractors. They suggest that the oscillations occurring during high-rate iron dissolution are due to an interplay between the formation and dissolution of two types of oxides: a thin, nonporous inner film and a porous anodic outer film layer. The latter quickly self-destructs at a critical potential, and building begins anew. The work lends support to the hypothesis that these electrochemical oscillations can be modeled by a set of ordinary or partial differential equations of modest complexity. The role of the external potentiostat/galvanostat control circuit, however, was not considered.

It is apparent that nonlinear systems coupled with even small spatial and/or temporal variations in control parameters (temperature, concentration, potential, or geometry) can be inherently unstable and lead to long-term results which are not satisfied by steady-state, continuum model solutions which assume that, in the long-term, transients will be damped and some average state be clearly dominant. While equilibrium, steady-state, continuum models have been useful and enlightening in studying and engineering with many practical systems, there are many systems which would become more understandable and serviceable and others less unpredictable and destructive if viewed from a more appropriate far-from-equilibrium, dynamic model point of view.

Jensen and Ray [15] observe that while reaction-diffusion systems are usually treated as macroscopic continua they are actually collections of microscopic subsystems. Nonuniform microstructures produce long-term steady-state macroscopic behavior inconsistent with continuum model solutions. Multiple hysteresis loops for reactions such as the oxidation of CO or H_2 on platinum are better explained by discrete or domain models.

Prigogine [4] outlines the principles of self-organization of microstructures in non-linear systems. These principles might apply to the intricate fern-like, branched aggregates created in electro-deposition of copper or zinc from an electrolyte confined to a thin layer between two transparent plates observed by Barkey [2]. The process, referred to as morphology selection, is attributed to a cellular mixing process resulting from a coupling of a hydrodynamic instability at the interface between the metal ion-depleted and bulk solution with the development of the aggregate morphology.

Walgraef, et. al. [16] observed that two kinds of chemical patterns: *chemical waves* and *mosaiclike structures*. The *waves* are more likely due to "long-range

fluctuations of the phase of the limit cycle" and a "lack of true long-range order in two-dimensional systems" while the mosaiclike patterns result from "true self-organization of the medium" and the "long-range phase fluctuations manifest themselves by the presence of topologic defects, dislocations, or grain boundaries." Jorne [17] used a linear stability analysis applied to an electrochemical system with a thin layer of an adsorbed species to show that coupling between diffusion and chemical reactions would lead to "chemical oscillations and pattern formations." The patterns could be idealized as repetitive hexagonal, triangular, or square cells. The model, he suggests, could be a "transformation mechanism between electrical and chemical waves, and vice versa, which might be of great interest in biological and engineering systems."

The discovery of electrochemical *strange attractors* has important implications for the quest for a *rational* design strategy for electrochemical processes in general. If a significant portion of the systems of interest fall into a category which is inherently *chaotic*, are they to be excluded from the effort? What kinds of processes fall into this category, how can they be identified, and is there perhaps some special strategy for dealing with them as well? As an example, Epstein [1] suggests that perhaps all catalytic reactions, on sufficiently small time scales, proceed in an oscillatory manor. Heterogeneous catalytic reactions could alternate between active and passive states, some switching mechanism determining just which *stable* state a given surface reaction site would be most likely in at any given point in time; what surface fraction is in an *on* versus an *off* phase at any given time under given conditions. What schemes of apportionment will most reliably describe the switching mechanisms in time and space, must be determined.

Because of their fundamental importance to the stability of electronic devices and memory media, phase transitions and the theory of switch stability in (electrically) noisy

environments have been the object of considerable attention in recent years. An electrode surface can be viewed as being in one of two states: active or passive, conductive or non-conductive. Here the bistable system is idealized as two potential wells separated by a local maximum or barrier. The state of the system is marked by the position of a single particle which must be in either of the two wells, or somewhere between them. If the system exists in a noisy environment, what level of noise can be tolerated? How stable is the particle in either of the two wells? If the particle is at the local maximum, it is clearly unstable and would be expected to be very sensitive to any kind of perturbation but which of the two wells will it settle into assuming the potential field is symmetric? What model will give a realistic distribution? Horsthemke and Lefever [18] demonstrate, mathematically, phase transitions induced by external noise in non-linear macroscopic systems which are far from equilibrium. Using a Fokker-Planck equation for a continuous diffusion process, they apply an external noise to a system represented by a phenomenological equation; "...by increasing the strength of the external noise, without changing its mean value, the system can be made to undergo a phase transition well above the deterministic critical point." As long as the variance in the fluctuating parameters is large enough to place the system under non-equilibrium constraints during finite time intervals, ..."this type of phase transition may take place in systems where the mean values of the fluctuating parameters correspond to chemical equilibrium values."

In other work exploring the effect of microscopic fluctuations on the macroscopic evolution of non-linear systems, van Kampen [19] asserts that, "No approximation scheme based on a separation of macroscopic behavior and small fluctuations will be able to handle this process of magnifying fluctuations." In particular, with regard to the distribution of the particle in a bistable potential, he argues that "the Fokker-Planck or diffusion approximation ... is subject to serious objections. The reason is that in many-

body systems the only way to make the individual jumps small is by increasing the size of the system, which, however, at the same time reduces the influence of nonlinearity on the fluctuations. In particular, near a point of instability the master equation cannot be replaced with a Fokker-Planck equation, because the finite size of the individual jumps is decisive." He points out that the importance of the fluctuations in the development of the system is that their existence "allows the system to probe the entire space of state x and search for the lowest potential minimum." He goes on to demonstrate that a Kramers' treatment leads to a equation of the form of a time-independent Schrodinger equation which then yields a satisfactory distribution for the particle between two potential wells.

Smythe, Moss, and McClintock [20] use a Fokker-Planck probability function (Stratanovic as opposed to Ito version) and an analog simulator to observe *noise-induced phase transitions* (NIPT) in a phenomenological equation with a noisy parameter. Using a similar technique, Moss [21] analyzes the NIPT responses of two generic switch types. Both are first order, nonlinear, stochastic, differential equations with either parametric (multiplicative) or additive noise. One is nonlinear in a cubic term and inherently bistable. The other is nonlinear only in a quadratic term and its bistability is a result of the noise itself. Both switch models predict curves which match well with their electronically simulated performance. The S curve of the cubic, inherently bistable switch, incidently, resembles many characteristic electrochemical system active-passive curves.

Ideally, the impedance response of the electrochemical cell is a series RC circuit such that the complex impedance as a function of frequency is $Z(\omega) = R - j / \omega C$ where R is the resistance of the electrolyte between the two electrodes of the cell and C the capacitance of the two electrode-electrolyte interfaces one of which is the reference electrode. In real cells, however, the impedance is more accurately described as

$Z(\omega) = R\text{-}A(\omega)^{-n}$ wherein the interface impedance is the second term, the constant phase angle (CPA) impedance. Here, $j = \sqrt{-1}$ and A and n are constants, $n < 1$.

Liu [24-26] suggests that this power law impedance response is modeled fairly well by assuming a cantor bar (self-similar) surface structure for the interface. When an RC network is used to show the accumulation over time of charge "random walked" (diffused) through the cantor bar interface, there appears to be a good correlation between the fractal dimension of the surface model (the network) and the power law exponent, n.

Bates and Chu [27], however, argue that while there may be a correlation between the RC network and a power law response, the correlation between the impedance response and the fractal dimension of actual rough surface electrochemical interfaces is not good. They find a much more suitable model in the nearly two-dimensional growth of metal *leaves* (similar to fern-like structures observed by Barkey [2]) formed by electrode deposition which suggests a simulation of accumulated charge distribution down through the peaks and valleys of a surface as though these features were fixed, non-growing clusters. Basic to this model is the assumption that local regions of the electrode are screened by protrusions on the surface; an assumption that seems justified by actual impedance measurements. Charge distribution, flow of charge across the interface to the electrode; ions "random walking" through this cluster-array, protrusion charge-shielded landscape, gives an impedance response which correlates well with the n exponent.

It is interesting to note that the phenomena of oscillating states dealt with here was first described by Joule in 1843 [23] at a time when Ohm, Fechner, and De la Rive had just established what we know today as Ohm's Law and Joule was using the *new* law as the basis for experiments to measure "the Intensities of various Voltaic Arrangements". Joule made very careful observations of the angle of his galvanometer needle, and the

appearance of a white film over an iron electrode surface immersed in a sulfuric acid solution, and then the sudden disappearance of the film followed by the rapid evolution of oxygen from the surface. He noted the competition between processes..."we can readily perceive that oxygen must inevitably rise from the iron, whenever the oxysulphion cannot be produced as quickly as is demanded by the intensity of the battery." He also concluded simply and accurately on the matter of threshold that, "In general a current of a certain degree of intensity is requisite in order to produce the intermittent effects." Today, with our potentiostats and galvanostats, lock-in amps, impedance and Raman spectrographs, the mechanisms behind these phenomena are still a curiosity and a challenge.

CHAPTER 9

EXPERIMENTAL

A Measurement-Based Model and Cycle Design

Of the many systems that might be considered for periodic control, there is hardly a more appropriate or more promising application than the electrodeposition of thin, laminar alloys. When applied in sufficiently thin layers (typically less than 1000 Angstroms), two metals, which may have any degree of miscibility, produce in combination an alloy with properties of the individual metals [1-18]. A silver-lead laminar alloy, for example, has the high conductivity of silver and low corrosivity of lead. Of particular current interest are *cyclic multilayer alloys* (CMA) exhibiting magnetoresistance and giant magnetoresistance [6, 13, 15-18] which is highly dependent on metal layer spacing. Conventionally, these alloys are produced by vapor deposition or by alternating between two electroplating bath compositions. Under pulsed-plating conditions, however, it is possible to electrodeposit CMAs from a single electrolyte.

Designing a pulse schedule and electrolyte composition for a laminar alloy system is based on the layer spacing required to achieve the desired alloy property. The pulse schedule (simple *on* - *off* or superposition on a dc condition) takes advantage of the difference in reduction potentials for the two metals (one being more noble than the other) and an electrolyte composition (very much more concentrated for one than the other) such that the deposition of metal 2 is negligible during the time required for metal 1 to be deposited to design thickness. The dissolution (or continued deposition) of metal 1 must be negligible during deposition of metal 2. The pulse current-*off* time must be just sufficient to allow time for the *relaxation* to initial conditions at the interface (or return to the dc condition which favors the plating of the more noble metal).

The electrodeposition pulse schedules for single metals such as copper, silver, or zinc are more likely to be designed by their interface relaxation times than deposit thickness. The object with single metal deposits is more likely uniformity, grain size, and elimination of hydrogen or hydroxide inclusions. Applications include copper plating on printed circuit boards requiring increasingly fine detail and electroplating zinc for galvanic protection on steel wire with minimum hazard of hydrogen embrittlement. The approach is to work with the relaxation times to achieve current leveling in order to ensure deposit control.

A good approximation of the relaxation time can be made by calculating the *transition* time required to attain zero concentration at the interface from the bulk concentration of an electrodepositing ion at a given constant current density. This is the time required to reach the steady-state reaction layer thickness for a given current density. The calculation is made by using Sands equation [19] which shows that the square root of the transition time is proportional to the bulk concentration of the electroactive species and inversely proportional to the current density.

An optimal pulse plating schedule exploits the dynamic nature of the electrochemical interface. Modern electrochemical instrumentation presents the opportunity to base pulse plating schedules on *measured*, rather than calculated, time constants. The experiments conducted in this work utilize the information in *electrochemical impedance spectra*, EIS, (impedance and phase angle versus frequency) to obtain the relevant process time constants for a *measurement-based* model for cycle optimization and control. Gabrielli [20] reported the development of a combined EIS-QCM system to characterize electrochemical systems by their transfer functions. Work by Hager, Ruedisueli, and Buehler [21] reported the use of the PCE (or QCM) to monitor the

deposition and anodic polarization (corrosion and passivation) of iron. Buehler and Hager [22] used the QCM to measure the pulse efficiency for single pulses of different durations in copper plating. Ruedisueli [24, 25, 26] first reported the idea to utilize EIS-QCM specifically for the purpose of measuring time constants for the optimization of cyclic electrochemical processes such as pulsed electrodeposition of metals.

As discussed in Chapter 3, a state-of-the-art frequency response analyzer, FRA, with a lock-in phase amplifier, can perform complex impedance measurements at a single frequency or sweep a range of frequencies. The complex impedance vector is $Z = R + jX$, where R is the ohmic resistance, and X the reactance (capacitive or inductive), while j is the complex unit vector, $j = \sqrt{-1}$. The absolute value of the impedance vector is $|Z| = \sqrt{R^2 + X^2}$. R is independent of frequency, while X varies with frequency. The vector Z is the transfer function for an input voltage, V, to a device resulting in an output current, I, with a corresponding phase angle, θ, indicating the amount by which the current *leads* or *lags* the input voltage. This relation is expressed as $V/I = Z(\omega)$ and $\mathrm{Tan}(\theta) = X/R$. For a purely resistive device, X and $\theta = 0$. For an ideally capacitive device, $R = 0$, $X = -j\frac{1}{\omega C}$, and $\theta = 90$ degrees; the current charging a capacitor leads the voltage by 90 degrees. For an ideally inductive device, $R=0$, $X = j\omega L$, and $\theta = -90$ degrees; the current carried by an electric field expanding in an inductor lags the voltage by 90 degrees. For all practical purposes resistors, capacitors, and inductors are common place, *pure* components. (Ideally, *pure* components do not exist; beyond a certain voltage and frequency range, a component becomes non-linear, and may show characteristics of other components. A resistor, for example, at very high frequencies will show some capacitance.)

Choosing a simple R_S-RC_p series-parallel circuit as our impedance measurement model, shown in Figure 9.1, we define the optimum pulse current to be that which most nearly maintains a continuous charge on the capacitor; more precisely, maintaining it at a pending discharge. At very low frequencies (or long pulses), $\omega \rightarrow 0$, essentially dc conditions, the capacitor is fully charged, continuously with no discharge, $Z = R_S + R$. At very high frequencies, the capacitor never fully charges, but rather appears as a short circuit and $Z = R_S$. The phase angle at both these extremes approaches zero. At a certain point between the extremes, the frequency would be just right to maintain some charge on the capacitor, but never overcharge it, or allow it to completely discharge. At this point, the temporal derivative of the charge on the capacitor is zero, $i_C = dq / dt = 0$. The average time rate of discharge equals the average time rate of charging. A steady state, quasi-equilibrium, is reached between the extremes of the capacitor being fully charged (engaged) continuously at low frequencies and not charged at all, in effect, by-passed at high frequencies. At this operating level, the phase angle reaches a maximum lag (which is also the point of maximum interface work, shown in Figure 3.4c); this is the *characteristic frequency*, $f = 1/RC_p$ (sec^{-1}), where $\omega = 2\pi f$ (radians/sec).

In an FRA impedance, log ω vs. $|Z|$, *Bode* plot of a *lumped component* electrical circuit of this type, the characteristic frequency is quite distinct; the phase peak is very pronounced and the *roll-off* of the impedance magnitude from a high value, $R_S + R$, (at low frequencies) to a low value, R_S, at high frequencies) is exponential. The reciprocal of the characteristic frequency, f, is the *relaxation time*, t_r, required for the capacitor to either exponentially charge from zero to a value which is $\exp(-t / t_r)$, 63%, of its fully charged state or discharge 63% of a full charge. Note that all the FRA has actually measured is the impedance, the *resistance* to current flow, to charging and discharging the capacitor in this particular circuit. The object is to *keep the capacitor charged*, so the

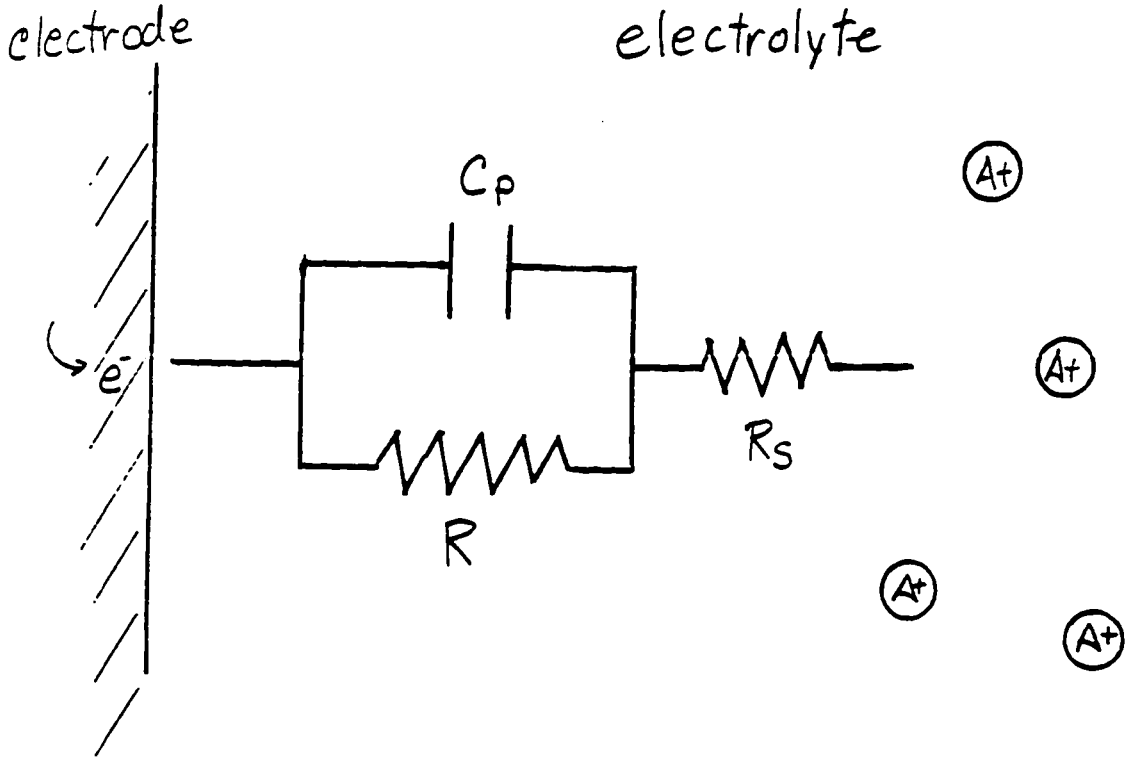

Figure 9.1. THE R_s-RC_p MODEL of the dynamic electrochemical interface describes roughly, but simply, the impedance behavior of the charge transfer process.

C_p	is parallel capacitance (double layer and chemical inventory)
R	is polarization or charge transfer or faradaic resistance
R_s	is electrolyte solution (series) resistance

Time constant, $t_r = C_pR$

current necessary to charge it in the time, t_r , must be selected. If the capacitance is unknown, it can easily be computed from the measured values, $(R_S + R)$, R_S and ω. Now, to charge the capacitor, a constant current, $i = q/t_r = CV/t_r$, is turned *on* at t= 0, and *off* at, $t = t_r$.

As suggested earlier this *on - off* schedule has applications apart from exercising the capacitor and saving power by having the current off part of the time. This simple circuit is a precise electrical analog for the *timing* of energy input or throughput to any physical system consisting of series - parallel, energy dissipative (a resistor) and energy storage (a capacitor) components. If the timing is right, the storage, time dependent, or *anelastic* element is neither over-driven or by-passed, but just *fully engaged*. Staying with the electrical analog components just a bit longer, consider the *other* energy storage component, the inductor, a simple coil of wire, wherein the voltage would *lead* the current. The R_S -RL circuit would behave mathematically and, in the FRA plot, very much like the R_S -RC circuit above, accept that it would be its mirror image. A capacitor stores a *static* electrical charge, electrons, a *condensed* electric field; an inductor stores an expanded electric field, a flux of electrons, a *kinetic* electrical charge. At low frequencies, the inductor acts as a short circuit; at high frequencies the inductor acts as a *choke*, no current gets through it. At some intermediate frequency, current flows equally through both inductor and resistor. If the two energy storing components, capacitor and inductor, are combined in parallel, they compliment each other in a complete cycle, passing energy in one form to another and back again, at the *right* frequency, indefinitely as an *oscillator*, were it not for the dissipative, resistor, element. An ohmic versus reactive (real vs. imaginary) resistance phase or *Nyquist* plot of an R-L-C parallel component circuit would result in a pair of opposing semi-circular loops, a complete circle, representing the frequency response of the two reactive (energy storing) components. An R-L-C circuit

tuned to some particular frequency of electromagnetic energy is the heart of a radio receiver.

The R-L-C circuit is also the electrical analog of many mechanical oscillator systems: a simple spring - mass system, a pendulum, or a gas expansion chamber mechanically linked to a flywheel. It also describes the behavior of an electro-mechanical device: the piezoelectric quartz crystal. In each of these systems energy is stored alternately in a kind of compression or potential energy of position and then a kind of expansion or kinetic energy of motion. The former is energy of displacement, the latter of *inertia*. The general equation for motion of all these systems is:

$$m\, d^2x/dt^2 + b\, dx/dt + k\, x = F$$

For the electrical circuit, this is expressed as:

$$L\, di/dt + Ri + c\int i\,dt = F_e$$

Recalling that the current through the circuit, $i = dq/dt$, the rate of change of charge on the capacitor; thus,

$$L\, d^2q/dt^2 + R\, dq/dt + C\, q = F_e$$

The first term is the *inertia*-like term which shows why it is not possible to *accelerate* (expand) an electro-magnetic field through a coil instantaneously. The third term is the displacement or Hooke-like restorative term. The middle term is the dissipative or damping term. The sum of these terms must equal the applied *electromotive force*, or voltage.

In the conventional dc operating mode, only the final steady-state is of concern. But in an ac (or pulsed) mode, the dynamics of a system are crucial. It is, therefore, tempting to ask if the electrical, mechanical circuit analog could also be extended to an electrochemical interface [24]. The double layer acts as a capacitor in storing charge as does the *pseudo-capacitive* effect of the interface as an inventory of chemical intermediaries is accumulated in multi-step reactions. The charge transfer of electrons between electroactive species at the interface and the electrode surface is impeded by a *polarization* or *faradaic* resistance factor. The dissipation by hydration and diffusion of charge transfer products or their inclusion in the structure of an electrode surface film or in the lattice of the electrode itself could be interpreted as a *pseudo-inductive* or inertial process. These latter processes being *storage* elements to the extent that they are reversible and therefore conservative. Charge stored in the electrochemical double layer is recoverable as is that stored in a chemical intermediary. An electron transferred to a metal ion subsequently incorporated as an atom in the lattice is also recoverable as are the components of a surface film. But the hydrogen ion, the most mobile of the electrochemical species, reduced by an electron transfer at an electrode surface to atomic hydrogen and discharged as gas is, like species removed as insoluble precipitates, not recoverable; the process is irreversible.

As discussed in previous sections, there are many electrochemical systems which show oscillatory behavior. Typically they are systems involving some kind of alternate film-building / film-dissolution mechanisms. When FRA Nyquist (phase) plots are made on such systems they are likely to show an inductive loop, in the low frequency range, as well as the capacitive semi-circle. But the inductive loop is quite small. It seems that most electrochemical systems are very well *damped*; their inductances, vanishingly small, and charge transfer resistances comparatively large.

In fact, the electrochemical interface is most likely to be successfully modeled as an R-C_l,RC circuit known as a Randles circuit [27], in which the C_l is in parallel with an RC series. But for many systems the simpler R_s-RC_p model, pictured in Figure 9.1, has worked quite well and will be considered here initially. In this model R_s is the solution resistance at the interface; R, the polarization resistance for charge transfer, and the parallel capacitor C_p includes capacitance for both double layer and pseudo-capacitance of chemical intermediaries. This model and the experimental apparatus and procedures described hereafter will be used to arrive at the time constants and the current levels to design pulsed current metal and metal alloy plating schedules.

Experimental Objectives

The objectives of the following experiments are fourfold:

1) Check and calibrate the FRA method(s) for obtaining electrochemical data, such as metal dissolution and deposition rates and time constants.

2) Test the effects of cell electrolyte sparge condition and electrode surface roughness on the Ecorr starting reference and on the FRA spectra.

3) Obtain FRA spectra on PCE substrates in metal plating solutions for the purpose of acquiring pulsed plating time constants, current levels, and duty cycles.

4) Observe and measure the interface resistance-parallel capacitance (CpR) response of the metal-electrolyte interface (PCE surface and cell) using an oscilloscope.

5) Prepare pulse plated samples on PCE substrates to determine the effectiveness of selected pulse plating schedules.

Experimental Apparatus

For most of the experiments, the FRA was a Solartron Model 1260 operated with a Princeton Applied Research (PAR) Model 273 potentiostat/galvanostat. The standard three electrode cell configuration was used with either an 800 ml cell with a PAR K47 working electrode sample holder (which exposes 1 cm^2 circular area of sample surface to the electrolyte) and high density graphite counter electrodes or, a small 6 ml cell with a piezoelectric quartz crystal working electrode (PCE) holder and a platinum foil counter electrode. Either a calomel (SCE) or a silver-silver chloride (Ag-AgCl) reference electrode was used depending on the particular experiment. The PCE was oscillated at a constant amplitude by a crystal oscillator board (designed by Sheldon Danniels, built by the UW chemistry electronics shop) and its frequency was monitored by an HP frequency counter Model 5384A. The FRA data was plotted with the 1260's onboard software on an HP plotter, Model 7470A. The conventional dc polarography (linear polarization, Tafel intercept corrosion rate measurement) experiments for comparison with FRA data, were run on a PAR Model 350 with its onboard plotting software and printer. The initial FRA measurements on the copper / cupric sulfate and gold / seawater interfaces were done on a Solartron 1250 (very similar to the 1260) with a PAR 273 supported by Stanford Research Institute (SRI) impedance calculation and plotting software on a MACINTOSH computer loaned to the researcher in the electrochemistry laboratory at SRI, Palo Alto, CA. Interface pulse response measurements were conducted using a Gould oscilloscope Model DM3010.

Procedures

Variation in Ecorr (rest potential or polarization *starting point*) due to electrolyte sparge condition was tested by stabilizing a specimen in one condition and measuring the

change with time when a sparge condition change was initiated. A shiny platinum electrode was placed in a nitrogen sparged 800 mL cell of 3.5 percent sea salt at 25 deg C. Once a stable Ecorr was attained, the sparge gas was switched to air, oxygen, or CO_2 and the Ecorr shift with time monitored with the PAR 273 programmed procedure. (See Appendix A for experiments and the results to observe the long-term platinum/seawater interface response.)

Test impedance scans were conducted using the 1260 alone and the 1260 in combination with the 273 on real electronic component R-R,C *dummy cell* circuits, per Figure 9.2, (1) to check the measured resistive and capacitive response spectrum against expected values, (2) to see what effect the instrument combination would have on the measurement process, and (3) to compare the model system impedance spectra with real, electrochemical cells.

Surface roughness effects were measured on low carbon steel, LCS, at 120 and 600 grit. The 800 mL cell was filled with 3.5 percent sea salt solution and sparged with nitrogen gas. The cell temperature was 25 deg. C. and at a pH of 7.2. The same specimen of 1018 LCS was resurfaced, alternating between the smooth finish 600 grit and the rough finish 120 grit emery paper, and tested five times in this same cell. Just prior to being placed in the sample holder each time, the freshly resurfaced sample was rinsed with water, quickly dried with a Kimwipe towelette, then covered with a drop of ethyl alcohol and blow dried with a hot air gun. This was done to minimize the time the sample surface would be under a film of oxygenated water had it been left to dry naturally after wet polishing.

Once a stable Ecorr (varying only a few mV over a half hour period) was obtained, an impedance scan was made on the sample using the 1260/273 arrangement. The scan

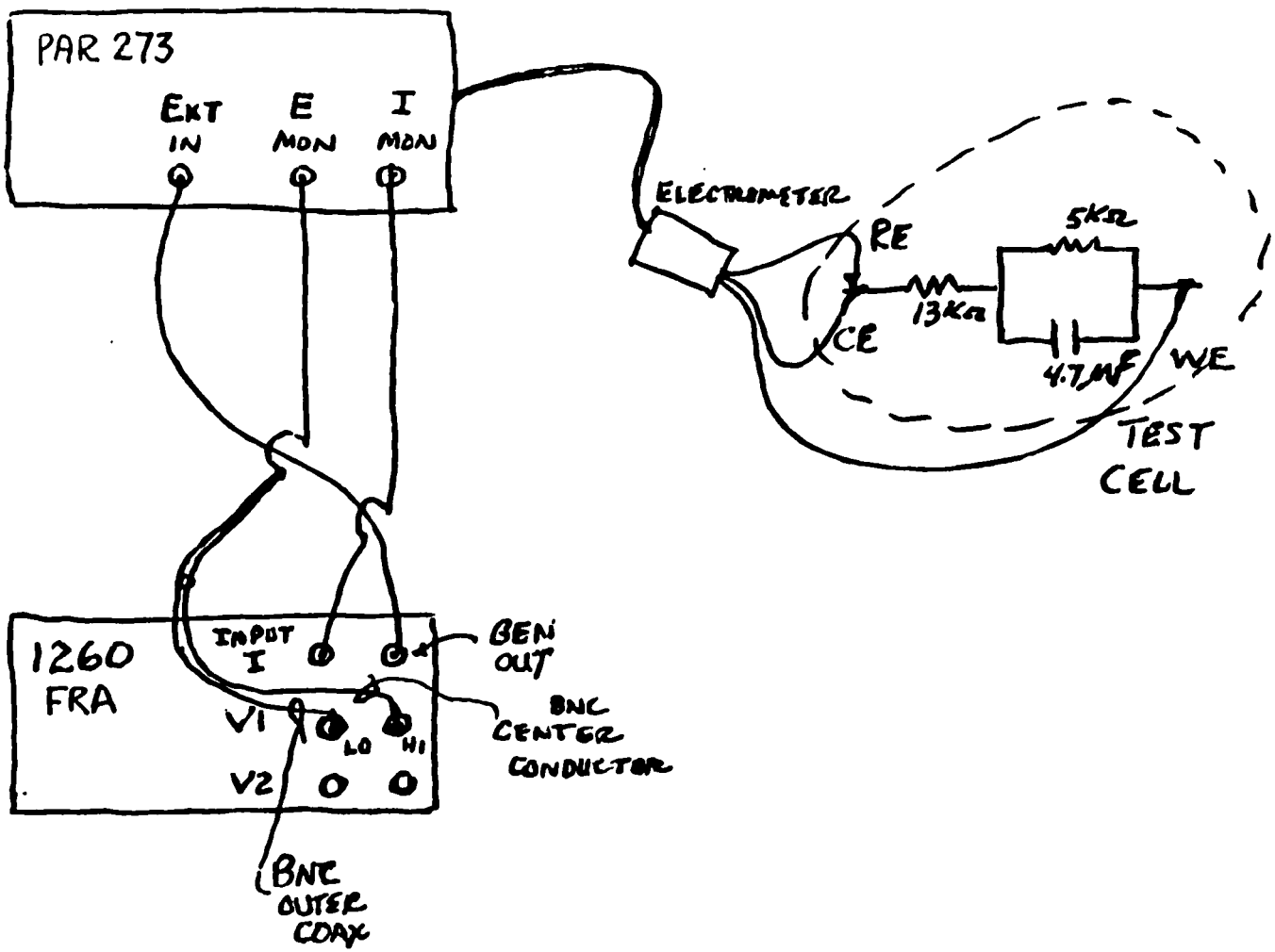

Figure 9.2. TEST SET-UP FOR DUMMY CELL MEASUREMENTS.

was made from 10 mHz to 10 kHz at an amplitude of 10 mV. Following the impedance scan, an anodic polarization scan was made on the sample using the PAR 350. The AP-scan was run from -250mV to +500mV relative to Ecorr at a scan rate of 1 mV per second.

The 1260/273 set-up was applied to measuring electrochemical cell parameters in a corrosivity study of several metals and metal alloys (LCS and Bronze) under various extremes of electrolyte, temperature, and sparge condition, and the results compared with PAR 350 corrosion measurements on the same samples. Each sample was polished to a 600 grit finish and placed in the PAR K47 holder in the 800 ml cell filled with fresh tapwater or sea water and sparged with nitrogen, air, oxygen, or carbon dioxide and held at 0, 25, or 50 deg C. Upon attaining a stable Ecorr, an impedance scan was run from 10 mHz to 10 kHz at an amplitude of 5 mV. In some cases, the sweep was run in both directions up and down the frequency range in order to check the stability of the system and the reproducibility of the data. Following the impedance scan on the sample, an AP-scan was run from -250 to +1200 mV with respect to the measured Ecorr.

Impedance scans on piezoelectric crystal electrodes in the small (6 mL) cell were performed on the 1250/273 set-up at SRI. The crystals were not oscillating. The purpose of the tests was to measure the electrode/interface impedance response only. All scans were conducted from 10 mHz to 10 kHz at a sinusoidal signal amplitude of 5 mV, taking five measurement points per frequency decade. Three scans were run on a gold electrode in aerated seawater. The first scan was run from an Ecorr of 0.063 volts (SCE); the second was run following a linear potentiodynamic scan of 10 mV per second down to -1.0 volts (SCE); and the third was conducted again at the Ecorr value.

The gold piezoelectric electrode was also used to obtain copper under-potential deposition data in a 1N cupric sulfate electrolyte; the impedance scan was made at the PAR 273-measured rest potential, 0.323 volts (SCE).

Four scans were made on a copper electrode in cupric sulfate at three different concentrations. The first was made at 0.02 N cupric sulfate; the second in the same concentration after ramping down from the rest potential to -0.5 volts (SCE); the third, was conducted at 0.2 N at the rest potential of -0.013 volts (SCE); and the final run was at 1 N at the rest potential of 0.053 volts (SCE).

FRA impedance scans were conducted, using the 1260/ 273 combination, (as shown in Figure 9.3) on a series of PCEs under various cell, electrolyte, and operating conditions: various electrolyte concentrations, aerated and de-aerated; with crystals oscillating and not oscillating; at the equilibrium potential, as measured by the PAR273, and at potentials displaced from equilibrium by PAR273-applied potentials. The experiments were conducted in order to determine the effects of key parameters on the range of measured interface impedance, R and C values. The resulting RC time constants would be the basis for pulsed deposition schedules for copper, nickel, silver, or zinc.

The oscilloscope was used (as shown in Figure 9.4) to observe and measure the RC time constant behavior of various metal/electrolyte interfaces in the 6 mL cell. The pre-cell resistor, R_1, was chosen such that its time constant would be large compared to that of the cell and the interface charge/discharge cycle would be visible on the scope. The perturbing signal was a square-wave (.1 to .5 sec at .5 to 1.0 volts) generated by the PAR273 and applied across the cell. This is a very different kind of perturbation than that utilized by the FRA (1250 or 1260) which uses a low amplitude, single sine wave of

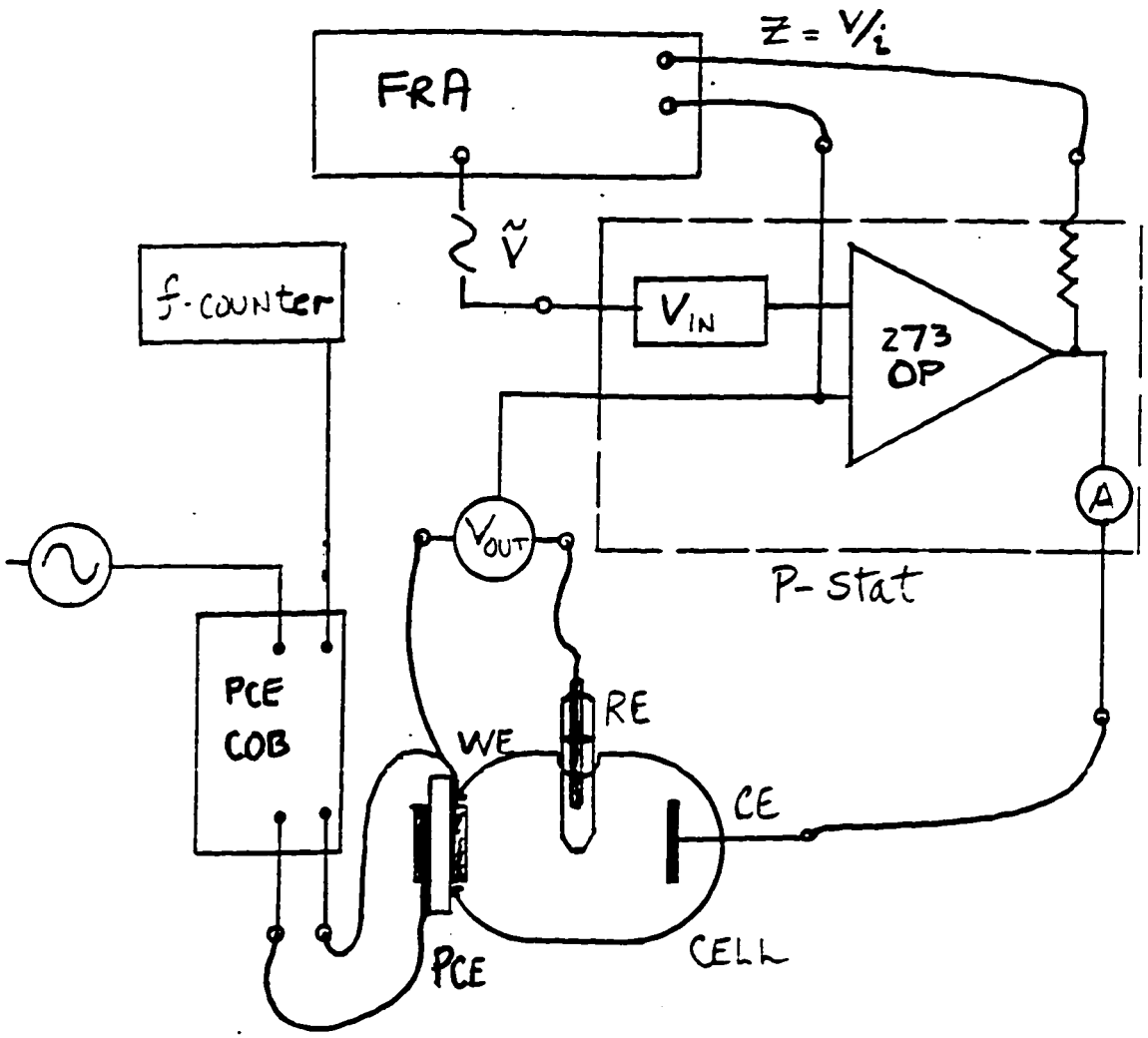

Figure 9.3. INSTRUMENTATION TO MEASURE EFFICIENCY OF THE INTERFACE PROCESS as a function of operating schedule:

$$charge \quad Q = \int i dt$$

$$mass \quad m = \frac{\Delta f}{S}$$

efficiency, mass-to-charge ratio

$$M_q = \frac{\Delta f F}{SQ}$$

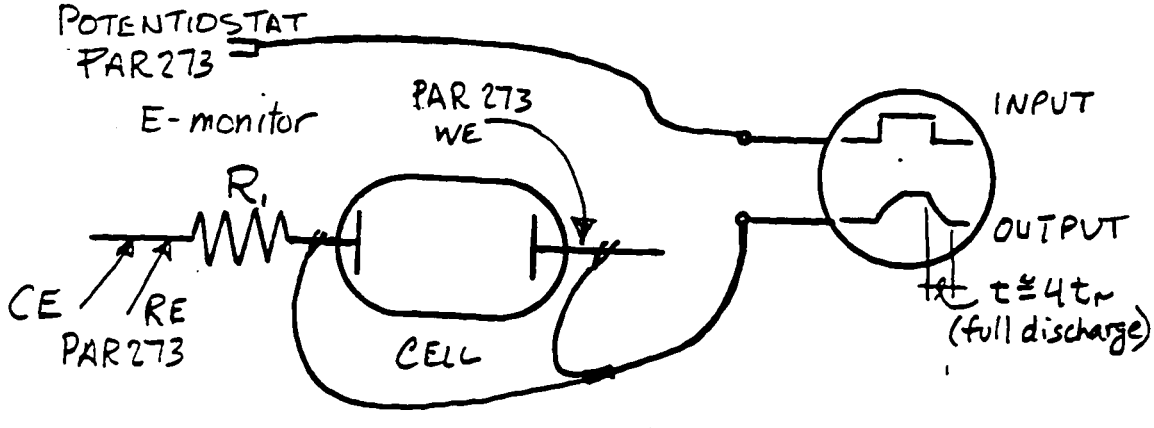

Figure 9.4. OSCILLOSCOPE METHOD for observing and measuring the electrochemical interface time constant, t_r

varying frequency. The scope trace shows both the input step and the charge-discharge curve of the cell response.

The PCEs were used to test the efficiency (charge-to-mass ratio, Mq) versus electrodeposition (cell) current, under galvanostatic control by the PAR273 (setup is shown in Figure 9.3), for (1) electrolyte concentration, under dc conditions, (2) PCE size (frequency, and electrode diameter), under dc conditions, and (3) RC time constant-based electrodeposition schedules.

(1) Plating solutions of 0.02, 0.2, and 1.0 N CuSO4 were prepared and test-plated in the 6 mL cell onto a gold, 10 Mhz, 150 mil dia., PCE under dc (galvanostatic) conditions at a series of cell currents. The PCE fundamental frequency shift and the integrated cell current were monitored for each test.

(2) With a plating solution of 0.2N CuSO4, the plating efficiency (as Mq) was checked for three different gold PCEs (10 Mhz 150 and 250 mil dia, and 5Mhz 150 mil dia), under dc (galvanostatic) conditions at a series of cell currents. The PCE fundamental frequency shift was recorded for each plating condition along with the integrated current for the plating period.

(3) Using the 10 Mhz gold PCE, in a solution of 0.2N CuSO4, a series of plating schedules were tested which were based on multiples of the FRA-measured RC time constant (t = 518 ms) to obtain current *on - off* and cycle durations. The PCE frequency shifts and integrated cell current values were recorded to compute efficiency as Mq for each of several different pulse cell current values.

Results

Once stabilized within the fresh or seawater cell, the platinum Ecorr (Ag/AgCl) shows rapid ***response to changes in sparge condition***. The three curves plotting Ecorr versus time for the experiments, on abrupt sparge changes (nitrogen to air, or oxygen, or carbon dioxide, or air to nitrogen) show the greatest and most rapid to be that caused by the switch from nitrogen to carbon dioxide; air to nitrogen is the slowest (see Figure 9.5). The air-nitrogen curve suggests a fairly lengthy sparge time would be required to purge the effects of dissolved gases (such as oxygen and carbon dioxide) on an electrode immersed in an aerated electrolyte. (Additional results of sparge condition experiments are shown in Appendix A.)

The 1260 FRA impedance plots for scans on the ***Rs-RC dummy cell models*** (see Figure 9.6 a and b) show the maximum phase angle at the frequency, $f = 1/RC$, and $R = |Z|_{lo} - |Z|_{hi}$, on the Bode plot, as expected. Note that $|Z|_{lo} - |Z|_{hi}$ in Figure 9.6a corresponds to the diameter of the semicircle in the Nyquist Plot, Figure 9.6b. (Additional dummy cell models are shown in Appendix C.)

The results of tests to measure the ***effects of surface roughness*** on frequency of maximum phase angle, polarization resistance, and corrosion current of LCS in nitrogen sparged seawater are summarized in Appendix B. No clear distinction can be made between the two degrees of surface roughness tested (120 and 600 grit polishes). There is reasonably good agreement between corrosion current measurements arrived at with the 1260/273 set up and those from the PAR350. At the same time, tests on samples having the same surface finish have as much as an order of magnitude variation in corrosion current though the cell conditions for successive tests is nominally the same. Ordinarily a factor of two or three might be expected in corrosion rate measurements on the same

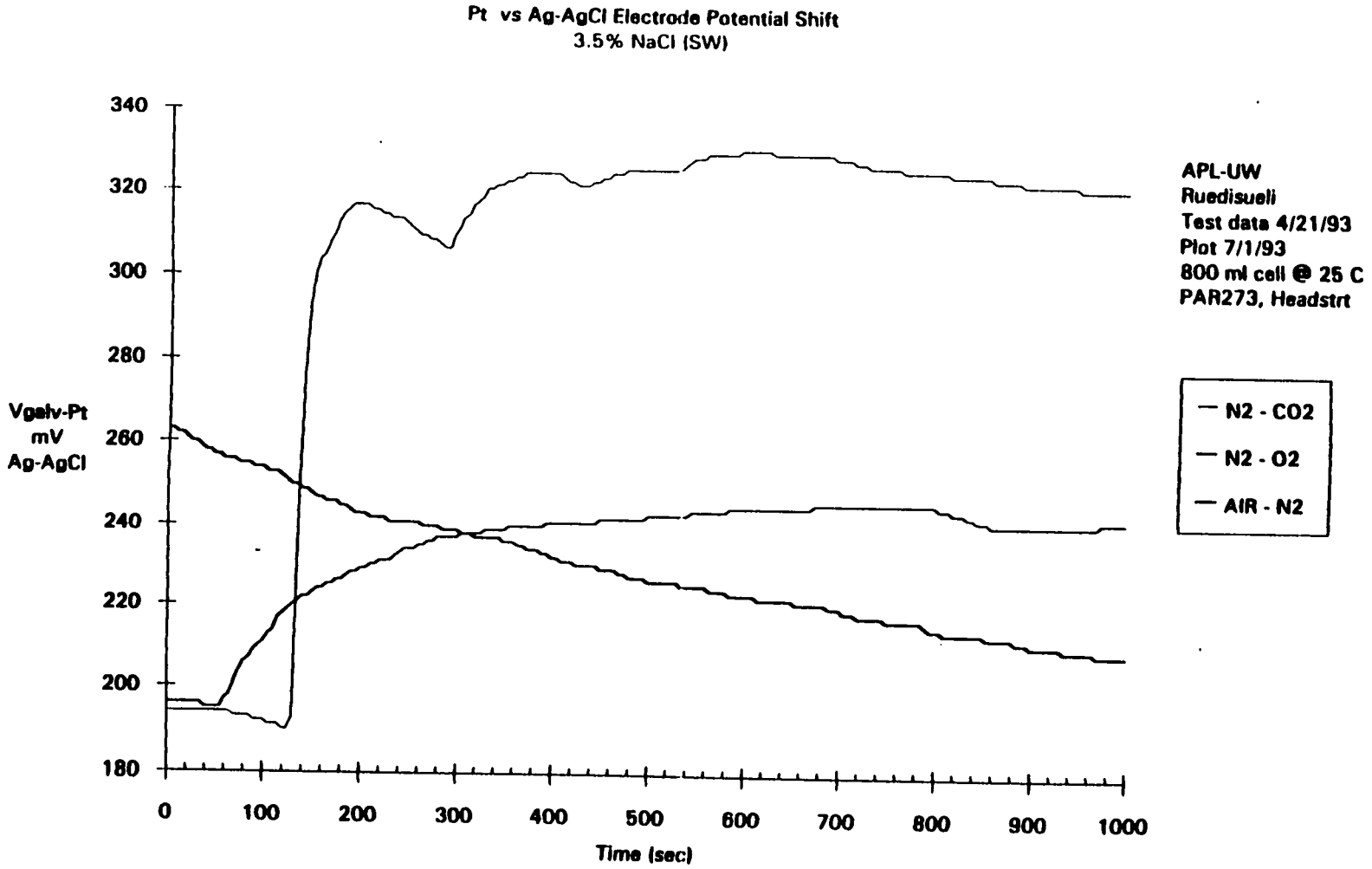

Figure 9.5. SPARGE CONDITION EFFECTS on platinum electrode rest potential, Ecorr (shown here as Vgalv-Pt).

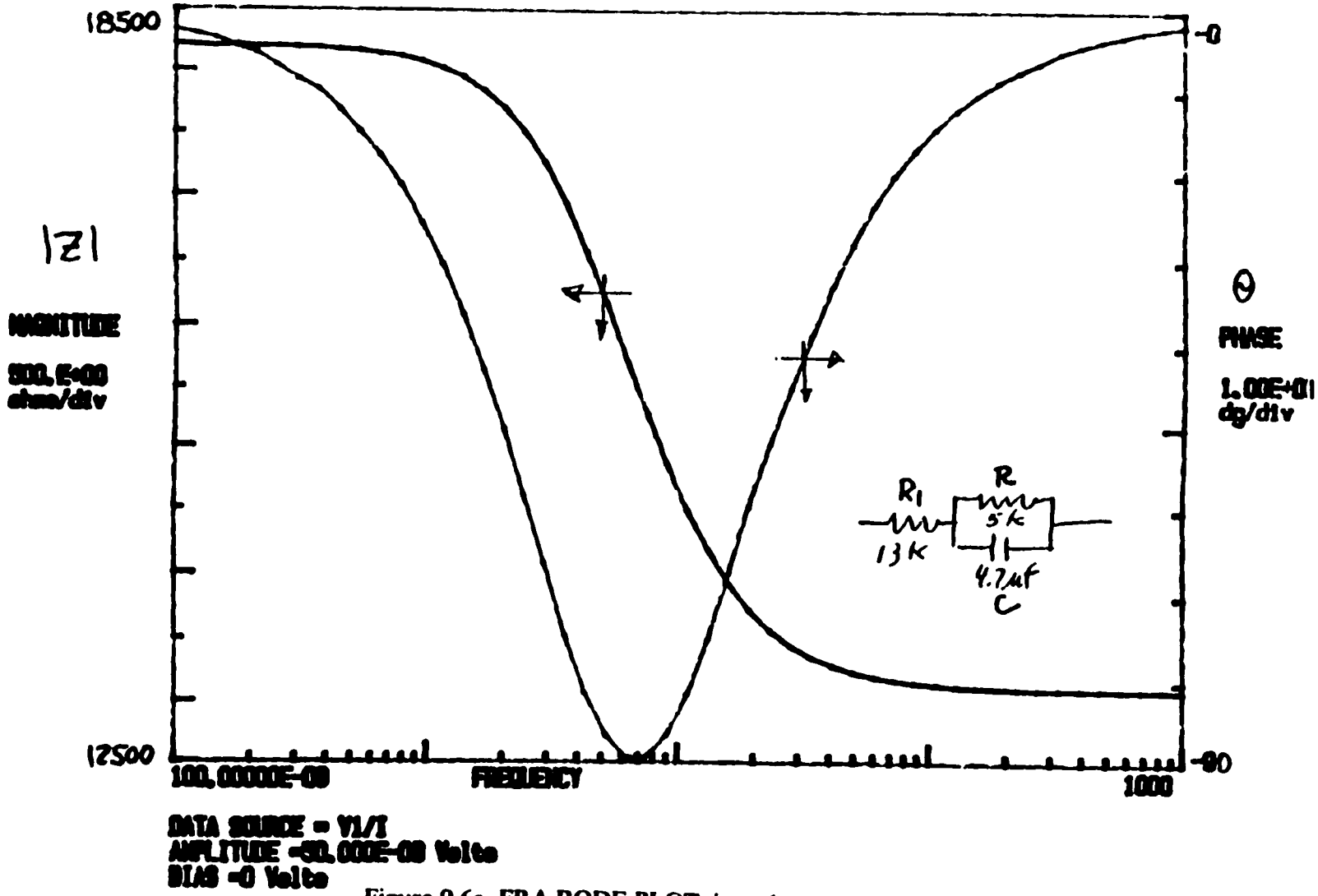

Figure 9.6a. FRA BODE PLOT, impedance magnitude, |Z|, and phase angle, θ, vs. log frequency for the R_1-RC dummy cell model.

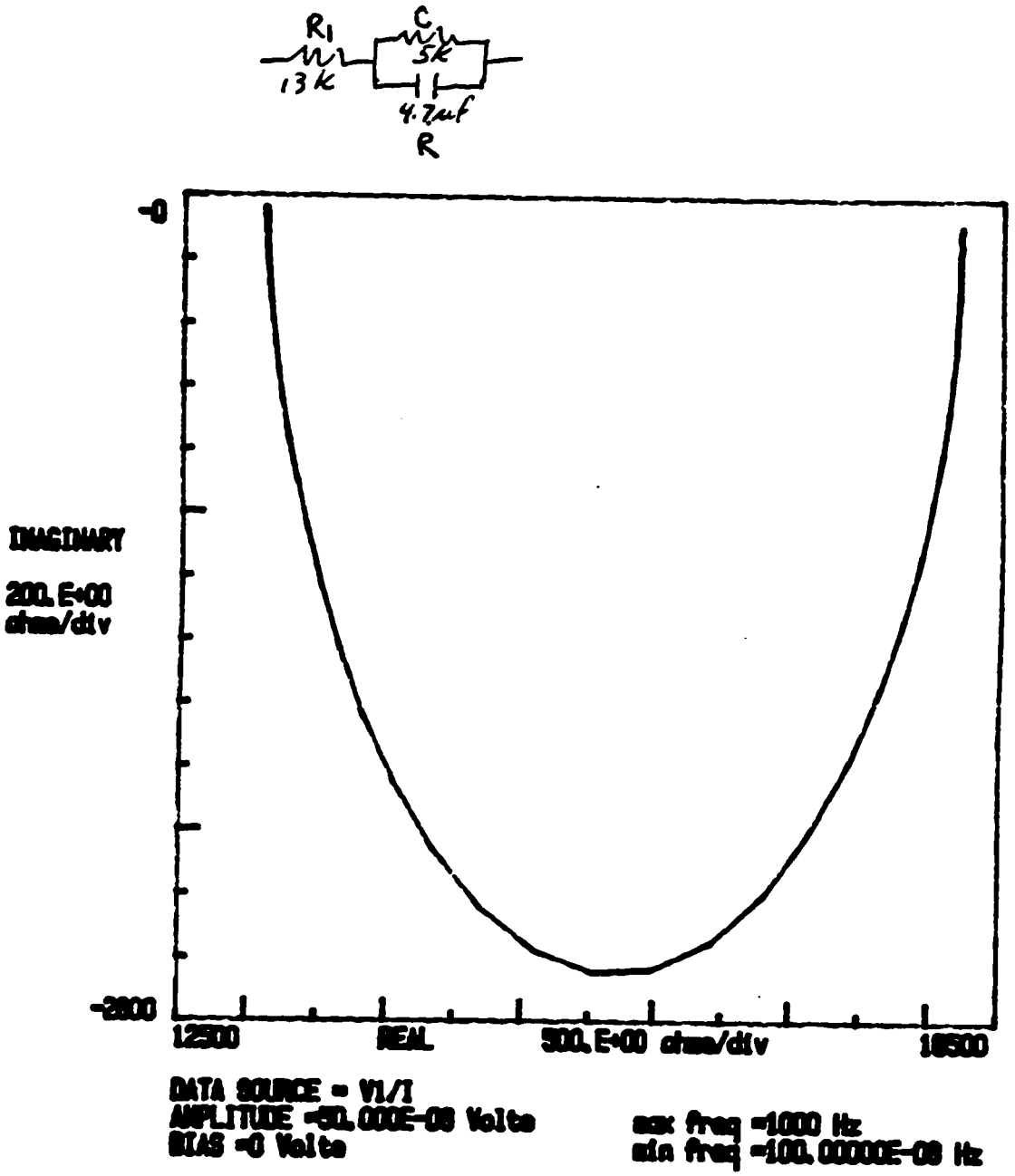

Figure 9.6b. FRA NYQUIST PLOT, real vs.imaginary impedance components for the R_1-RC dummy cell model.

sample, the actual active area of the sample involved being a likely variant from test to test. The 800 mL cell volume may not be large enough to assume negligible changes in composition of electrolyte over successive tests, especially if the test scan extends into high anodic potentials. The changes seen in a separate platinum-Ag/AgCl reference electrode system, referred to as $V_{galv\text{-}Pt}$, show the cumulative effect of changing electrolyte composition due to corrosion of the working electrode sample over successive tests. The shiny platinum electrode exposed directly to the cell electrolyte ordinarily would have a potential in deaerated seawater of between 0 and 100 mV. But due to the increasing presence of Fe^{2+} ions, the potential drops to between -300 and -600 mV (Ag/AgCl).

The ***tabulated data for the corrosion of LCS and Bronze*** (Cu-Ni-Al) in fresh and seawater under various sparge conditions as measured by (1) the 1260/273 system and (2) the PAR 350 show very good agreement (see Appendix D). In the 1260/273 system the corrosion rate (current density) is computed from the polarization resistance which is taken as the difference between the impedance magnitude measured at very low frequencies $|Z|_{\omega=lo}$ and that measured at high frequencies, $|Z|_{\omega=hi}$. The PAR 350 uses the linear polarization/Tafel intercept method wherein the voltage vs. log current anodic and cathodic curves are projected back from their linear high field (or Tafel) regions to their intercepts with the current axis at the Ecorr potential to give the corrosion current density (as shown in Figure 2.8). These corrosion measurement results, on two independent electrochemical measurement systems, check the performance of the 1260/273 system for electrochemical measurements [23].

The SRI lab ***1250/273 FRA impedance spectra data*** for copper in copper sulfate solutions, gold in copper sulfate solutions, and gold in seawater are tabulated in

Appendix E and are shown in the Bode, Nyquist, and the phase angle vs. log ω plot formats. From this data, the polarization resistance, maximum phase angle frequency, double layer capacitance, and RC time constant data are to be derived as the basis for pulsed-process schedule design. While the phase angle plots for these experiments, generally, show no clear maximum values as seen in the ideal lumped-circuit model FRA plots (Figure 9.6a), there is a clear difference in all the Bode plots between the impedance magnitude, | Z |, at low frequencies and that at high frequencies; and the influence of the double layer (parallel) capacitance is evident in the linear *roll-off* region of the Bode plots. The polarization resistance, R, is taken as the low frequency - high frequency impedance magnitude difference,

$$R = | Z |_{\omega=lo} - | Z |_{\omega=hi}$$

and, the intercept of the roll-off line with the Bode plot ordinate, log | Z |, axis, shown in Figure 9.7, is taken as:

$$\log 1 / Cp = \log | Z |_{intercept,\ \omega=0}$$

Then the EIS-measured relaxation *time constant* for the WE interface is:

$$t_r = Cp\ R$$

And the corresponding frequency is:

$$f = 1 / CpR,\ \omega=2\ \pi\ f$$

The time constant can also be measured, as discussed previously (Chapter 4), by using a pulsed PCE. The *time constant* is taken, as shown in Figure 9.8, to be the decay time of the crystal frequency response after the pulse is shut off. Values for both the EIS

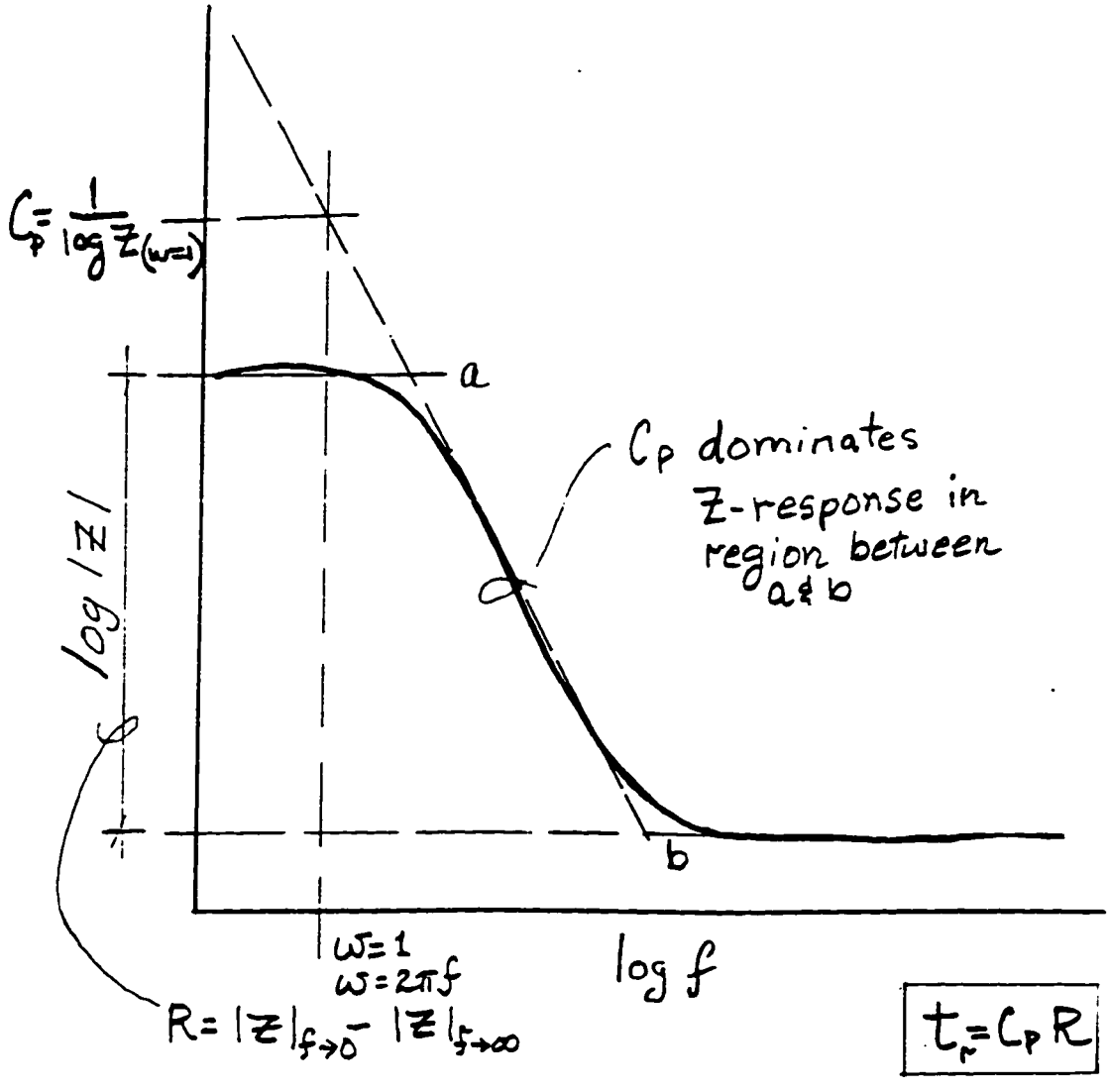

Figure 9.7. TIME CONSTANT FROM BODE PLOT

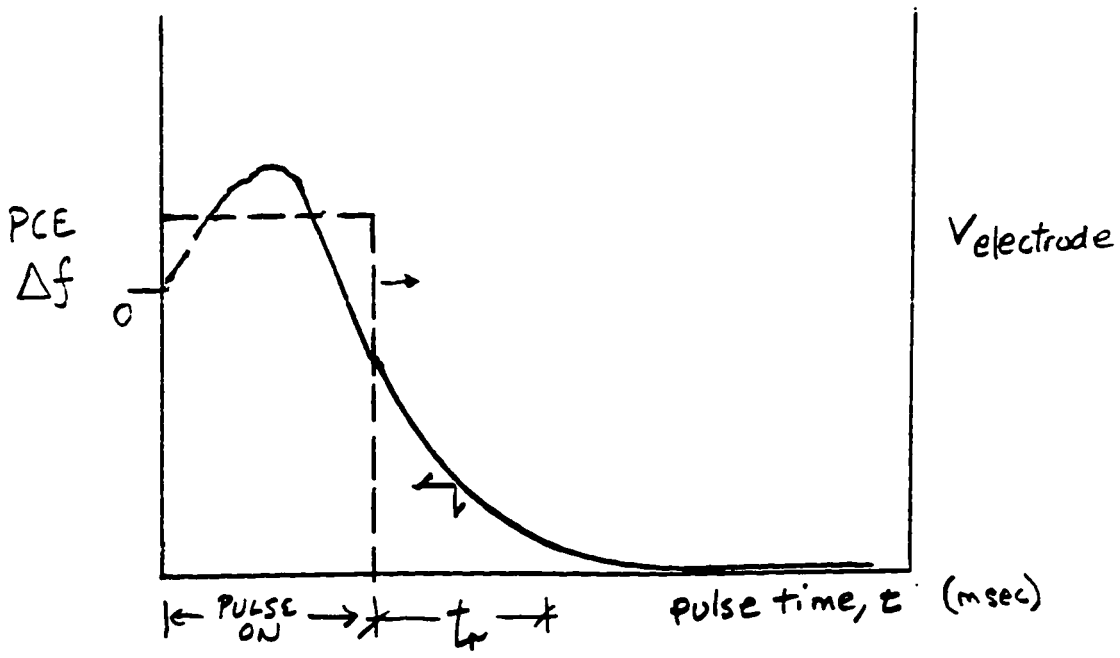

Figure 9.8. TIME CONSTANT FROM PCE

and PCE techniques [22] and those obtained by calculations [8, 19] are summarized in tables in Appendix E.

The ***tabulated values for the FRA (1260/273) RC time constant measurements*** on PCEs of various metals in various electrolytes are shown in Appendix E. Vapor deposited Cu PCE's (which had performed well during the SRI tests) corroded unexpectedly in the CuSO4 solution in follow-up tests. The corrosion resistance of copper in copper sulfate solutions is ordinarily *good* for wrought or cast copper (as opposed to *excellent* or *poor*) [28]. The exact nature of the vapor deposited Cu surface is not known, but compared to wrought or cast specimens, they are very thin and relatively granular. Copper corrosion resistance to acids, in general, is quite good, and to sodium chloride as well; but not in the presence of ferric or ferrous sulfate (or chloride). A small amount of iron contamination in the vapor deposit or the solution would present a problem, especially if the solution were aerated.

The range of values for the EIS-measured *time constants* for the (WE) interface obtained from the follow-on (1260/273) tests support the method used, and values measured, in the earlier (1250/273) tests. The measured *time constant*, t_r=518 ms, for $Cu/CuSO_4$ (0.2N cupric sulfate) interface was selected as the basis for an optimized electrodeposition schedule to be tested using the PCE method of determining mass-to-charge ratios of candidate pulse plating schedules.

The ***tabulated results of the oscilloscope measurements*** of the RC time constants are shown in Appendix E. The ohmic and capacitive components were clearly distinguishable in the scope trace and further demonstrated the measurable dynamic properties of the electrochemical interface.

The results of the ***PCE tests for optimized pulsed Cu electrodeposition schedules*** are shown in Figures 9.9, 9.10, and 9.11; a plate showing the (PCE) subjects for these tests is included in Appendix F. The *figure of merit* in these tests is the *charge-to-mass ratio* (efficiency) as a function of cell currents for the various parameters tested cell solution concentration, PCE diameter and crystal fundamental frequency, and pulse-schedule). The test PCE 's were gold, providing background contrasting with the copper deposit which aided the visual evaluation of the deposit.

The results of the ***dc plating tests on 10 Mhz Au PCEs in 0.02, 0.2, and 1.0 N cupric sulfate solutions*** are shown in Figure 9.9 (end of chapter), indicate the best solution concentrations would be 1N or 0.2N with the second highest Mq and a sharper response to cell current variation.

The results of the ***dc plating tests on Au (10 Mhz 150 and 250 mil, and 5Mhz 150 mil dia) PCEs in 0.2 N cupric sulfate,*** shown in Figure 9.10 (end of chapter), indicate that the most responsive test PCE (high Mq and variation with cell current) is the 10 Mhz, 150 mil diameter.

The results of the ***ac (pulsed-plating schedule) optimization tests on Au 10 Mhz , 150 mil PCE in 0.2 mil cupric sulfate*** in Figure 9.11 (end of chapter), indicate the optimum plating schedule to be one time constant ON and OFF at a cell current of 2mA, which is, approximately, the calculated limiting current density.

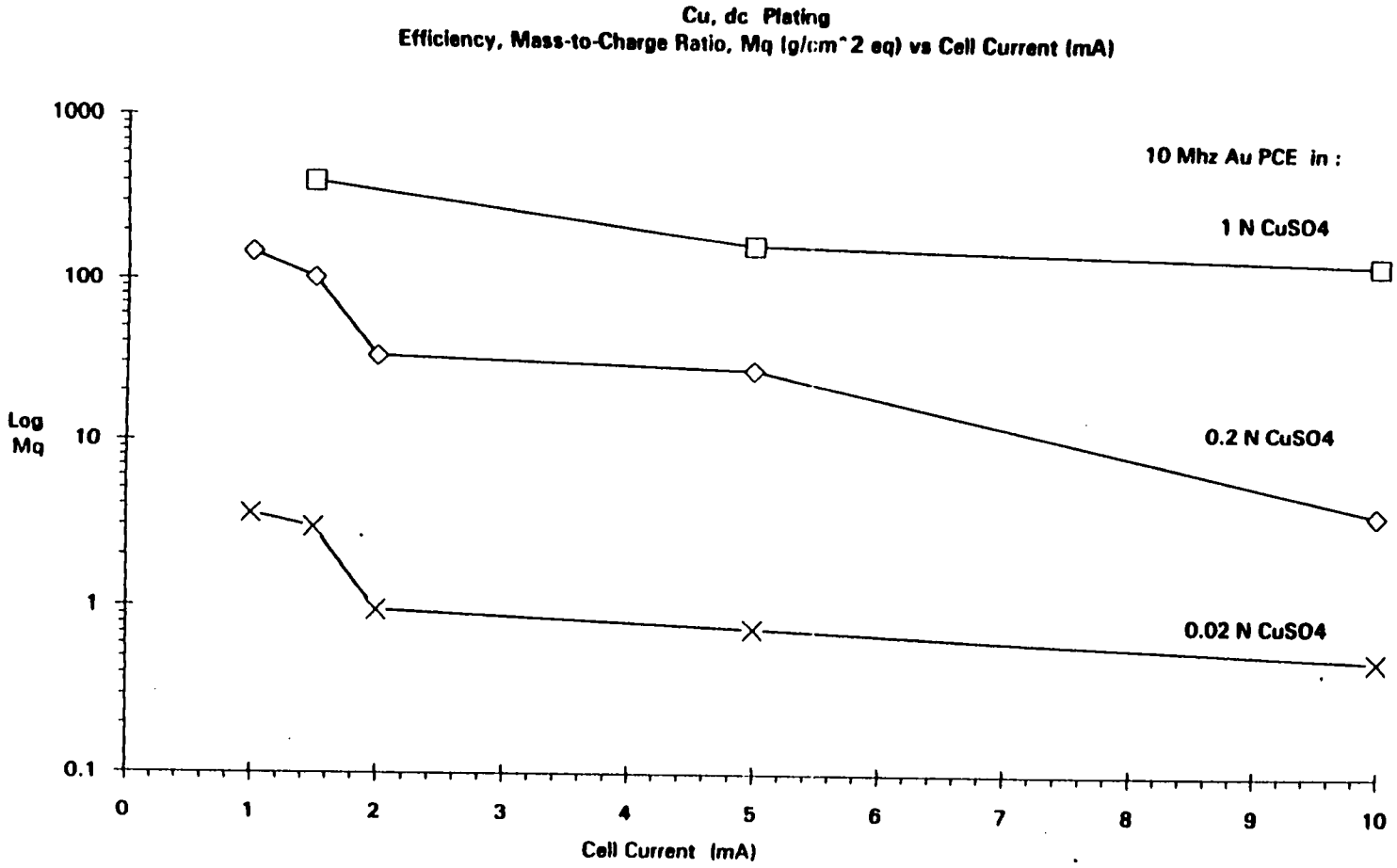

Figure 9.9. **dc** PLATING TESTS on 10 Mhz Au PCEs in 0.02, 0.2, and 1.0 N cupric sulfate solutions

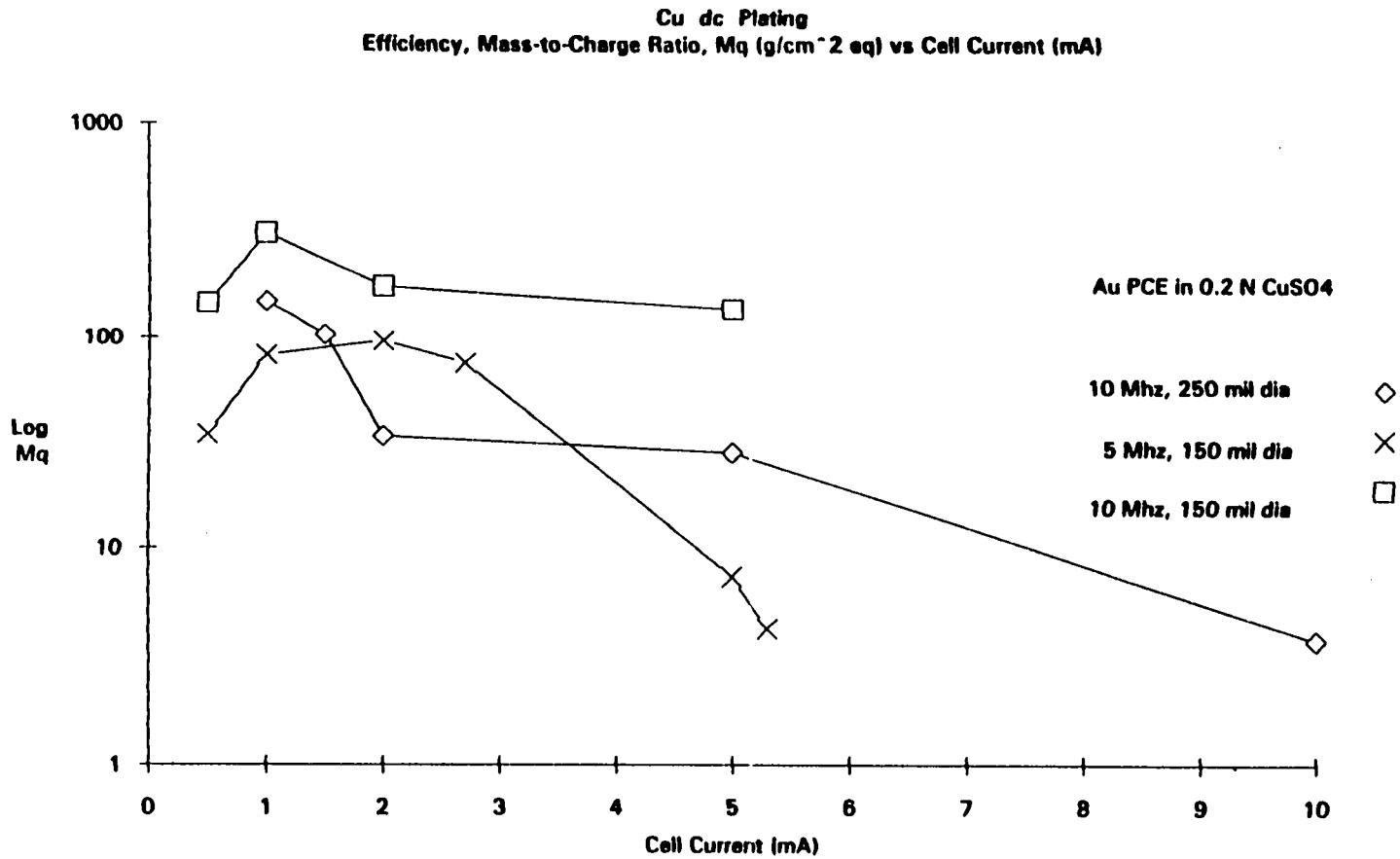

Figure 9.10. **dc** PLATING TESTS on Au (10 Mhz 150 and 250 mil, and 5Mhz 150 mil dia) PCEs in 0.2 N cupric sulfate

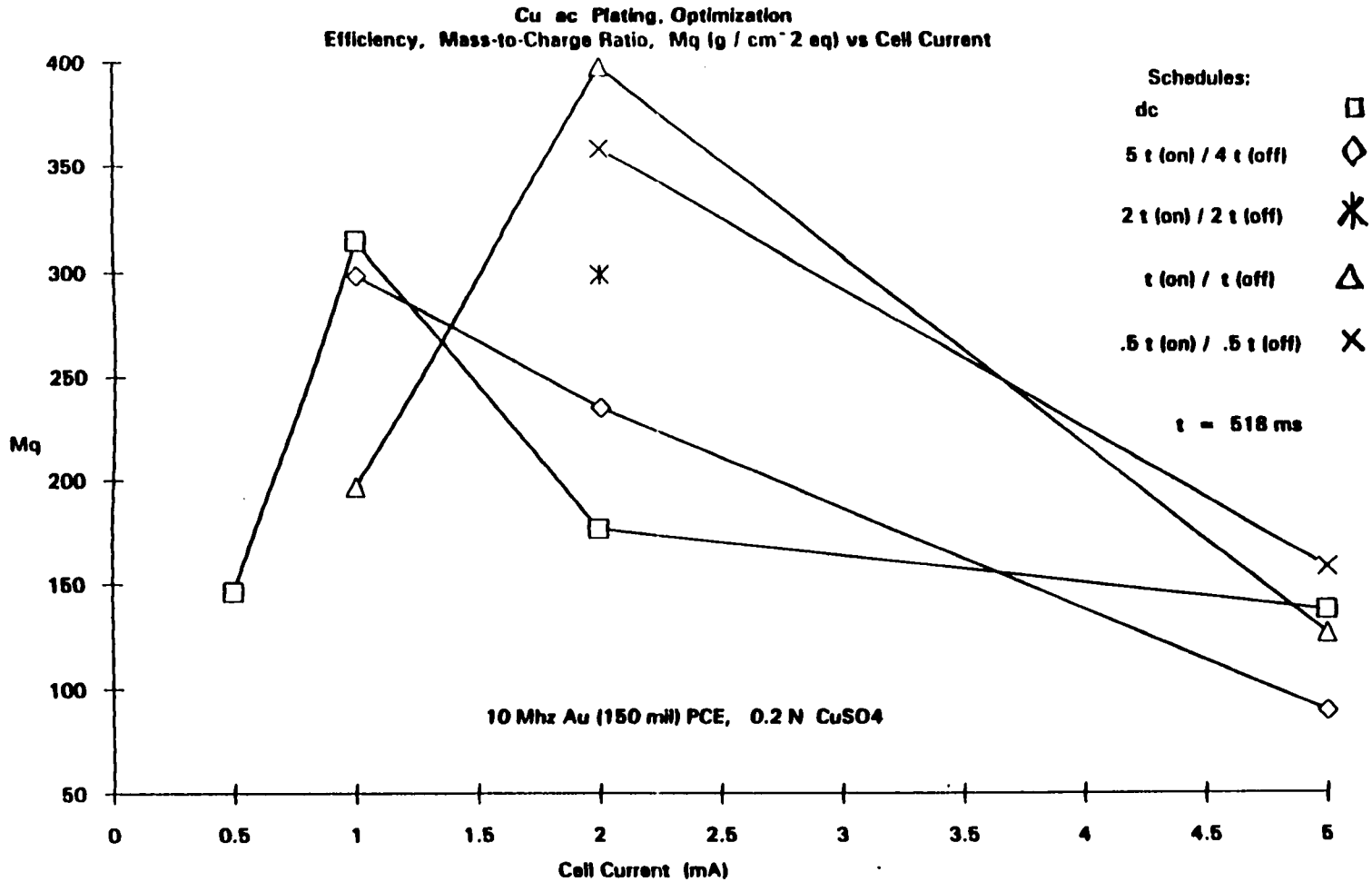

Figure 9.11. ac (PULSED-PLATING SCHEDULE) OPTIMIZATION TESTS on Au 10 Mhz , 150 mil PCE in 0.2 mil cupric sulfate

CHAPTER 10

Discussion, Summary, and Conclusion

Recap and Discussion

State-of-the-art electrochemical impedance spectroscopy and piezoelectric crystal electrode techniques, combined with conventional electrochemical potentiostatic and galvanostatic control methods, have been used to develop a strategy for the rational design of cyclically optimized *ac* electrochemical processes. The desired optimum operating cycle in many cases is expected to lie between two conventional operating extremes: dc approaching limiting current density and short, high frequency pulses at high current density. The dc mode is based on steady-state equilibrium models. Other models, based on certain restrictive assumptions about the dynamics of the interface, predict best performance at high (exceeding limiting) current densities at pulse frequencies approaching infinity.

In the present work the *optimum apportionment* of cell current among the reactions in the interface is achieved with *operating cycles based on the measured dynamics of the fully engaged electrochemical interface*. The dynamics of the electrochemical system are analogous to those of mechanical and electrical systems and result in natural periods corresponding to system time constants. Other approaches to the study and control of reactions in the electrochemical interface have been reviewed. The present study applies the electrolyte series resistance, parallel capacitor and polarization resistance interface model to obtain *measured time constant* [1,2]. The time constants are measured by electrochemical impedance spectroscopy. The periodic control, current/

potential schedules based on these time constants are tested by the *in situ* piezoelectric crystal electrode measurement of mass-to-charge ratio.

The parameters of primary interest for periodic control schedules are the polarization resistance, R , and the parallel capacitance, C_p, which is assumed to consist of the double layer capacitance and an intermediary product inventory pseudo-capacitance. The second capacitance being parallel to the double layer, the two are additive. The two systems studied in the SRI-EIS data set, see Appendix E, copper redox, and noble metal (gold) in natural water (seawater), each demonstrate two very different regimes of reaction control. Systems with EIS Nyquist real vs. imaginary (R vs. X) plots which form a semi-circle intersecting the abscissa at both high and low frequency, are reaction rate or charge transfer controlled. Those which intersect the abscissa at low frequency but approach linear behavior at high frequency, are mass transfer (diffusion) controlled. Note that the three cases which exhibit the semi-circular Nyquist plots all have R values equal to the semi-circle, are diameter which are in good agreement with the R value derived from their respective Bode plots. In the copper redox system, at low concentrations and low field (no or only very small, applied cell voltage), the reaction is charge transfer controlled, while at high field or high concentration, it is more likely diffusion controlled. The noble metal/water system, on the other hand, is most likely charge transfer controlled when a high field (high cell voltage) is applied; diffusion controlled in a low field.

With the exception of the 0.2 and 1 N copper/copper sulfate systems, all the measured parallel capacitances are considerably smaller than expected. The double layer capacitance is typically 20 to 60 μF. The observed behavior of the diffusion controlled interface systems argues for a more exact model. The Rs-RCp model may be over simplified to assist in mechanistic explanations and is frequently replaced with an R-R-

Z_W,C where the Z_w represents the *Warburg* impedance which is in series with the polarization resistance and in parallel with the double layer capacitance. However, for present purposes, the over-riding factor in many (if not most) cases is that there *is* a *measurable* characteristic capacitive reactance, charge-discharge (RC) *time constant*, t_r, which is a reasonable basis for a pulsed-process schedule.

This work has discussed but not dealt experimentally with systems where in a pseudo inductive element has been observed. Systems with both capacitive and inductive, properly proportioned, would be oscillatory.

The *RC* time constants arrived at using EIS can be compared to similar parameters arrived at by other methods. A calculation (i.e. using Sands' equation) based on assumed values for the diffusion layer thickness, the diffusion coefficient and the bulk concentration of the electro-active species can yield order of magnitude estimates of the characteristic time constant, $t_r = 1/f$. Values obtained from such calculations are around 0.3 Hz and in reasonable agreement with the values in Appendix E, measured for the copper/copper sulfate system.

The time constant measurement results of the non-oscillating crystal electrode study can be compared with time constants derived from the Buehler [3] PCE work on pulsed-plating of copper from copper sulfate. The same electrodes and cell were used in the Buehler-PCE work as in the SRI-EIS work; the copper sulfate concentration was 0.2 N, but in this case the PCE was actually oscillating at 10 Mhz, and the frequency response of the crystal to the electrode activity was recorded for single current pulses of varying length. The oscillating electrode frequency vs. time curve (see Figure 9.8) had three regions: (1) a non-linear, frequency-increasing indicating mass loss, or, liquid viscosity decrease; (2) a nearly linear, frequency-decreasing, mass gain, region in which deposition

occurred; and (3) with the current *off*, an exponential, frequency-decreasing region believed to be caused by concentration gradient relaxation. This third region would correspond to a pseudo-capacitive relaxation region. The time constants for the curve fit to the relaxation region, depended on the pulse length, but corresponded to characteristic frequencies varying from about 224 Hz down to about 120 Hz. In the EIS work, the variation occurred with concentration and applied voltage, resulting in characteristic frequencies ranging from 10.6 Hz down to 0.2 Hz. (See table comparing characteristic frequencies in Appendix E.)

Two factors could be expected to produce differences between the impedance and crystal oscillation measurement methods. First, the crystal oscillating in the shear mode at 10 Mhz very likely has some convective effect on the interface boundary layer; and second, the current pulse must be carried out in a high field. The hydro-dynamic mass transfer boundary layer thickness is inversely proportional to $\omega^{1/2}$, where ω is the angular frequency of oscillation of the crystal surface. The typical electrochemical current vs. potential curve is highly non-linear and the double layer capacitance potential-dependent. The short, high current density pulses tested in the Buehler-Hager work address a different operating regime, and present a different approach to the optimization problem. Ideally, time constant measurements should be carried out near the actual cell operating potential. The length of time required to accomplish an impedance measurement scan, by single sine FRA, however, precludes this.

Summary

The rationale for developing periodically controlled electrochemical processes has been reviewed and an approach to the design of P-C process schedules has been described and demonstrated.

1) For an Rs-RCp model, the log Z vs. log ω curve tangent to the linear capacitance dominated region, the intercept with the ω=1 ordinate yields, as expected, $\log (1/Cp) = \log |Z|_{\omega=1}$ from which the parallel capacitance, Cp, is computed.

2) In cases where $|Z|_{(\omega=0)} > 10\,|Z|_{(\omega=\infty)}$, the intercept-measured C is in excellent agreement with actual measured values for C.

3) In many cases, therefore, (although not all), the Rs-RCp model can be applied and the time constant, $t_r = CpR$, where $R = |Z|_{\omega=lo} - |Z|_{\omega=hi}$, is a measure of the dynamic response of the interface across a wide range of frequencies.

4) The oscilloscope can be used to observe and measure $t_r = CpR$ directly, in potentiostatic control mode, in a limited range of perturbation frequencies, as long as the pre-cell resistor, R_1, is selected to be on the order of 10 R_{cell}. In such cases, the cell ohmic resistance and capacitive voltage drop values are discernible and dependent upon the cell electrodes and electrolyte composition.

5) The impedance, $|Z|_\omega$, measured $t_r = CpR$ values for Cu, Ag, Ni, and Zn are scattered over an order of magnitude and not as reproducible as expected, but do support the EIS measurement method.

6) The oscilloscope measured t_r values (with a large perturbation, 1 volt) for Cu, Ag, Ni, and Zn are in a narrower range than the EIS-measured values, and nearly an order of magnitude shorter.

7) The time constants for copper electrodeposition from cupric sulfate solutions as measured by EIS are one or two orders of magnitude longer than the results obtained by the PCE method.

8) Cu plating experiments demonstrate the use of the PCE as an *in situ* microbalance which, together with the PAR273 integrated current measures the relative efficiencies as mass-to-charge (surface density) ratios for different EIS measured, time constant, t_r-based pulse current schedules: steady *dc* versus periodic current t_r/n, nt_r (*ON/OFF*) schedules (where n= some integer).

9) In order to achieve the desired *fully engaged*, dynamic interface operating condition: the best results, the highest values for the piezoelectric crystal electrode measured mass-to-charge ratio, were obtained with pulse current schedules based on alternate *ON, OFF* symmetric periods equal to *one* time constant in duration, at current density levels approaching limiting current.

Conclusion

This work demonstrates that a periodically controlled current schedule can be based on a time constant derived from electrochemical impedance measurements of the properties responsible for the dynamic behavior of the interface. The dynamic behavior of the interface is a function of its polarization resistance and parallel capacitance. The product, C_pR, is the desired time constant and, functionally, the basis for the natural cycle of the interface. The optimality of the schedule based on the C_pR time constant was determined by the *in situ* piezoelectric crystal electrode measurement of the deposition

mass-to-charge ratio, which serves as a figure of merit to compare candidate electro-deposition schedules.

Most significantly this work proves, in principle, the method of cyclic optimization by operating the process at current densities approaching the limiting current on schedules allowing the alternating charge and discharge of the interface for one full, measured interface time constant each cycle.

The present work demonstrates the effectiveness of C_pR timing as a basis for optimization of pulsed-current electrodeposition schedules for the (diffusion) limiting current density case. This work tests one optimization scheme in a broader spectrum of possibilities which includes conventional pulsed deposition conducted with short, high (exceeding limiting) current density pulses on schedules which may be asymmetric as well as symmetric and include reverse current phases. In this work, pulsed deposition schedule optimization tests, applied to copper deposition schedules based on the EIS-measured time constant, indicate the optimal schedule to be alternate current ON/OFF periods equal to the *measured time constant* at current densities approaching the limiting current density.

Based on the work reviewed and the experimental evidence presented here, it is reasonable to hypothesize further that many electrochemical processes driven at current levels approaching the mass transport limiting current density will be optimized by operating in a pulsed current mode at the measured C_pR time constant. Multiple process time constants and asymmetry of charge versus discharge time characteristics could also be reflected in the schedule design.

NOMENCLATURE

a_i activity of species i

A electrode surface area (cm^2)

B elctrochemical polarization resistance proportionality contstant (volts)

C capacitance (microfarads, μF), or concentration ($moles/cm^3$)

C^b bulk concentration ($moles/cm^3$)

C_i concentration of species i ($moles/cm^3$)

D diffusion coefficient (cm^2/sec)

E cell potential (volts)

E^o half-cell potential, standard state (volts)

E_{corr} electrode equilibrium potential, (volts, with respect to reference electrode)

f_o piezoelectric crystal fundamental frequency of oscillation (hz, sec^{-1})

F Faraday's constant (charge, 96487 coulombs/equivalent)

G Gibbs free energy (joules)

H enthalply (joules)

I cell current (amperes, A)

i current density ($amperes/cm^2$)

i_o exchange current density ($amperes/cm^2$)

i_L limiting current density ($amperes/cm^2$)

m electrode surface mass, areal density (gm/cm^2)

M molecular weight (gms)

n number of moles or equivalents

n electrode overpotential (volts, with respect to reference electrode)

Ni ionic flux of species i ($moles/cm^2$-sec)

Q integrated charge passed during some time interval (coulombs)

Q integrated charge passed during some time interval (coulombs)

r reaction rate (moles/cm^2-sec)

R electrical resistance (ohms), or gas constant (8.314 joules/mole-°K)

S piezoelectric crystal sensitivity factor (gms-sec/cm^2)

t time (sec)

t_r relaxation time (sec)

T temperature (°K or °C)

V velocity of cell convective fluid motion (cm/sec)

W weight (gravimetrically measured mass) of electrochemical reaction product (gm)

X electrical reactance capacitive (μF), or inductive (henrys)

z_i charge of oxidation number of species i

Z electrical complex impedance (ohms)

Greek Symbols

α electrochemical reaction symmetry factor

β Tafel constant (anodic or cathodic) (volts)

Δ change in parameter

Φ potential profile

μ ionic mobility, or micro-

θ phase angle

τ relaxation time constant (sec)

ω angular frequency (radians/sec)

Subscripts

a anodic
b bulk

c cathodic

i species

p polarization, parallel

r relaxation

s series, surface

REFERENCES

CHAPTER 1

1. Fechner, G.T., *J. Chemie u Physik*, 23, 121, 1828. (see also, *Schweigg. J.*, 53, 141, 1828.)

2. Wojtowicz, J., *Modern Aspects of Electrochemistry*, Vol. 8, J. O'M. Bockris and B.E. Conway, Editors, pp. 47-120, Plenum Press, New York, 1972.

3. Li, W., Nobe, K., and Pearlstein, A.J., "Electrodissolution Kinetics of Iron in Chloride Solutions: VIII. Chaos in Potential/Current Oscillations", *J. Electrochem. Soc.*, Vol. 140, No. 3, March 1993, pp. 721-728.

4. Ruedisueli, R.L., Hager, H.E., and Sandwith, C.J., "An Application of a State-of-the-Art Corrosion Measurement System to a Study of the Effects of Alternating Current on Corrosion," *Corrosion*, Vol. 43, No. 6, June, 1987, pp. 331-338.

5. Kwiatkowski, L., and Mansfeld, F., "Surface Modification of Stainless Steel by an Alternating Voltage Process," *J. Electrochem. Soc.*, Vol. 140, No. 3, March 1993, pp. L39-L41.

6. Beck, T.R., "Industrial Electrochemical Processes", *Techniques of Electrochemistry*, E.Yeager and A.J. Salkind, eds., John Wiley & Sons, New York, 1978, Vol. 3, Ch1, pp. 1-47.

7. Spotnitz, R.M., Spillman, R.W., and Lundquist, J.T., Jr., "Economics of Electrolytic Processing," *J. Electrochem. Soc.*, Vol. 134, No. 10, October 1987, pp. 2435-2441.

8. Bich, Nguyen N. and Bauman, J., "Pulsed Current Cathodic Protection of Well Casings," *Materials Performance*, Vol. 34, No. 4, 1 April 1995, pp.17-21.

9. Dabowski, J., "Pulsed Rectifier Limitations for Well Casing Cathodic Protection," *Materials Performance*, Vol. 34, No. 10, 1 October 1995, pp. 25-28.

10. Berube, L. PH. and Piron, D.C., "Zinc electrowinning under Periodical Reverse Current (PRC)," *J. Electrochem. Soc.*, Vol. 134, No. 3, March 1987, pp. 5562-5572.

11. Varjian, R.D., "Electrolytic Processing," *Interface*, Vol. 3, No. 3, Fall 1994, pp. 24-28.

12. Douglas, J.M. and Gaitonde, N.Y., *Ind. & Eng. Chem. Fundamentals*, June 1967, pp. 265.

CHAPTER 2

1. Jones, D. A., *Principles and Prevention of Corrosion*, Macmillan Publishing Company, New York, 1992, pp. 39-70.

2. Pourbaix, M., *Lectures on Electrochemical Corrosion*, Plenum Press, New York, 1973, pp. 201-295.

3. Pourbaix, M., *Atlas of Electrochemical Equilibria in Aqueous Solutions*, NACE, Houston, 1974.

4. Snoeyink, V. L. and Jenkins, D., *Water Chemistry*, John Wiley & Sons, New York, 1980, pp. 316-378.

5. Bockris, J. O'M. and Reddy, A.K.N., *Modern Electrochemistry*, Plenum/Rosetta, New York, 1977, Vol. 2, pp. 876-878, 1126, 1126.

6. Rao, Y.K., *Stoichiometry and Thermodynamics of Metallurgical Processes*, Cambridge University Press, New York, 1985, pp. 410-427.

7. Barrow, G.M., *Physical Chemistry*, McGraw-Hill Book Company, Inc., New York, 1961, pp. 585-616.

8. Stumm, W. and Morgan, J.J., *Aquatic Chemistry*, John-Wiley & Sons, New York,1981, pp. 418-428.

9. Wagner, C. and Traud, W., *Z. Elektrochem.*, Vol. 44, 1938, pp.391.

10. Stern, M. and Geary, A.L., *J. Electrochem. Soc.*, Vol. 104, 1957, pp.56.

CHAPTER 3

1. Van Vlack, L.H., *Elements of Materials Science and Engineering*, Addison-Wesley Publishing Co., Reading, MA.,1980, pp. 50.

2. Halliday, D. and Resnick, R., *Physics of Students of Science and Engineering*, John Wiley&Sons, New York, 1965, pp. 854-859.

3. MacDonald, D.D., *Transient Techniques in Electrochemistry*, Plenum Press, New York, 1977, pp. 47-67.

4. Macdonald, J.R., *Impedance Spectroscopy*, John Wiley & Sons, New York, 1987, pp. 83.

5. Bockris, J.O'M. and Reddy, A.K.N., *Modern Electrochemistry*, Plenum/Rosetta, New York, 1977, Vol. 1, pp. 730.

6. Mansfeld, F., "Recording and analysis of AC impedance data for corrosion studies", *Corrosion*, Vol. 36, No. 5, NACE, May 1981, pp. 301-307.

7. Reed-Hill, R.E., *Physical Metallurgy Principles*, Litton Educational Publishing, Inc., Monterey, CA, 1973, pp. 441.

8. Barrow, G.M., *Physical Chemistry*, McGraw-Hill Book Company, Inc., New York, 1961, pp. 528-546.

9. Stumm, W. and Morgan, J.J., *Aquatic Chemistry*, John-Wiley & Sons, New York,1981, pp. 112-116.

10. Randles, J.E.B., "Kinetics of Rapid Electrode Reactions," *Discussions of the Faraday Society*, No. 1, 1947, pp. 11-19.

11. Taylor, S.R. and Gileadi, E., "Physical Interpretation of the Warburg Impedance," *Corrosion*, Vol. 51, No. 9, September 1995, pp. 664-671.

CHAPTER 4

1. Van Vlack, L.H., *Elements of Materials Science and Engineering*, Addison-Wesley Publishing Co., Reading, MA.,1980, pp. 303-306.

2. Buehler, M.F., "Quantification of Iron Corrosion and Copper Pulse Plating Using Piezoelectric Quartz Crystals," MS Thesis, University of Washington, 1986.

3. Deakin, M.R. and Melroy, O., "Underpotential Metal Deposition on Gold, Monitored *In Situ* with a Quartz Microbalance," *J. Electroanal. Chem.*, 239, 1988, pp. 321-331.

4. Hager, H.E., Ruedisueli, R.L., and Buehler, M.F., "The Use of Piezoelectric Crystals as Electrode Substrates in Iron Corrosion Studies: the Real-Time, *In Situ* Determination of Dissolution and Film Formation Rates," *Corrosion*, Vol. 42, No. 6, June, 1986, pp. 345-351.

5. Simpson, R.L., "*In Situ* Surface Analysis at Solid-Liquid Interfaces Using Piezoslectric Quartz Crystals and Total Internal Reflectance Spectrometry," PhD Dissertation, University of Washington, 1985.

6. Buttry, D.A., "The Quartz Crystal Microbalance as an *In Situ* Tool in Electrochemistry," *Electrochemical Interfaces: Modern Techniques for In-Situ Interface Characterizaion*, Ed. H.D. Abruna, VCH Publishers, Inc., 1991, Ch. 10, pp. 529-567.

7. Buttry, D.A., and Ward, M.D., "Measurement of Interfacial Processes at Elextrode Surfaces with the Electrochemical Quartz Crystal Microbalance," *Chem. Rev.*, Vol. 92, 1992, pp. 1355-1379.

8. Hillier, A.C., and Ward, M.D., "Scanning Electrochemical Mass Sensitivity Mapping of the Quartz Crystal Microbalance in Liquid Media", *Anal. Chem.*, Vol. 64, 1992, pp. 2539-2554.

9. Deakin, M.R., and Melroy, O.R., "Monitoring the Growth of an Oxide Film on Aluminum *In Situ* with the Quartz Crystal Microbalance," *J. Electrochem. Soc.*, Vol. 136, No. 2, February 1989, pp. 349-352.

10. Feldman, B.J., and Melroy, O.R., "The Mechanism of Electroless Cu Deposition: Extraction of the Oxidative and Reductive Electrochemical Half-Cell Currents from a Complete Bath," *J. Electrochem. Soc.*, Vol. 136, No. 3, March 1989, pp. 640-643.

11. Deakin, M.R., and Byrd, H., "Prussian Blue Coated Quartz Crystal Microbalance as a Detector for Electroinactive Cations in Aqueous Solution," *Anal. Chem.*, Vol. 61, 1989, pp. 290-295.

12. Ivanov, D.V., and Yelon, A., "Chemical Sensitivity of the Thickness Shear-Mode Quartz-Resonator Nanobalance," *J. Electrochem. Soc.*, Vol. 143, No. 9, September 1996, pp. 2835-2841.

CHAPTER 5

1. Schumacher, R., Gordon, J.G., and Melroy, O., "Observation of Surface Reconstruction of Copper and Silver Electrodes in Solution Using a Quartz Microbalance," Research Report, IBM Almaden Research Center, San Jose, California, 1985.

2. Thirsk, H.R., and Harrison, J.A. *A Guide to the Study of Electrode Kinetics. Academic Press*, New York, 1972, pp.83, 88.

3. Ibl, N., "Some Theoretical Aspects of Pulse Electrolysis," *Surface Technology*, 10, (1980), pp. 81-104.

4. Simpson, R.L., "*In Situ* Surface Analysis at Solid-Liquid Interfaces Using Piezoslectric Quartz Crystals and Total Internal Reflectance Spectrometry," PhD Dissertation, University of Washington, 1985.

5. Liu, S.H., "Fractal Model for the ac Response of a Rough Interface", *Physical Review Letters*, Vol. 55, No. 5, 29July1985, pp. 529-532.

6. Bates, J.B., and Chu, Y.T.,"Surface Topography and Electrical Response of Metal-Electrolyte Interfaces", *Solid State Ionics*, 28-30 (1988), pp. 1388-1395.

CHAPTER 6

1. Szabo, T.T., Lloyd, W.A., Cannon, M.R., and Speaker, S.S., "Controlled-cycling extraction," *Chemical Engineering Progress*, Vol. 60, No.1, January 1964, pp. 66-70.

2. Schrodt, V.N., Sommerfeld, J.T., Martin, O.R., Parisot, P.E., and Chien, H.H., "Plant-scale study of controlled cyclic distillation," *Chemical Engineering Science*, Vol. 22, 1967, pp. 759-767.

3. Wade, H.L., Jones, C.H., Rooney, T.B., and Evans, L.B., "Cyclic Distillation Control," *Chemical Engineering Progress*, Vol. 65, No. 3, March 1969, pp. 40-45.

4. Breuer, M.E., Yoon, C.Y., Jones, D.P., and Nurry, M.J., "Countercurrent Controlled Cycle Liquid-Liquid Extraction," Chemical Engineering Progress, June 1977, pp. 95-96.

5. Avila, A.J., and Brown, M.J., "Design Factors in Pulse Plating," *Plating*, Vol. 57, November 1970, pp. 1105-1108.

6. Raub, Ch. J., and Knodler, A., "The Electroplating of Gold by Pulse Plating," *Gold Bulletin*, Vol. 10, April 1977, pp. 38-44.

7. Missel, L., and Montelbano, T., "Comparison of Electroplated Gold Deposits for Internal Stress and Grain Size," *Electronic Packaging and Production*, April 1978, pp. 166-170.

8. Missel, L., Duke, P., and Montelbano, T., "Square Profile Gold by Pulse Plating," *Semiconductor International*, February 1980, pp. 67-78.

9. Berube, L.Ph., and Piron, D.L., "Zinc Electrowinning under Periodical Reverse Current (PRC)," J. Electrochem.Soc., Vol. 134, No. 3, March 1987, pp. 562-570.

10. Bich, Nguyen N. and Bauman, J., "Pulsed Current Cathodic Protection of Well Casings," *Materials Performance*, Vol. 34, No. 4, 1 April 1995, pp.17-21.

11. Dabowski, J., "Pulsed Rectifier Limitations for Well Casing Cathodic Protection," *Materials Performance*, Vol. 34, No. 10, 1 October 1995, pp. 25-28.

12. Varma, R., Shimotake, H., Hoeller, T.L., and Agarwala, V., "Electrodeposition of cadium from aqueous fluoborate electrolytes," *Materials Performance*, May 1988, pp. 39-44.

13. Dyer, C.K., and Alwitt, R.S., "Surface Changes during A.C. Etching of Aluminum," *J. Electrochem. Soc.*, Vol. 128, No. 2, February 1981, pp. 300-305.

14. Kwiatkowski, L. and Mansfeld, F., "Surface Modification of Stainless Steel by an Alternating Voltage Process," *J. Electrochem. Soc.*, Vol. 140, No. 3, March 1993, pp. L39-L41.

15. Mansfeld, F., Lin, S.H., and Kwiatkowski, L., "Optimization of the Alternating Voltage Passivation Process for Stainless Steel," *Corrosion*, Vol. 50, No. 11, November 1994, pp. 838-847.

16. Yeager, E., and Salkind, A.J., *Techniques of Electrochemistry*, John Wiley & Sons, New York, 1978, Ch. VI. "Electrodeposition", pp. 369-436.

17. Raub, E., and Muller, K., *Fundamentals of Metal Deposition*, Elsevier Publishing Company, New York, 1967, pp. 1-35, 152-173.

18. Hobbs, F.B., *Traffic Planning & Engineering*, Pergamon Press, New York, 1974, pp. 353-358.

19. Varjian, R.D., "Electrolytic Processing," *Interface*, Vol. 3, No. 3, Fall 1994, pp. 24-28.

CHAPTER 7

1. Bakshi, R., and Fedkiw, P.S., "Optimal Potential Control of Electroorganic Reactions", *Electrochemical Engineering and Small Scale Electrolytic Processing*, Symposium Proceedings, Industrial Electrolytic Division Proceedings Volume 90-10, The Electrochemical Society, Inc., Pennington, NJ, 1990, pp. 3-18.

2. Smeltzer, J.C., and Fedkiw, P.S., "Selectivity Enhancement of an Electroorganic Synthesis in a Parallel-Plate Reactor under Periodic Cell-Voltage Control", *Ibid.*, pp. 125-140.

3. Nolen, T.R., and Fedkiw, P.S., "Reaction Selectivity Enhancement under Periodic-Current Control: The Reduction of Nitrobenzene on the Rotating Disk Electrode", *Ibid.*, pp. 141-163.

4. Hager, H.E., "Current levelling behaviour under pulse current electroplating conditions: the role of eaction pseudocapacitance", *Journal of Applied Electrochemistry*, 16, (1986), pp. 189-195.

5. Cheh, H.Y., "Electrodeposition of Gold by Pulsed Current", *J. Electrochem. Soc.*, Vol. 118, No. 4, April 1971, pp. 551-557.

6. Chin, D-T., "Mass Transfer and Current-Potential Relation in Pulse Electrolysis", *J. Electrochem. Soc.*, Vol. 130, No. 8, August 1983, pp. 1657-1667.

7. Ibl, N., "Some Theoretical Aspects of Pulse Electrolysis," *Surface Technology*, 10, (1980), pp. 81-104.

8. Viswanathan, K., Farrell Epstein, M.A., and Cheh, H.Y., "The Application of Pulsed Curent Electrolysis to a Rotating-Disk Electrode System, I. Mass Transfer," *J. Eectrochem. Soc.*, Vol. 125, No. 11, November 1978, pp. 1772-1776.

9. Viswanathan, K., and Cheh, H.Y., "The Application of Pulsed Curent Electrolysis to a Rotating-Disk Electrode System, II. Electrochemical Kinetics," *J. Electrochem. Soc.*, Vol. 125, No. 10, October 1978, pp. 1616-1618.

10. Viswanathan, K., Cheh, H.Y., and Standart, G.L., "Electrolysis by intermittent potential," *Journal of Applied Electrochemistry*, 10, (1980), pp. 37-41.

11. Verbrugge, M.W., and Tobias, C.W., "A Mathematical Model for the Periodic Electrodeposition of Multicomponent Alloys," *J. Electrochem. Soc.*, Vol. 132, No. 6, June 1985, pp. 1298-1307.

12. Macdonald, D.D., *Transient Techniques in Electrochemistry*, Plenum Press, New York, 1977, pp. 47-67.

13. Denn, M.M., *Optimization by Variational Methods*, McGraw Hill, New York, NY (1969).

14. Athans, M. and Falb, P.L., *Optimal Control*, McGraw Hill, New York, NY (1966).

15. Petrov, Iu. P., *Variational Methods in Optimal Control Theory*, Academic Press, New York, NY (1968).

16. Ray, W.H., *Admanced Process Control*, McGraw Hill, New York, NY (1981).

17. Au, T. and Stelson, T.E., *Introduction to Systems Engineering, Deterministic Models*, Addison-Wesley Publishing Co., Reading, MA, (1969).

CHAPTER 8

1. Epstein, I.R., Kustin, K., De Kepper, P, and Orban, M., "Oscillating Chemical Reactions", *Scientific American*, Vol. 248, No. 3 (March 1983), pp. 112-123.

2. Barkey, D., "Morphology Selection and the Concentration Boundary Layer in Electrochemical Deposition," *J. Electrochem. Soc.*, Vol. 138, No. 10, October 1991, pp. 2912-2917.

3. Bearman, G., editor for The Oceanography Course Team, *Seawater: Its Composition, Properties, and Behaviour*, 2nd Ed, 1995, Elsevier Science Inc., Tarrytown, NY, pp. 49-56.

4. Prigogine, I., *From Being to Becoming*, W. H. Freeman and Company, San Francisco, 1980, Ch.4, pp. 74-101.

5. Stewart, I., *Does God Play Dice?, The Mathematics of Chaos*, Basil Blackwell Inc., New York, 1989, Ch.9, pp. 165-191.

6. Gleick, J., *Choas, Making a New Science*, Penguin Books, New York, 1987, pp. 121-153.

7. Boyce, W.E., and DiPrima, R. C., *Elementary Differential Equations*, 3rd Ed., John Wiley & Sons, Inc., New York, 1977, Ch.9, pp. 378-449.

8. Wojtowicz, J., *Modern Aspects of Electrochemistry*, Vol. 8, J. O'M. Bockris and B.E. Conway, Editors, Plenum Press, New York, 1972, pp. 66.

9. Thompson, J.M.T., and Stewart, H.B., *Nonlinear Dynamics and Chaos*, John Wiley & Sons, New York, 1986, pp.15-59.

10. Hudson, J.L., and Bassett, M.R., "The Oscillatory Electrodissolution of Copper in Acidic Chloride Solution, I. 0.1M Chloride", *J. Electrochem. Soc.*, Vol. 137, No. 3, March 1990, pp. 922-932.

11. Hudson, J.L., and Bassett, M.R., "The Oscillatory Electrodissolution of Copper in Acidic Chloride Solution, II. 0.3 and 0.5 Chloride", *J. Electrochem. Soc.*, Vol. 137, No. 6, June 1990, pp. 1815-1826.

12. Cattarin, S.,and Tributsch, H., "Interfacial Reactivity and Oscillating Behavior of Chalcopyrite Cathodes during H_2O_2 Reduction, I. Electrochemical Phenomena", *J. Electrochem. Soc.*, Vol. 137, No. 11, November 1990, pp. 3475-3483.

13. Hibbett, D.B., and Murphy, S.V., "Kinetic Model of Iron Corrosion and Passivity", *J. Electrochem. Soc.*, Vol. 138, No. 8, August 1991, pp. L30-L32.

14. Li, W., Nobe, K., and Pearlstein, A.J., "Electrodissolution Kinetics of Iron in Chloride Solutions: VIII. Chaos in Potential/Current Oscillations", *J. Electrochem. Soc.*, Vol. 140, No. 3, March 1993, pp. 721-728.

15. Jensen, K.F. and Ray, W.H., "The Role of Surface Structures in the Dynamic Behavior of Heterogeneous Catalytic Systems", Ch.4, pp. 111-153, in *Dynamics of Nonlinear Systems*, V. Hlavacek, ed., Gordon and Breach Science Publishers, New York, 1986.

16. Walfraef, D., Borckmans, P., and Dewel, G., "Dissipative Structures in Diffusion-Chemical Reaction Systems", Ch. 7, pp. 221-245, in *Dynamics of Nonlinear Systems*, V. Hlavacek, ed., Gordon and Breach Science Publishers, New York, 1986.

17. Jorne, J., "Oscillations and concentration patterns in electrochemical systems", *Electrochimica Acta.*, Vol. 28, No. 12, pp.1713-1717, 1983.

18. Horsthemke, W. and Lefever, R., "Phase Transition Induced by External Noise", *Physics Letters*, Vol. 64A, No. 1, 28 November 1977, pp. 19-21.

19. van Kanpen, N.G., "A Soluble Model for Diffusion in a Bistable Potential," *Journal of Statistical Physics*, Vol. 17, No. 2, 1977, pp. 71-88.

20. Smythe, J., Moss, F. and McClintock, P.V.E., "Observation of a Noise-Induced Phase Transition with an Analog Simulator", *Physical Review Letters*, Vol. 51, No. 12, 19September1983, pp.1062-1065.

21. Moss, F., "Noisy Switches", *Chaos in Nonlinear Dynamical Systems*, J. Chandra, ed., SIAM, Philadelphia, 1984, Ch. X, pp.119-129.

22. Moss, F. and Wiesenfeld, K., "The Benefits of Background Noise", *Scientific American*, August 1995, pp. 66-69 & 100-103.

23. Joule, J.P., "On the Intermittent Character of the Voltaic Current in certain cases of Electrolysis; and on the Intensities of various Voltaic Arrangements", *Philosophical Magazine and Journal of Science*, London,Vol XXIV, Jan-June, 1844, pp. 106-115.

24. Liu, S.H., "Fractal Model for the ac Response of a Rough Interface", *Physical Review Letters*, Vol. 55, No. 5, 29July1985, pp. 529-532.

25. Liu, S.H., and Kaplan, T., "AC Response of Fractal Interfaces," *Solid State Ionics*, 18 & 19, 1986, North-Holland, Amsterdam, pp. 65-71.

26. Liu, S.H., Kaplan, T., and Gray, L.T., "Theory of the AC Response of Fractal Interfaces," Proceedings of the IEEE International Symposium on Circuits and Systems, Philadelphia, PA, May 4-7, 1987, pp. 942-947.

27. Bates, J.B., and Chu, Y.T.,"Surface Topography and Electrical Response of Metal-Electrolyte Interfaces", *Solid State Ionics*, 28-30 (1988), pp. 1388-1395.

28. MacDonald, D.D., private communication, SRI, Palo Alto, CA, Apr 1989.

29. Horowitz, P., and Hill, W., *The Art of Electronics*, Cambridge University Press, NewYork, 1980, pp. 650-652.

30. Angelo, E.J., Jr., *Electronic Circuits*, McGraw-Hill, New York, 1964, pp. 128.

31. Degn, H., *Transactions of the Faraday Society*, Vol. 64, 1968, pp. 1348.

32. Epelboin, I., Gabrielli, C., Keddam, M., and Takenouti, H., "A Model for the Behaviour of Iron in Sulphuric Acid Medium," *Electrochimica Acta*, Vol. 20, 1975, pp. 913-916.

CHAPTER 9

1. Brenner, A., *Electrodeposition of Alloys, Principles and Practice*, Vol. I, Academic Press, New York, 1963, pp.276.

2. Kovac, Z., "The Effect of Superimposed A.C. on D.C. in Electrodeposition of Ni-Fe Alloys," *J. Electrochem. Soc.*, Vol. 118, No. 1, January 1971, pp. 51-57.

3. Horkans, J., "Effect Plating Parameters on Electrodeposited NiFe," *J. Electrochem. Soc.*, Vol. 128, No. 1, pp. 45-49.

4. Cohen, U., Koch, F.B., and Sard, R., "Electroplating of Cyclic Multilayered Alloy (CMA) Coatings," *J. Electrochem. Soc.*, Vol. 130, No. 10, pp. 1987-1995.

5. Verbrugge, M.W., and Tobias, C.W., "A Mathematical Model for the Periodic Electrodeposition of Multicomponent Alloys," *J. Electrochem. Soc.*, Vol. 132, No. 6, June 1985, pp. 1298-1307.

6. Dariel, M.P., Bennett, L.H., Lashmore, D.S., Lubitz, P. and Rubinstein, M.; Lechter, W.L., and Harford, M.Z., "Properties of electrodeposited Co-Cu multilayer structures," *J.Appl. Phys.*, Proceedings of the Thirty-First Annual Conference on Magnetism and Magnetic Materials, Vol. 61, No. 8, 15 April 1987, pp. 4067-4069.

7. Lashmore, D.S., and Dariel, M.P., "Electrodeposited Cu-Ni Textured Superlattices," *J.Electrochem. Soc.*,Vol. 135, No. 5, May 1988, pp. 1218-1221.

8. Despic, A.R., and Jovic, V.D., "Electrochemical Formation of Laminar Deposits of Controlled Structure and Composition, I. Single Current Pulse Galvanostatic Technique," *J. Electrochem. Soc.*,Vol. 134, No.12, December 1987, pp. 3004-3011.

9. Despic, A.R., Jovic, V.D., and Spaic, S., "Electrochemical Formation of Laminar Deposits of Controlled Structure and Composition, II. Dual Current Pulse Galvanostatic Technique," *J. Electrochem. Soc.*,Vol. 136, No.6, June 1989, pp. 1651-1657.

10. Grimmett, D.L., Schwartz, M., and Nobe, K., "Pulsed Electrodeposition of Iron-Nickel Alloys," *J. Electrochem. Soc.*, Vol. 137, No. 11, November 1990, pp. 3414-3418.

11. Akayama, T., and Fukushima, H., "Recent Study on the Mechanism of the Electrodeposition of Iron-group Metal Alloys," *ISIJ Inernational*, Vol. 32, No. 7, 1992, pp. 787-798.

12. Grimmett, D.L., Schwartz, M., and Nobe, K., "A Comparison of DC and Pulsed Fe-Ni Alloy Deposits," *J. Electrochem. Soc.*, Vol. 140, No. 4, April 1993, pp. 973-978.

13. Alper, M., Aplin, P.S., Attenborough, K., Dingley, D.J., Hart, R., Lane, S.J., Lashmore, D.S., and Schwarzacher, W., "Growth and characterization of electrodeposited Cu/Cu-Ni-Co alloy superlattices," Journal of Magnetism and Magnetic Materials, Vol.126, 1993, pp. 8-11.

14. Intrater, R., and Yahalom, J., "Electrochemical parameters for electrodeposition of compositionally modulated alloys of iron-copper," *Journal of Material Science Letters*, Vol. 12, No. 19, October 1993, pp. 1549-1551.

15. Alper, M., Attenborough, K., Baryshev, V., Hart, R., Lashmore, D.S., and Schwarzacher, W., "Giant magnetoresistance in electodeposited Co-Ni- Cu/Cu superlattices," *J. Appl. Phys.*, Vol. 75, No. 10, 15 May 1994, pp. 6543-6545.

16. Bird, K.D., and Schlesinger, M., "Giant Magnetoresistance in Electrodeposited Ni/Cu and Co/Cu Multilayers," *J. Electrochem. Soc.*, Vol. 142, No. 4, April 1995, pp. L65-L66.

17. Lebad, N., Voiron, J., Nguyen, B., and Chainet, E., "Electrodeposition of Cu/Ni multilayers with pulsed electric regimes," *Annales de Chimie (Science des Materiaux)*, Vol. 20, Nol 7-8, May 1995, pp. 391-394.

18. Chassaing, E., Nallet, P., and Trichet, M.F., "Electrodeposition of Cu/Fe20Ni80 Magnetic Multilayers," *J. Electrochem. Soc.*, Vol. 143, No. 5, May 1996, pp. L98-L100.

19. Bockris, J. O'M. and Reddy, A.K.N., *Modern Electrochemistry*, Plenum/Rosetta, New York, 1977, Vol. 2, pp. 1019, 1045, 1058.

20. Gabrielli, C., Keddam, M., and Takenouti, H., "New Trends in the Investigation of Electrochemical Systems by Impedance Techniques: Multi Transfer Functions Analysis," (Extended abstract in proceedings for) First International Symposioum on EIS, BomBannes, France, May 25, 1989, pp. PL 9.

21. Hager, H.E., R.L. Ruedisueli, M.F. Buehler, "The use of Piezoelectric Crystals as Electrode Substrates in Iron Corrosion Studies; the Real-time, In Situ Determinaiton of Dissolution and Film Formation Reaction Rates," NACE Journal of Corrosion, Vol. 42, No. 6, June, 1986, pp. 345-351.

22. Buehler, M.F., "Quantification of Iron Corrosion and Copper Pulse Plating Using Piezoelectric Quartz Crystals," MS Thesis, University of Washington, 1986.

23. Ruedisueli, R.L., "Two Corroison Rate Measurement Methods," Spring Meeting of the Northwest Chapter of the Electrochemistry Society, Seattle, WA, April 28, 1990, (unpublished).

24. Ruedisueli, R.L., "Experimental Techniques for the Analysis of Non-Steady Electrochemical Processes," Spring Meeting of the Northwest Chapter of the Electrochemical Society, Seattle, WA, April 29, 1989, (unpublished).

25. Ruedisueli, R.L., "On the Application of Electrochemical Impedance Spectroscopy and Piezoelectric Crystal Techniques to the Study of Mass Accretion Processes," (Extended abstract in proceedings for) First International Symposioum on EIS, BomBannes, France, May 25, 1989, pp. C6.2.

26. Ruedisueli, R.L., "Relaxation Phenomena in Electrochemical Systems," Poster, International Discussion Meeting on Relaxations in Complex Systems, Heraklion, Crete, Greece, June 28, 1990, (unpublished).

27. Randles, J.E.B., "Kinetics of Rapid Electrode Reactions," *Discussions of the Faraday Society*, No.1, 1947, pp. 11-19.

28. Poan, N.W. "Corrosion of Copper and Copper Alloys," in *Metals Handbook*, Vol. 13, *Corrosion*, 9th ed. ASM International, Metals Park, OH, 1987, pp. 617-619.

CHAPTER 10

1. Ruedisueli, R.L., "Experimental Techniques for the Analysis of Non-Steady Electrochemical Processes," Spring Meeting of the Northwest Chapter of the Electrochemical Society, Seattle, WA, April 29, 1989.

2. Ruedisueli, R.L., "On the Application of Electrochemical Impedance Spectroscopy and Piezoelectric Crystal Techniques to the Study of Mass Accretion Processes," First International Symposioum on EIS, BomBannes, France, May 25, 1989.

3. Buehler, M.F., "Quantification of Iron Corrosion and Copper Pulse Plating Using Piezoelectric Quartz Crystals," MS Thesis, University of Washington, 1986.

Appendix A

Sparge Condition Effects

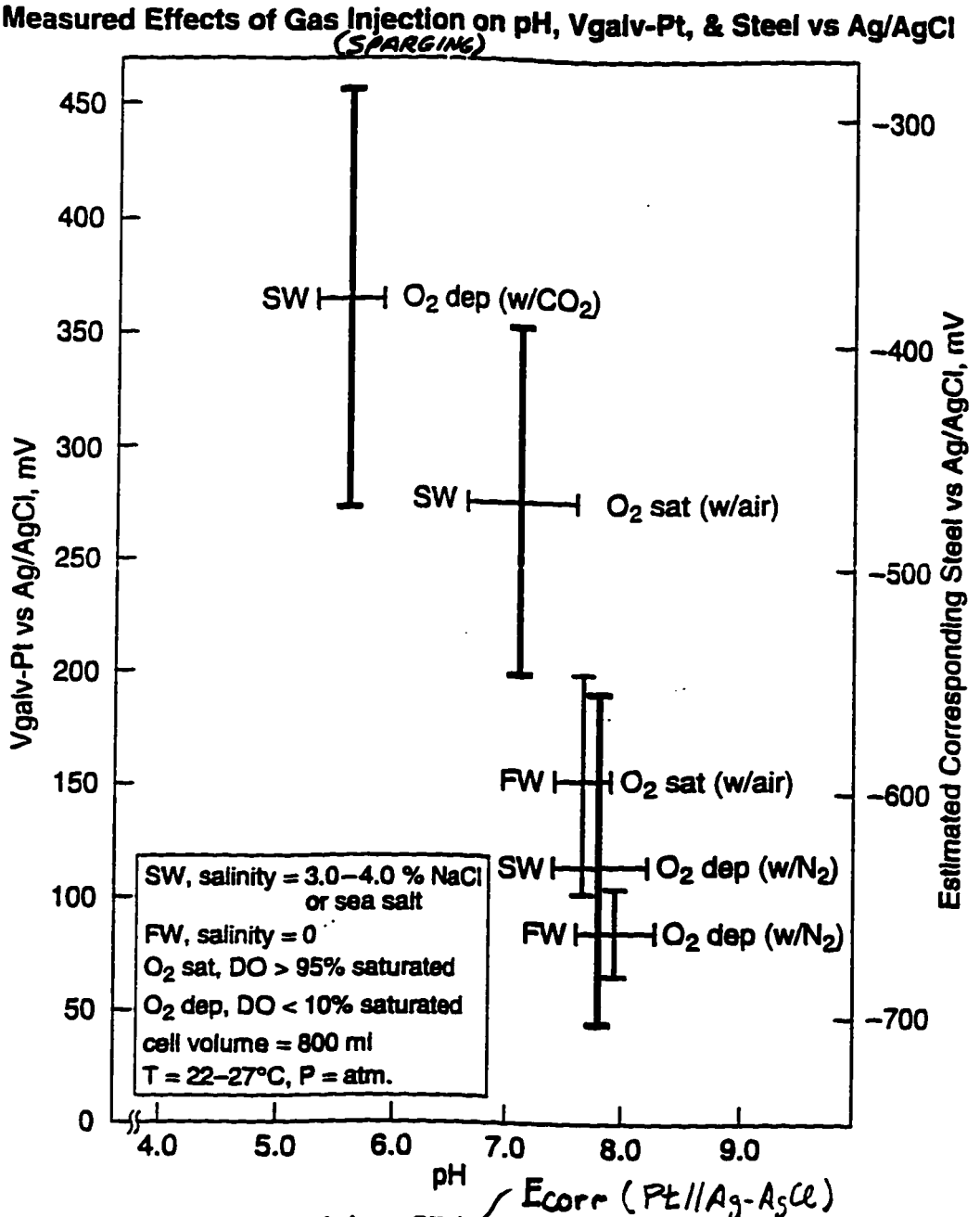

The range of responses of the platinum (Vgalv-Pt) electrode and pH in artificial seawater (SW) and fresh (tap) water (FW) cells is shown along with the estimated, corresponding potential of a freshly surfaced low carbon steel a Ag/AgCl electrode in seawater.

Figure A1. Sparge Condition Effects (a) Steel. (Sandwith-Ruedisueli, OCEANS'94)

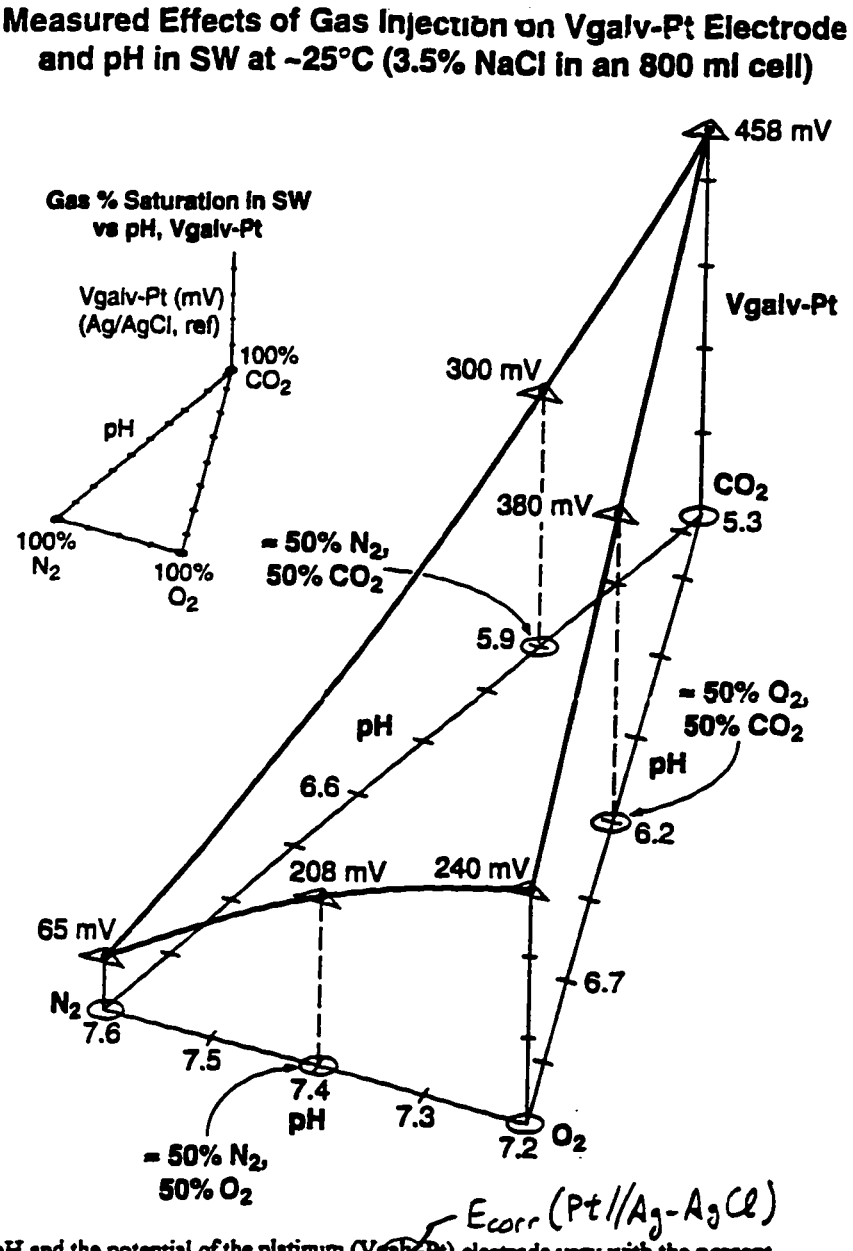

The cell pH and the potential of the platinum (Vgalv-Pt) electrode vary with the percent saturation of gases bubbled (injected) into the cell. The vertices of the base triangle represent 100% saturation, at atmospheric pressure, by injecting one of three gases (nitrogen, oxygen, or carbon dioxide). Intermediate points are the result of injecting an approximately 50/50 (mass flow) mixture of two gases.

Figure A1. Sparge Condition Effects (b) Platinum (Sandwith-Ruedisueli, OCEANS'94)

Table B1

Roughness Experiment Summary

(Data from 4/6 - 4/8/93)

LCS 8.5% SW/N_2

RUN #	SURFACE (grit)	E_{corr} (mV, Ag/AgCl)	ω_{DMAV} (Hz)	R_p (ohms)	$\dot{i}_{corr}$ (1260/273) (10^{-6} A)	$\dot{i}_{350}$ (10^{-6} A)	$V_{galv-Pt}$ (mV, Ag/AgCl)
1	120	-630	1.0	8700	1.47	2.0	+106
2	120	-680	1.2	1400	9.16	20.0	+176
3	600	-642	4.5	1370	9.36	9.90	-324
4	120	-636	1.5	1100	11.66	7.58	-434
5	600	-622	1.2	2500	5.13	20.0	-388

$$\dot{i}_{corr\ (1260/273)} = \frac{B}{R_p}$$

$$B = \frac{RT}{nF} = \frac{8.31\,(J/mole.K)\cdot 298\,(K)}{2\,(equiv/mole)\cdot 96500\,(C/equiv)} = 12.83\ mV$$

(file - Z-scan data, sparge/surface conditions)

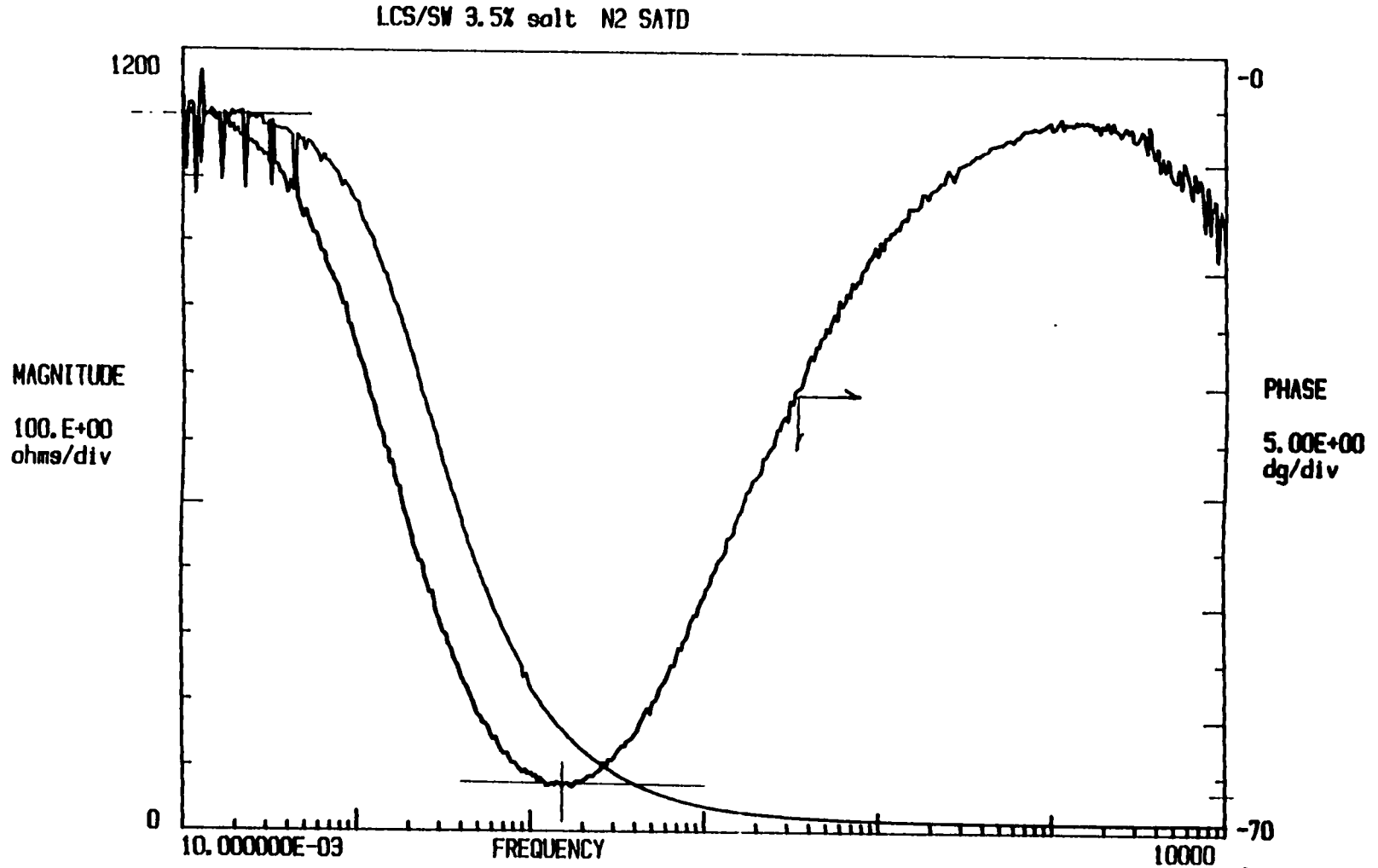

Figure B1. Roughness Effects, EIS Test Scan

Appendix C

R-RC Circuit Impedance Test Models

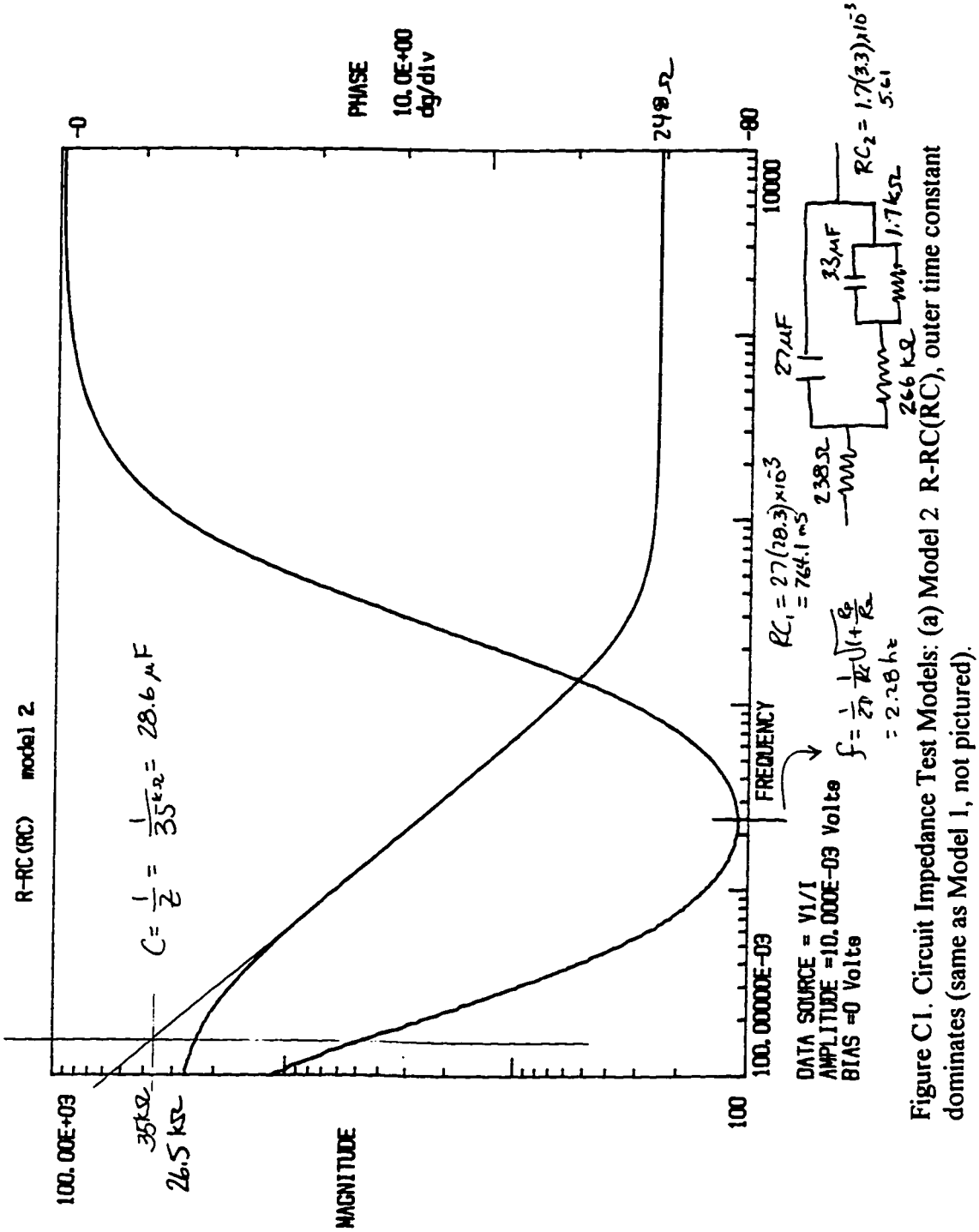

Figure C1. Circuit Impedance Test Models: (a) Model 2 R-RC(RC), outer time constant dominates (same as Model 1, not pictured).

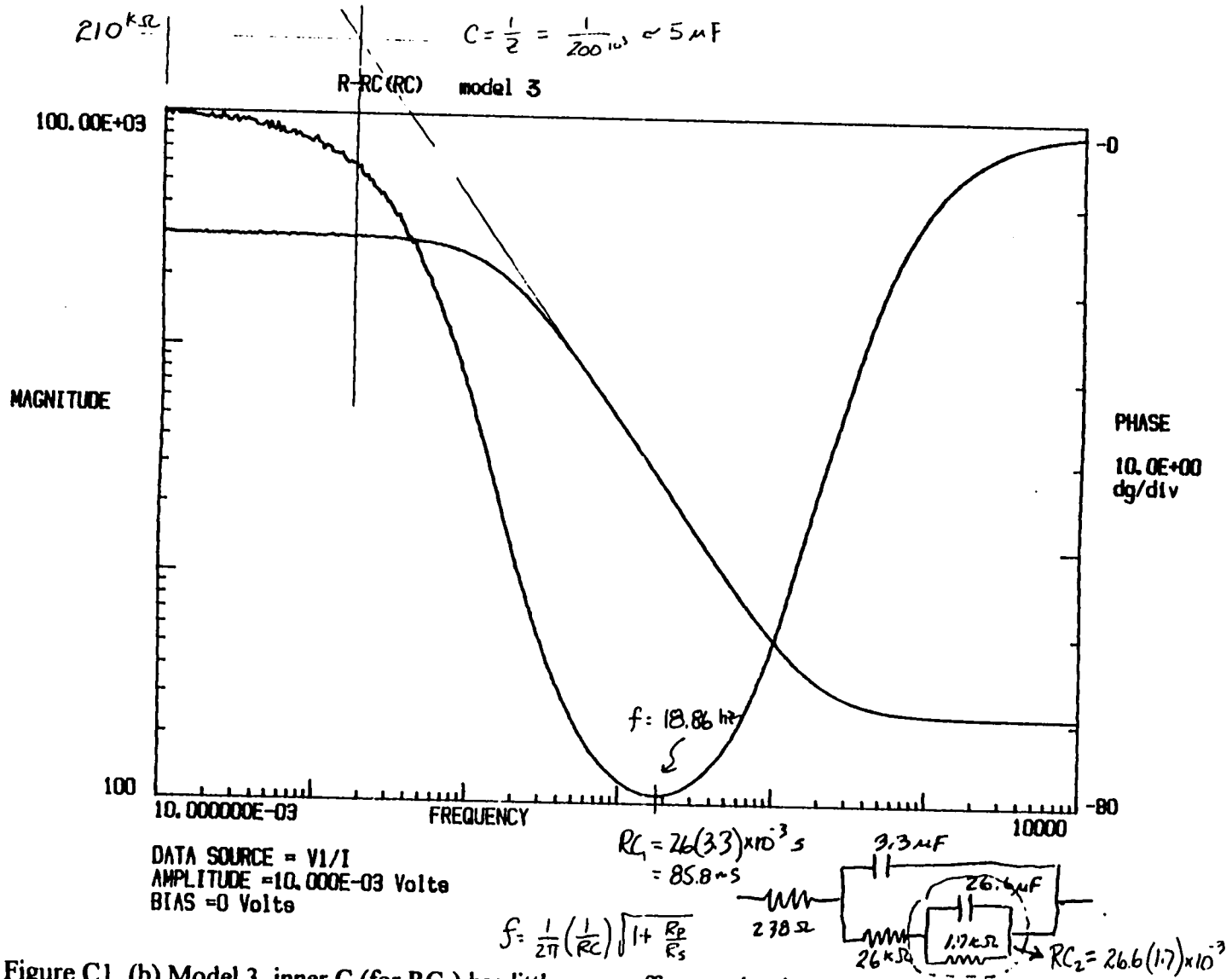

Figure C1. (b) Model 3, inner C (for RC_2) has little or no effect on dominant, outer C (for RC_1).

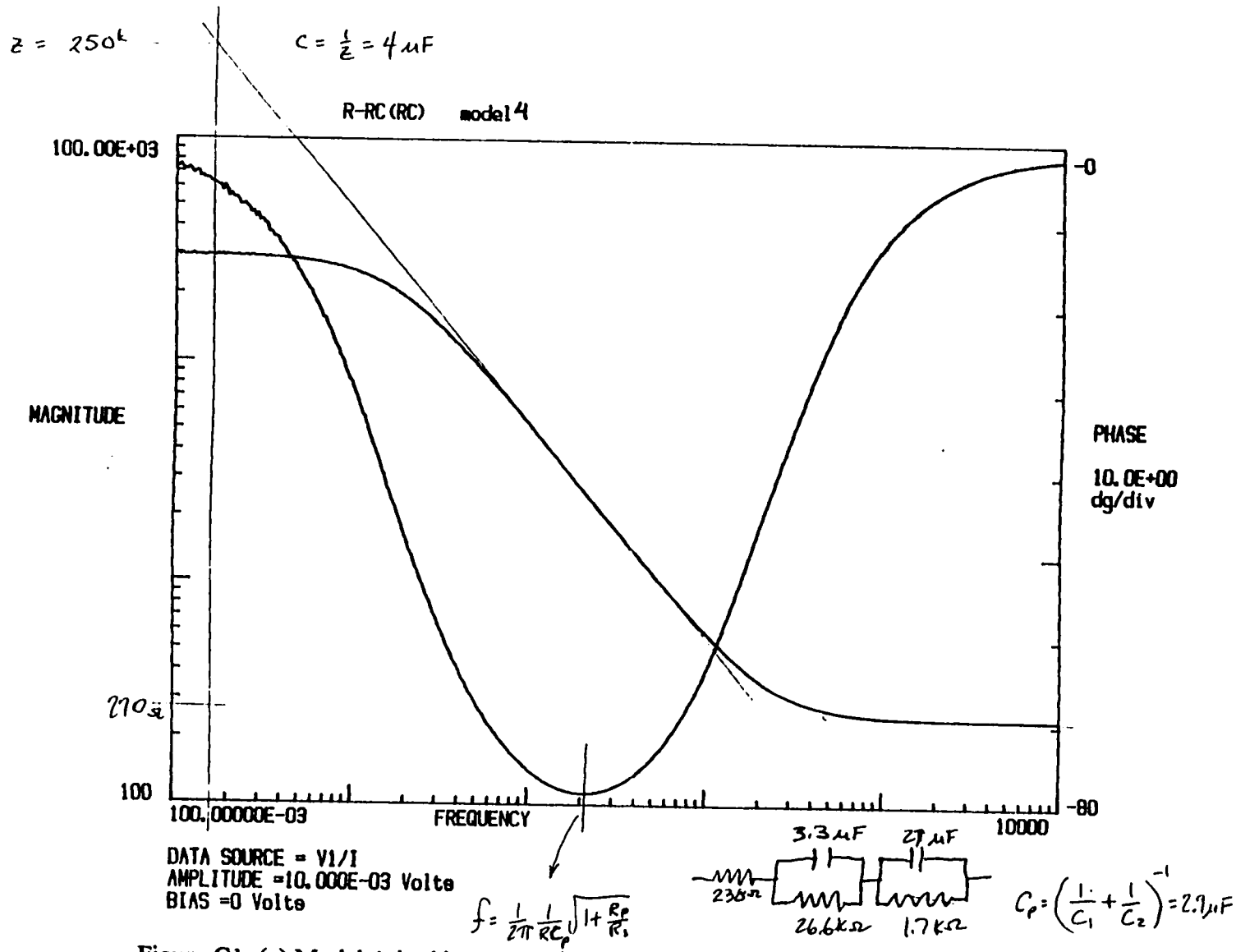

Figure C1. (c) Model 4, in this case, the capacitors add as the sum of their reciprocals.

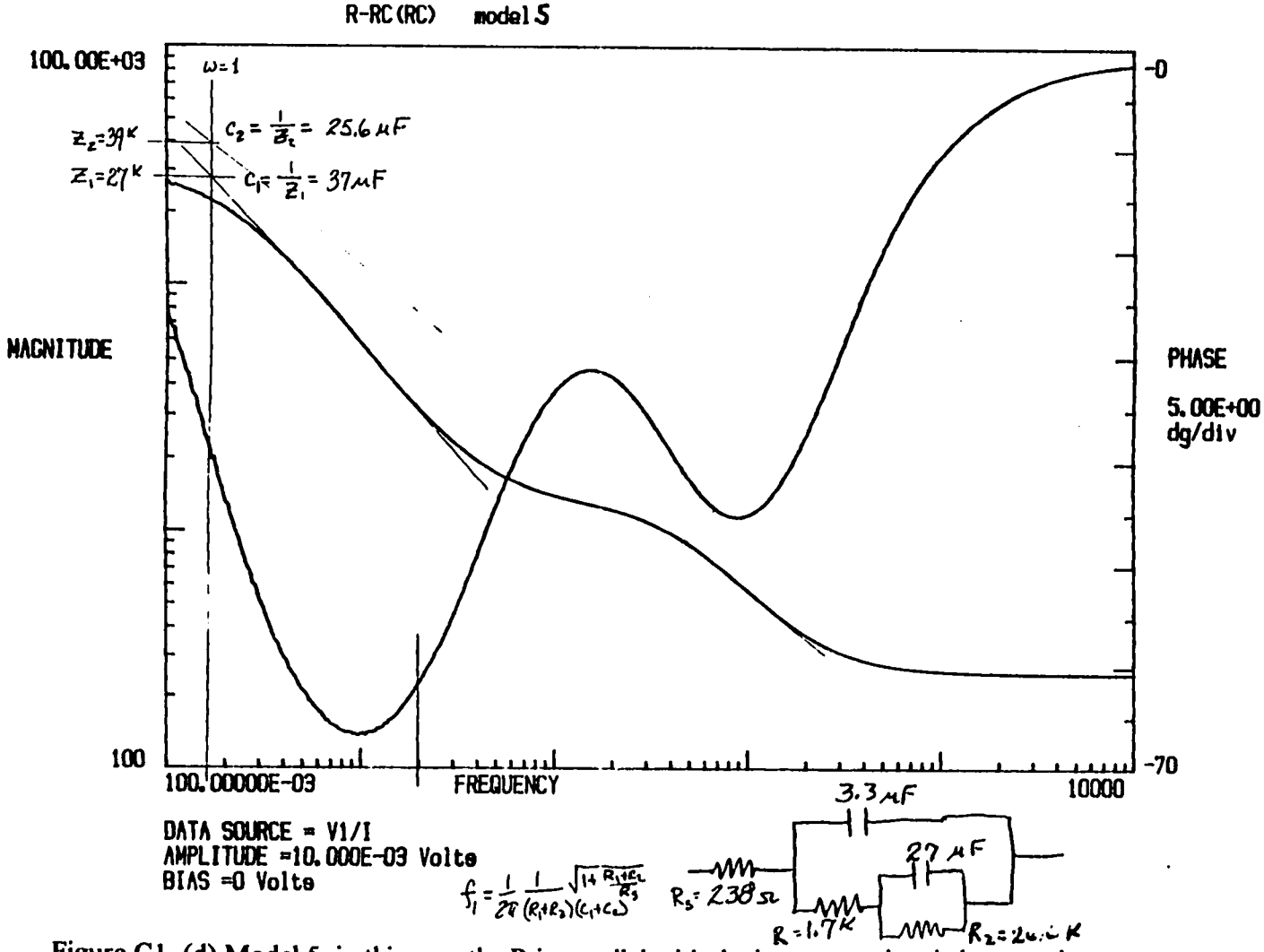

Figure C1. (d) Model 5, in this case the R in parallel with the inner capacitor is large and its large RC time constant is expressed.

Table D1. PAR 350 / Solartron 1260-PAR 273 Corrosion Measurements, compared.

PAR 350 (DC) VS. 1260 (AC) CORROSION CURRENT (Icorr)
MEASUREMENT METHODS

FOR DOME MATERAILS: LOW CARBON STEEL AND BRONZE
IN SEA WATER (SW) AND TAP WATER (TW)
SPARGED WITH AIR, OXYGEN (O2), NITROGEN (N2), OR CARBON DIOXIDE (CO2)

BRONZE SAMPLES:

Sample Number	Solution	Sparge Gas	1260, Rp (Ohms)	350 Icorr (mA/cm^2)	1260 Icorr (mA/cm^2)
#1	SW	N2	25000	6.20E-04	5.08E-04
#1	TW	AIR	18800	6.58E-04	6.76E-04
#2	TW	AIR	20800		6.11E-04
#1	SW	O2	900	3.43E-02	1.41E-02
#2	SW	O2	950		1.34E-02
#1	SW	AIR	1450	1.03E-02	8.76E-03
#2	SW	AIR	1875		6.77E-03

Table D1, continued.

LOW CARBON STEEL SAMPLES:

Sample Number	Solution	Sparge Gas	1260, Rp (Ohms)	350 Icorr (mA/cm^2)	1260 Icorr (mA/cm^2)
#1	SW	N2	11000	3.53E-03	1.15E-03
#2	SW	N2	9500		1.34E-03
#1	SW	AIR	550	3.50E-02	2.31E-02
#2	SW	AIR	475		2.67E-02
#1	SW	O2	330	8.24E-02	3.85E-02
#2	SW	O2	305		4.16E-02
#1	SW	CO2	285	5.50E-02	4.46E-02
#2	SW	CO2	280		4.54E-02
#1	TW	N2	22300	9.50E-04	5.70E-04
#2	TW	N2	18200		6.98E-04
#1	TW	AIR	1550	2.63E-03	8.19E-03
#1	TW	AIR	2000		6.35E-03
#2	TW	AIR	1850		6.87E-03
#1	TW	CO2	10000	2.94E-03	1.27E-03
#2	TW	CO2	6000		2.12E-03

See Notes on Following page

Table D1, continued.

NOTES:

1) PAR 350 Icorr obtained from Potentiodynamic / Tafel intercept polarization scans (average values)

2) 1260 impedance spectra are used to obtain polarization resistance, Rp = [Z](lo freq) - [Z](hi freq).

3) 1260 Icorr = B/Rp
Where B = RT/ZF * 1000 (mV)
for Z=2 , T=295 K , B=12.702

$R = 8.31\ J/^{o}k$

$F = 96500\ C$

Appendix E

Table E1
Time Constants, Measurements/Calculation
Compared by Characteristic Frequency, fc = 1 / tr

Source	Method	System		Range, fc
Ruedisueli (SRI tests)	EIS	Cu/SO4	[C]lo, Vlo	10.64
			[C]mid, Vlo	1.92
			[C]hi, Vhi	0.63
		Cu/SO4	[C]lo, Vhi	0.24
			[C]hi, Vlo	3.77
		Au/SW	[C]hi, Vhi	1.01
			[C]hi, Vlo	0.039to0.0
Buehler-Hager (Ref. [9.22] pp. 91)	PCE (10Mhz)	Cu/SO4	[C]hi, Vhi	223.7 to 1
Bockris (Ref. [9.19] pp.1058))	Calculation	KI3 I3(-)+2e(-)=>3I(-)		
	diffusion layer, static, d=0.05cm		[C]lo, Vhi	0.005
	for RDE, w=240 rpm, d=0.005cm			0.51
	@limiting current, D=1.0x10^(-5) cm2/sec			
	d=2/(pi)*sqrt(Dt), tr=pi/D*(d/2)^2			
Despic&Jovic (Ref [9.8])	C-V measured potential response to current puls 2-5 mA tr = 2 - 10sec	Cu(2+) [C]=0.02N	[C]lo, Vhi	0.1 to 0.5

[C]=concentration
V=applied voltage

fctable.xls

Table E2

SRI-EIS TIME CONSTANT MEASUREMENT RESULTS SUMMARY (4/6/89)

TEST#	CONDITIONS	Rp k ohms	C micro Farads	RC(ms)	freq (hz)
CuAuFRA& (Cu/Au/FRA01)	Au(150mil) 1N CuSO4/AIR E273=-0.323V (SCE)	31.6	50.12	1583.8	0.1
CuCuFRA& (Cu/Cu+/FRA01)	Cu(150mil) 0.02N CuSO4/Al E273=-0.013V (SCE)	9.4 (9.1*)	17.8	94	1.69
CuCuFRA0 (Cu/Cu+/FRA02)	Cu(150mil) 0.02N CuSO4/AIR E273=-0.5V (SCE)	11.95	354.8	4239.9	0.038
CuCuFRA1 (Cu/Cu+/FRA03)	Cu(150mil) 0.2N CuSO4/AIR E273=-0.013V (SCE)	6.68 (6.95*)	77.6	518.4	0.31
CuCuFRA2 (Cu/Cu+/FRA04)	Cu(150mil) 1N CuSO4/AIR E273=-0.053V (SCE)	2.11	125.9	265	0.6
SWFRA01& (SW/FRA01)	Au(150mil) SW E273=0.063V (SCE)	126	31.6	3982	0.039
SWFRA02& (SW/FRA02)	Au(150mil) SW E273=-1.0V (SCE)	15.8 (17.0*)	10	158	1.01
SWFRA03& (SW/FRA03)	Au(150mil) SW E273=0.063V (SCE)	100	31.6	3160	0.05

NOTES:
1) Cu(150), Au(150),; Cu and Au PCE, respectively, 150 mil diameter
2) SW = Seawater, salinity approx 35%
3) Polarization resistance, Rp = |Z| - |Z|w=hi, BODE plot
4) Capacitance, C for 1/C intercept on |Z| axis of BODE plot
5) *, Rp value from Nyquist plot semi-circle diameter
6) frequency , freq = 1/(2 pi T), (hz); T = RC

Table E3

SCHLUMBERGER 1260 (FRA) EIS RESULTS SUMMARY, APL

TEST#	CONDITIONS	Z (k ohms) high	Z (k ohms) low	Rp kohms	C(micro Farads) Calc	C(micro Farads) Meas	RC(ms)
12(1A-1)) (10/11/94)	Au(150mil) 0.02N CuSO4/Air E273 = +0.279V (SCE)	28	0.50	27.5	45.5	39	1251
12(2A-1)) (10/11/94)	Au(150mil) 0.02N CuSO4/N2 E273 = +0.300V (SCE)	100	1.00	99	10	10	990
12(3A-1)) (10/11/94)	Au(150mil) 0.02N CuSO4/N2 E273 = +0.298V (SCE)	83	1.15	81.9	15.9	13	1302
12(4A-1)) (10/12/94)	Au(150mil) 0.02N CuSO4/N2 E273 = +0.221SCE)	10	1.00	9	125	115	1250
12(2B-1)) (10/11/94)	Au(150mil) 0.2N CuSO4/AIR E273 = +0.333V (SCE)	90	0.27	89.7	13.7	13	1229
12(2B-1)) (10/11/94)	Au(150mil) 0.2N CuSO4/N2 E273 = +0.308V (SCE)	57	0.21	56.8	23.8	21	1352
12(4B-1)) (10/12/94)	Au(100mil) 0.2N CuSO4/N2 E273 = +0.279V (SCE)	14	0.23	13.8	76.9	75	1061
12(1C-1)) (10/11/94)	Au(150mil) 1.0N CuSO4/Air E273 = +0.333V (SCE)	49	0.20	48	19.2	20	937
12(2C-1)) (10/11/94)	Au(150mil) 1.0N CuSO4/N2 E273 = +0.340V (SCE)	43	0.08	42.9	21.7	23	930
12(4C-1)) (10/12/94)	Au(100mil) 1.0N CuSO4/N2 E273 = +0.301V (SCE)	27	0.09	26.9	32.3	38	868

Table E3 (continued)

TEST#	CONDITIONS	Z (k ohms) high	Z (k ohms) low	Rp kohms	C(micro Farads) Calc	C(micro Farads) Meas	RC(ms)
12(5B-1)) (10/12/94)	Au(150mil) 0.2N NiSO4/N2 E273 = +0.261V (SCE)	200	0.19	199.8	5.88	6.2	1174
12(6B-1)) (10/13/94)	Au(150mil) 0.2N AgNO3/NO2 E273 = +0.607V (SCE)	27	0.10	26.9	50	51	1345
12(7B-1)) (10/12/94)	Au(150mil) 0.2N ZnSO4/N2 E273 = +0.227V (SCE)	30	0.12	29.9	40	42	1196
13(1e-1)) (10/13/94)	Ag(150mil) 0.2N AgNO3/N2 E273 = Ecorr = +0.472V (SCE)	0.23	0.13	0.095	3571	1000	339
13(1d-1)) (10/13/94)	Ag(150mil) 0 .2N AgNO3/N2 E273 = Ecorr = +0.474V (SCE)	0.11	0.08	0.03	9090	600	273
15(1a-1)) (10/17/94)	Ni(150mil) 0.2N NiSO4/N2 E273 = Ecorr = +0.100V (SCE)	200	0.15	200	3.7	4.4	740
15(1b-1)) (10/17/94)	Ni(150mil) 0 .2N NiSO4/N2 E273 = Ecorr-50mv = +0.060V (SCE)	80	0.15	80	4.8	5.5	384
15(1c-1)) (10/18/94)	Ni(150mil) 0.2N NiSO4/N2 E273 = Ecorr-100mv = +0.005V (SCE)	80	0.12	80	5.9	7	472
15(1d-1)) 10/18/954	Ni(150mil) 0 .2N NiSO4/N2 E273 = Ecorr = +0.101V (SCE)	60	0.11	60	7.7	10	462

Table E3 (continued)

TEST#	CONDITIONS	Z (k ohms) high	Z (k ohms) low	Rp kohms	C(micro Farads) Calc	C(micro Farads) Meas	RC(ms)
15(2a-1)) (10/18/94)	Cu(150mil) 0 .2N CuSO4/N2 E273 = Ecorr = +0.047V(SCE)	2	0.12	1.88	43.5	3.3	82
15(1b-1) (10/18/94)	Cu(150mil) 0.2N CuSO4/N2 E273 = Ecorr-50mv = +0.003V(SCE)	4.3	0.12	4.18	52.6		220
16(1a-1) 10/18/954	Cu(150mil) 0 .2N CuSO4/N2 E273 = Ecorr = +0.058V (SCE)	3.7	0.12	3.58	6.25		22
16(2a-1) (10/19/94)	Ag(150mil) 0.2N AgNO3/N2 E273 = Ecorr = +0.500V (SCE)	0.15	0.08	0.07	4761	2300	333
16(2d-1) (10/18/94)	Ag(150mil) 0 .2N AgNO3/N2 E273 = Ecorr = +0.478V (SCE)	0.51	0.082	0.428	1961	900	839
17(1-1) (10/19/94)	Au(150mil) 0 .2N ZnSO4/N2 E273 = Ecorr = +0.301V (SCE)	36	0.13	35.87	23.8	26	854
17(3-1) (10/19/94)	Zn(Au)(150mil) 0 .2N ZnSO4/N2 (90sec) E273 = Ecorr = -1.050V (SCE)	0.13	0.083	0.047	7692	1300	362
17(4-1) (10/19/94)	Zn(Au)(150mil) 0 .2N ZnSO4/N2 (120sec) E273 = Ecorr = -1.050V (SCE)	0.17	0.065	0.125	10000	22000	1250

Table E4. Time Constant Measurement by Oscilloscope

Test #	Cell Electrolyte	CE/WE (d PCE -#)	273 In		Cell OUT (Volts)			
			Volts	t(sec)	V total	V ohmic	V capacitive	tau (sec)
31	0.1 M NaCl	Pt/Au(100)-1	1.00	0.50	0.94	0.20	0.74	0.01
	0.2 N ZnSO4		1.00	0.50	0.96	0.20	0.76	0.005
	0.1M NaCl		1.00	0.50	0.96	0.20	0.76	0.01
32	0.1 M NaCl	Pt/Au(100)-2	1.00	0.50	0.94	0.20	0.74	0.01
	0.2 N NiSO4		1.00	0.50	0.96	0.20	0.76	0.005
	0.1M NaCl		1.00	0.50	0.96	0.20	0.76	0.01
33	0.1 M NaCl	Pt/Au(100)-3	1.00	0.50	0.96	0.20	0.76	0.01
	0.2 N AgNO3		1.00	0.50	0.80	0.12	0.68	0.07
	0.1M NaCl		1.00	0.50	0.94	0.20	0.74	0.03
	0.2 N AgNO3		1.00	0.50	0.20	0.12	0.70	0.07
34	0.1 M NaCl	Pt/Au(100)-4	1.00	0.50	0.96	0.20	0.76	0.008
	0.2 N CuSO4		1.00	0.50	0.93	0.30	0.63	0.03
	0.1M NaCl		1.00	0.50	0.95	0.20	0.75	0.005

d PCE - # Piezo-electric crystal electrode diameter, sample number
tau (sec) Time constant

Appendix F

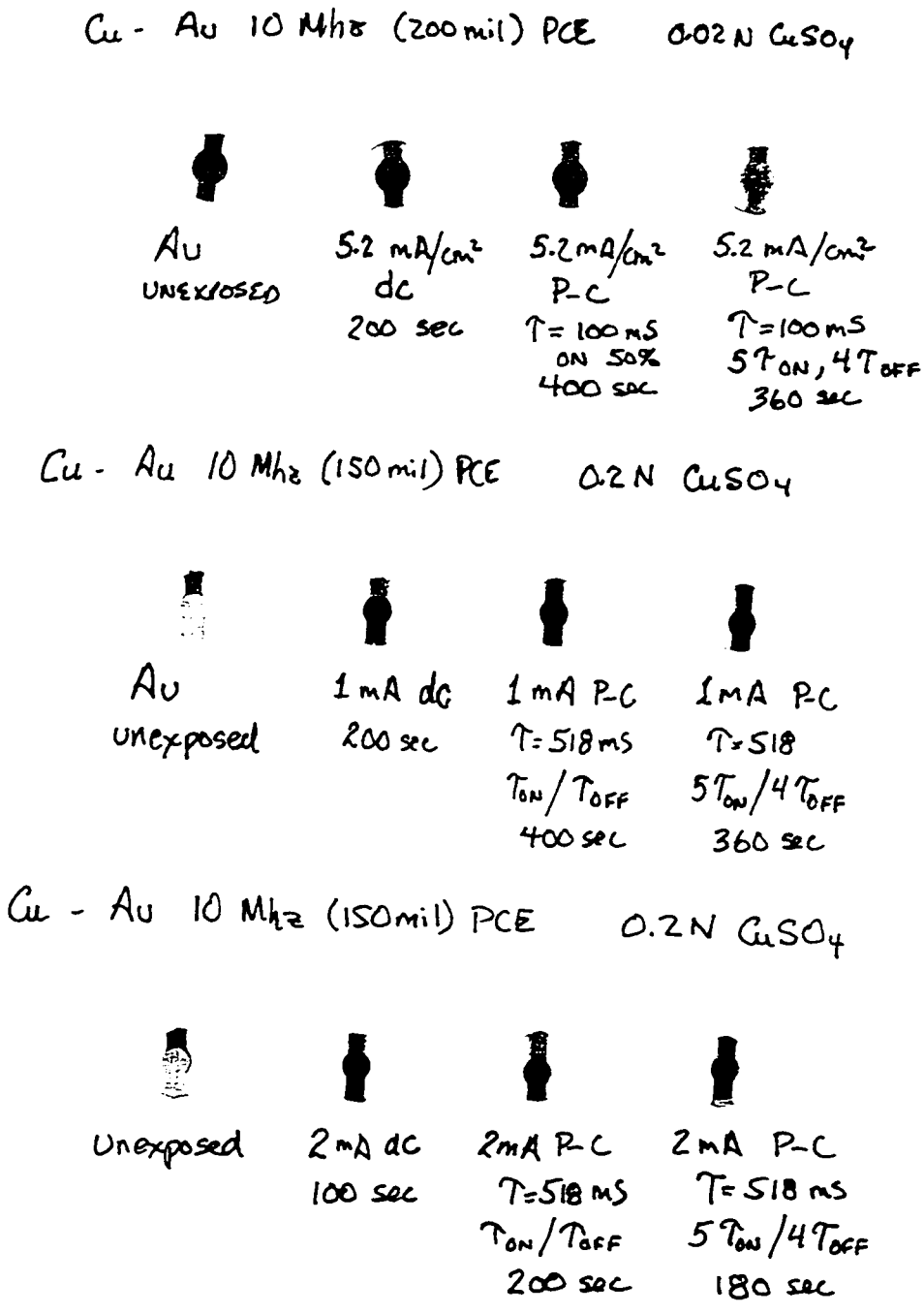

Figure F1. PCE Pulsed Electrodeposition Optimization Test Subjects and Results.

Table F1. DC Tests

10 Mhz/0.02N CuSO4

I (mA)	Mq (ug/cm2-eq)		I (mA)	Mq (ave)
1	6.83	3.551	1	3.551
1	1.369		1.5	2.93
1	1.614		2	0.9605
1	4.432		5	0.7545
1	3.51		10	0.513
1.5	2.93			
2	0.974	0.9605		
5	0.737	0.7545		
10	0.721	0.513		
2	0.947			
5	0.772			
10	0.305			

5 Mhz/0.2N CuSO4

I (mA)	Mq (ug/cm	I (mA)	Mq (ave)
0.5	39.04	0.5	34.27
0.5	29.5	1	82.53
1	76.18	2	96.43
1	91.98	2.7	75.69
1	79.43	5	7.43
2	96.43	5.3	4.26
2.7	75.69		
5	9.11		
5	5.75		
5.3	4.26		

10 Mhz/0.2N CuSO4

I (mA)	Mq (ug/cm2-eq)	I (mA)	Mq (ave)
1	193	1	150
1	28	1.5	103.7
1	107	2	33.7
1.5	103.7	5	28.2
2	33.7	10	3.77
5	28.2		
10	3.77		

10 Mhz/1 N CuSO4

I (mA)	Mq (ug/cm	I (mA)	Mq (ave)
1.5	406	1.5	406
5	171	5	171
10	137	10	137

dc_doc.xls

Table F2. AC Tests

10 Mhz/0.2N CuS04 t = 518 ms
SCHEDULE: dc

I (mA)	Mq (g/cm2-	I (mA)	Mq (ave)
0.5	146.1	0.5	146.1
1	315	1	315
2	183	2	177.2
2	221.7	5	138
2	138.7		
2	165.3		
5	138		

5 t(on)/ 4 t(off)

I (mA)	Mq (g/cm2-	I (mA)	Mq (ave)
0.5		0.5	
1	299	1	299
2	199	2	235.7
2	272.4	5	89.8
5	89.8		

2 t(on) / 2 t(off)

I (mA)	Mq (g/cm2-eq)
0.5	
1	
2	299.9
5	

t(on) / t(off)

I (mA)	Mq (g/cm2-	I (mA)	Mq (ave)
0.5		0.5	
1	197	1	197
2	331	2	398.9
2	466.8	5	127
5	127		

.5 t(on) / .5 t(off)

I (mA)	Mq (g/cm2-eq)
0.5	
1	
2	359.4
5	159

ac_doc.xls

Appendix G

Sample Calculations

Ruedisueli
10/8/96

"Cyclically Optimized Electrochemical Processes" 1/

Sample calculation for
(1) time constant, from FRA Z-plot
(2) limiting current, Sands Eq'n
(3) schedule efficiency, from PCE measurements

(1) Process time constant measurement/calculation
FRA impedance plot log |Z| vs log w

Cu PCE in 0.2N $CuSO_4$ @ -0.013 V(SCE)

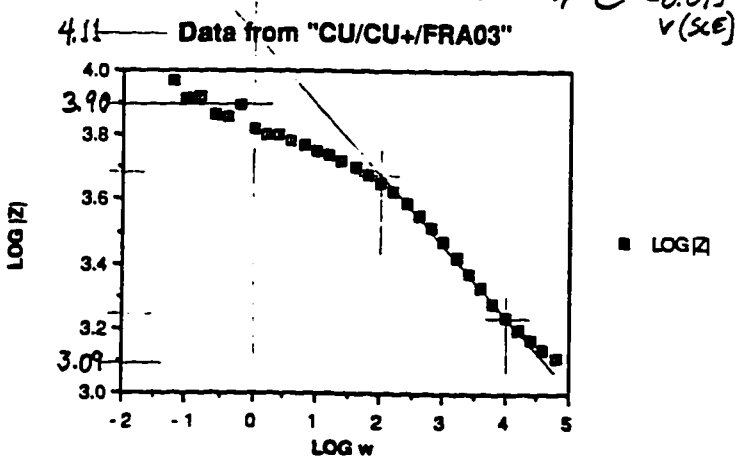

> the interface is modeled by an $R_s - C_\phi R$ circuit

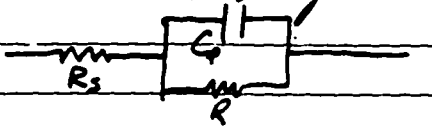

$$\bar{Z} = \bar{Z}_R + \bar{Z}_C$$

$$\bar{Z}_C = -\frac{1}{\omega C} j$$

Ruedeuel
10/8/96

(Sample calculation, cont'd) 2/

> at very low and very high frequencies the circuit (interface) response is dominated by the Z_R term

the polarization resistance, R_p, is determined as

$$R_p = |Z|_{\omega \to 0} - |Z|_{\omega \to \infty}$$

$$R_p = 10^{3.90} - 10^{3.09}$$

$$R_p = 7943 - 1230 = \underline{6712}$$

> at mid range frequencies, the capacitive reactance dominates

$$\log |Z| = -\log \omega - \log C_p$$

at $\log \omega = 0$, $\omega = 1$, $(f = 0.159)$

$$|Z| = \frac{1}{C_p}$$

in this example, at $\log \omega = 0$

$$|Z| = 10^{4.11}$$

$$C_p = \frac{1}{10^{4.11}} = 7.76 \times 10^{-5} = 77.6\ \mu F$$

> time constant $\tau = R_p C_p = 6.7 \times 77.6 \times 10^{-3} = \underline{520\ ms}$

tracked with
10/30/96

(Sample calc., cont'd) 3/

> The Nyquist plot (or Cole-Cole), Z'' vs. Z', (R_{imag} vs R_{real}), if found to plot as a semi-circle, whose diameter equals the R_p value, confirms the R-C model application.

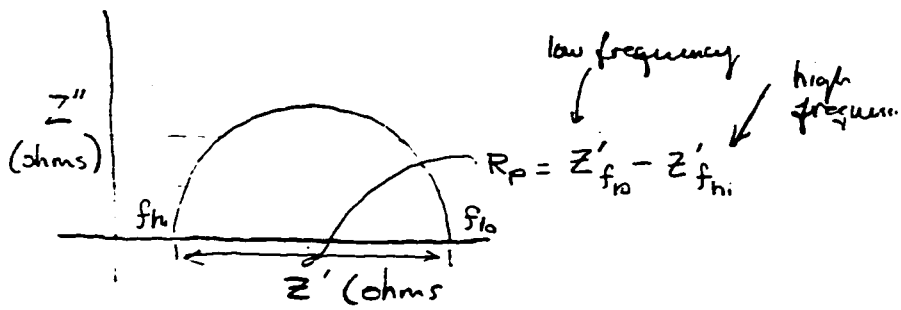

Cu PCE in 0.2N $CuSE_4$ @ -0.013 V(SCE)

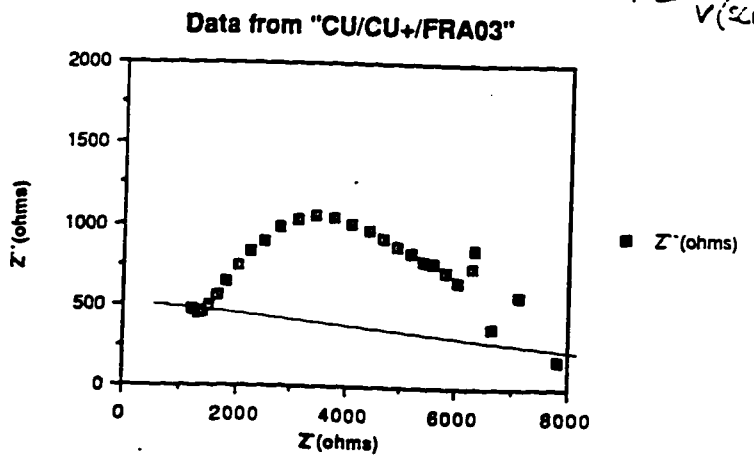

> In this example, $Z'_{(f=lo)} = 7.8\,k\Omega$

$Z'_{(f=hi)} = 1.2\,k\Omega$

$\therefore R_p = 7.8 - 1.2\,k\Omega = 6.6\,k\Omega$

(which is approx = 6.7 kΩ from Bode plot

Ruetschi
10/30/96

4/

(2) Calculation of expected limiting current value (or reasonable range).

Limiting current density,

$$i_L = \frac{D_A n F C_A^\circ}{\delta} \qquad (1)$$

where $D_A = 3.5 \times 10^{-6}$ cm²/sec, diffusivity of the electroactive species, Cu^{+2} ion, (value from Despic & Jovic)

$n = 2$, number of equivalents (oxidation number) involved in reaction

$F = 96500$ couls/eq, Faradays constant

$C_A^\circ = 0.1$ moles/1000 cm³ ($N = 0.2$)

δ = Diffusion boundary layer thickness

δ can be calculated from Sand's equation (2) when constant current is applied at $t = 0$

$$\delta = \frac{2}{\sqrt{\pi}} \sqrt{D_A t} = 1.128 \sqrt{D_A t}$$

where t can be taken here as the Pulse length (sec)

Rueda-Sound
10/30/96

5/

Limiting current, (cont'd)

for $t = T_{(Cu^{2+} = 0.2N)} = 520\ ms$

$$\delta = 1.128\left(3.5\times10^{-6}\ (0.52)\right)^{1/2}$$

$$\delta = 0.00152\ cm.$$

then $$i_L = \frac{3.5\times10^{-6}\ (2)\ (96500)\ (0.1)}{0.00152\ (1000)} \quad \frac{cm^2}{sec}\cdot\frac{coulomb}{mole}\cdot\frac{mole}{cm^3}$$

$$i_L = 0.044\ A/cm^2 = \underline{44\ mA/cm^2}$$

(if we use the Nernst BL eq'n $\delta = \sqrt{\pi D_A t}$, for the application of constant potential @ $t=0$, then $i_L = 0.028\ A/cm^2$)

Notes: (1) Eq'n results from Ficks first law for charge-transfer flux of a diffusion limited process

$$J = \frac{i}{nF} = -D\left(\frac{dc}{dx}\right)_{x=0} = -D\frac{C^o - C_{x=0}}{\Delta x}$$ B&R pg 1059

(2) SAND's Equation gives variation of electroactive species in the interface w/ time after application of a constant current. B&R pg 1045

Ruedisueli
11/4/96

4/

(3) Checking schedule efficiency by calculating mass-to-charge ratio, M_q, from PCE-measured frequency changes due to deposition on test electrode surface.

> deposition mass (areal density) is computed from the Sauerbrey formula.

$$\Delta f = - C_f \Delta m$$

$$\Delta m = - \frac{\Delta f}{C_f}$$

where Δf = frequency shift in fundamental frequency of oscillation of the quartz crystal (electrode substrate)

C_f = sensitivity factor (see Note 5)
for example an AT-cut, 10 Mhz, 250 mil ϕ quartz-crystal.

> $C_{f_{10}} = 2.75 \times 10^8$ cm^2/g-sec
[See Buehler, MS, PG 38]

$C_f \propto f^2$, where f is the fundamental resonance frequency of the crystal so for a 5Mhz crystal.

> $C_{f_5} = \left(\frac{5}{10}\right)^2 \times 2.75 \times 10^8 = 6.875 \times 10^7$

Ruedisueli
11/5/96

7/7

> deposition process efficiency, or figure of merit is the mass-to-charge ratio,

$$M_q = \frac{\Delta m\, F}{Q}$$

where Δm is computed from the measured frequency change and the appropriate C_f.

and Q is the measured (current-integrated) value of the charge passed during the process.

for example for the T_{ON}/T_{OFF} @ 2.0 mA (for 200 s)
(0.2N $CuSO_4$ on 10 Mhz PCE)

$\Delta f = 271796$ (hz)

$\Delta m = \frac{271796\ s^{-1}}{2.75\times10^{8}\ cm^2/gm\text{-}s} = 9.883\times10^{-4}\ gm/cm^2$

$\Delta Q = 204.3\times10^{-3}$ coul

$M_q = \frac{9.883\times10^{-4}(96500)\ coul/eq}{204.3\times10^{-3}\ coul} = 466.84\ gm/cm^2\text{-}eq$

Note. (3) $C_f = \frac{2f^2}{S\nu\rho} = \frac{2f^2}{S\sqrt{\rho\mu}}$

where (for Y-cut rotated 35°15', AT-cut quartz)

$\nu = 3320$ m/s, acoustic wave velocity of propagation

$S =$ ____ cm^2, active electrode area of the resonator

$\rho = 2.653\times10^{3}\ kg/m^3$, density of quartz

$\mu = \nu^2\rho$, stiffness modulus, $= 2.924\times10^{10}\ kg/ms^2$

Appendix H

Electrochemical Sign Conventions

Various conventions (American, Stockholm, etc.) address the issue of cell polarity and reaction sign consistency. The most generally accepted, IUPAC (International Union of Pure and Applied Chemistry), declares that when the half cell reactions involved are written as reduction reactions, their signs being taken consistent with the copper plus / zinc minus convention, the potential of the half-cell on the *left* is subtracted from the potential of the half-cell on the *right* to obtain the magnitude of the cell potential and the sign for the direction of spontaneous reaction. [See Bockris, vol. 2, pg.1119.] Another suggestion is to note that the more positive or noble half-cell is the reduction reaction while the more negative, more active, is the oxidation reaction of the cell. [See Fontana, 3rd ed., pg. 452.] All well and good if a table of standard half cell reactions, clearly identified as adhering to one convention or the other, is available, and an agreement is reached on which is *left* and which is *right* is reached. Perhaps it is best to simply remember three things:

1. Electrons flow from negative (a region of excess electrons) to positive (a region of electron defficiency).

2. The cathode is a region, an interface, where reduction takes place. Here electrons go from the external circuit, across the electrode surface, into the interface. (It is the positive terminal on a battery.)

3. The anode is a region, an interface, where oxidation takes place. Here electrons leave the electrode and enter the external circuit, move away from the interface. (It is the negative terminal on the battery.)

With a flashlight battery (whose poles are clearly marked) on hand in the laboratory or in the field, the instrument used to measure an unknown cell can be calibrated to determine unambiguously which electrode is the cathode and which is the anode.

The electrochemical half-cell is a very useful concept and in electrochemical studies the object of interest is often the reaction across a single interface. The absolute voltage across a single interface, a half-cell, however, can not be directly measured. It must always be measured with respect to some other half-cell. The voltmeter can only be connected across a complete, two-electrode cell. It is possible to define a reference half-cell reaction in the standard state and then measure other standard state reactions with respect to it. The reduction/oxidation reaction for hydrogen at STP (standard temperature and pressure, 25 deg C, 1 atmosphere) as hydrogen gas is bubbled over the surface of a platinum electrode immersed in a unit activity solution of hydrochloric acid, is arbitrarily assigned an equilibrium, reversible, half-cell potential, $E^{o}(H = H^{+}) = 0.0$ volts.

Any other half-cell may now be measured with respect to this standard hydrogen electrode (SHE). For example, if an interface consisting of a copper electrode immersed in a 1 normal solution of cupric ions (i.e., copper sulfate) at STP and connected to the SHE across a semi-permeable membrane (which allows charge transfer but no mixing), the reversible equilibrium potential for the reduction/oxidation of copper is measured by a voltmeter across the electrodes of this cell to be $E^{o}(Cu = Cu^{2+}) = +0.337$ volts (SHE). The E^{o} indicates the cell is in the standard state and the SHE indicates the measurement is with respect to the standard hydrogen electrode.

In this same manner, other half-cell reactions may be measured; zinc, for example, $E^{o}(Zn = Zn^{2+}) = -0.763$ volts (SHE); and so on, to construct the whole table of

equilibrium half-cell potentials, the EMF (electromotive force) series. Both oxidation and reduction tables are in print, however, and can lead to confusion. The copper plus, zinc minus, *reduction* reactions tables give signs which are consistent with the IUPAC. If the standard copper/SHE cell is connected to the battery-calibrated voltmeter, it will indicate a + potential; the copper is indeed the cathode and the Gibbs equation yields a $-\Delta G$ which means the copper reduction reaction is the spontaneous direction. Replacing the copper with the standard zinc/SHE would , on the other hand, result in a - potential on the voltmeter, meaning the zinc is the anode of this cell, while the Gibbs free energy change here is + (for the reduction reaction) and the spontaneous reaction direction is, therefore, the oxidation of zinc.

VITA

Robert Louis Ruedisueli was born to Robert W. and Elizabeth M. Ruedisueli on Staten Island in New York City, on May 11, 1947. Robert graduated from JEB Stuart High School in Falls Church, Virginia, in 1965. He attended Brown University in Providence Rhode Island on a US Navy ROTC scholarship. In 1970 Robert received his BS in Engineering from Brown and was commissioned as an officer in the Navy. During his four year tour in the Navy, Robert met Diana Eileen Garatoni in San Diego, California where he was stationed between cruises to Vietnam and the Western Pacific. They were married May 6, 1972.

Robert left the Navy in June of 1974. After a brief stay in Stockton, California where Robert worked as a project engineer in a paper mill, the couple moved to the San Fransisco Bay area where Robert worked as production foreman at a fiber glass pipe plant. Early in 1977, they relocated to Bellingham, Washington where Robert continued to work in the fiberglass industry first as production supervisor then in design and engineering.

Always intending to continue his education, Robert enrolled in the University of Washington College of Engineering as a graduate student in the Mechanical Engineering Ocean Engineering program, in the spring of 1981. Finding a particular interest in marine corrosion, he took courses in Chemical Engineering, broadening his interest to electrochemistry in general. He completed his studies for his Masters of Science in engineering under the direction of Professor Colin J. Sandwith and Dr. Harold E. Hager in December of 1983 with a thesis on the effects of alternating current on corrosion.

Robert continued his studies in electrochemistry and corrosion in the U of W Department of Materials Science and Engineering under the guidance and supervision of Professor Thomas F. Archbold. Meanwhile, he worked part time as an engineer with

Professor Sandwith on corrosion problems on Navy submarines and undersea cables at the Applied Physics Laboratory, U of W.

Robert continues to work at the Applied Physics Lab, doing research in electrochemistry and corrosion. He hopes to develope a course of laboratory instruction in electrochemistry techniques for seniors and graduate students. He is a member of the Northwest Chapter of the Electrochemistry Society and has been active in Puget Sound section of the National Association of Corrosion Engineers, International, recently serving as a section officer, 1992-1995. When not working on corrosion and electrochemistry problems, Robert enjoys playing the violin, hiking, and working in the garden with Diana at their home in Bellingham.

PUBLICATIONS

H.E. Hager, R.L. Ruedisueli, M.F. Buehler, "The use of Piezoelectric Crystals as Electrode Substrates in Iron Corrosion Studies; the Real-time, In Situ Determinaiton of Dissolution and Film Formation Reaction Rates," NACE Journal of Corrosion, Vol. 42, No. 6, June, 1986, pp. 345-351.

R.L. Ruedisueli, H.E. Hager, and C.J. Sandwith, "An application of a State-of-the-Art-Corrosion Measurement System to a study of the Effects of AC on Corrosion," NACE Journal of Corrosion, Vol. 43, No. 6, June, 1987, pp 332-338.

C.J. Sandwith, R.L. Ruedisueli, and M.L. Welch, "A Standardized Abrasion Resistance Test for Undersea Cable Jackets," OCEANS '91, Honolulu, Hawaii, USA, October 1-3, 1991, Procedings, Vol. 1, pp. 296-300.

C.J. Sandwith and R.L. Ruedisueli, "Corrosion Testing of the Steel Shield of a Small Deep-Sea Electro-Optic Cable," OCEANS '91, Honolulu, Hawaii, USA, October 1-3, 1991, Procedings, Vol. 1, pp. 301-305.

C.J. Sandwith, R.L. Ruedisueli, and K.G. Booth, "Seawater Monitoring Instrumentation System," MTS '92 (The Marine Technology Society), Washington, D.C., October 19-21, 1992, Proceedings, Vol. 2, pp. 1037-1043.

C.J. Sandwith, R.L. Ruedisueli, K.G. Booth, J.P. Papageorge, and B.A.Eng, "Monitoring Corrosion in Submarine Sonar Domes," OCEANS '93, Victoria, B.C., Canada, October 18-21, 1993, Procedings, Vol. 1, pp. 158-163.

C.J. Sandwith, R.L. Ruedisueli, J.P. Papageorge, and B.A. Eng, "Initial Results of Monitoring Corrosivity in Submarine Sonar Domes: The Dome Water Monitoring Instrumentation System (DWMIS) Experiment, January - August 1993," OCEANS '94, Brest, France, September 13-16, 1994, Procedings, Vol. 2, pp. 313-318.

C.J. Sandwith and R.L. Ruedisueli, "An Experiment to Reduce Corrosivity in Submarine Sonar Domes by Nitrogen," OCEANS '95, San Diego, CA, October 9-12, 1995, Procedings, Vol. 2, pp. 1134-1138.

C.J. Sandwith, R.L. Ruedisueli, A.L. James, and G.E. Gotthardt, "Resistance of Steel Strength Wires Used in Small Fiber-Optic Cables to Seawater Corrosion," OCEANS '96, Fort Lauderdale, FA, September 23-26, 1996, Procedings, Vol. 1, pp. 511-516.

PRESENTATIONS

"A Proposal for a Study on the Effects of AC on Corrosion and Other Electrochemical Processes," Ph D General Exam, Dept. of Materials Science and Engineering, University of Washington, Seattle, WA, March 8, 1988.

"Experimental Techniques for the Analysis of Non-Steady Electrochemical Processes," Spring Meeting of the Northwest Chapter of the Electrochemical Society, Seattle, WA, April 29, 1989.

"Electrochemistry of Corrosion," Seminar, Applied Physics Laboratory, University of Washington, Seattle, WA, May 9, 1989.

"On the Application of Electrochemical Impedance Spectroscopy and Piezoelectric Crystal Techniques to the Study of Mass Accretion Processes," First International Symposioum on EIS, BomBannes, France, May 25, 1989.

"Two Corroison Rate Measurement Methods," Spring Meeting of the Northwest Chapter of the Electrochemistry Society, Seattle, WA, April 28, 1990.

"Relaxation Phenomena in Electrochemical Systems," Poster, International Discussion Meeting on Relaxations in Complex Systems, Heraklion, Crete, Greece, June 28, 1990.

"Seawater Monitoring Instrumentation System," MTS '92 Conference, Washington, D.C., October 19, 1992.

"Monitoring Corrosion in Submarine Sonar Domes," OCEANS '93, Victoria, B.C., October 19, 1993.

"An Experiment to Reduce Corrosivity in Submarine Sonar Domes by Nitrogen," OCEANS '95, San Diego, CA, October 11, 1995.

"Resistance of Steel Strength Wires Used in Small Fiber-Optic Cables to Seawater Corrosion," OCEANS '96, Fort Lauderdale, FA, September 25, 1996.